UNIVERSITY OF OKLAHOMA

GRADUATE COLLEGE

ADSORBED SURFACTANT AT THE SOLID/LIQUID INTERFACE: USE OF ADSORBED SURFACTANT AGGREGATES IN THE SYNTHESIS OF ELECTRICALLY CONDUCTING POLYMERS

A Dissertation

SUBMITTED TO THE GRADUATE FACULTY

in partial fulfillment of the requirements for the

degree of

Doctor of Philosophy

By

ANDREW CARSWELL
Norman, Oklahoma
2003

Downloaded from SHAREOK. Persistent Handle URL: https://hdl.handle.net/11244/681

UMI Number: 3112345

INFORMATION TO USERS

The quality of this reproduction is dependent upon the quality of the copy submitted. Broken or indistinct print, colored or poor quality illustrations and photographs, print bleed-through, substandard margins, and improper alignment can adversely affect reproduction.

In the unlikely event that the author did not send a complete manuscript and there are missing pages, these will be noted. Also, if unauthorized copyright material had to be removed, a note will indicate the deletion.

UMI®

UMI Microform 3112345

Copyright 2004 by ProQuest Information and Learning Company.

All rights reserved. This microform edition is protected against unauthorized copying under Title 17, United States Code.

ProQuest Information and Learning Company
300 North Zeeb Road
P.O. Box 1346
Ann Arbor, MI 48106-1346

© Copyright by ANDREW CARSWELL 2003
All Rights Reserved

ADSORBED SURFACTANT AT THE SOLID/LIQUID INTERFACE: USE OF ADSORBED SURFACTANT AGGREGATES IN THE SYNTHESIS OF ELECTRICALLY CONDUCTING POLYMERS

A Dissertation APPROVED FOR THE
SCHOOL OF CHEMICAL ENGINEERING AND MATERIALS SCIENCE

BY

Dr. Brian P. Grady

Dr. Edgar A. O'Rear III

Dr. Lloyd A. Bumm

Dr. John F. Scamehorn

Acknowledgements

As is true for life in general, graduate school has been a time in which one encounters many obstacles and cross roads where decisions have to be made. I believe firstly that struggles can give rise to strength and that when one faces a cross road one either makes the *right* decision or if not has the ability to then make the decision *right*. In either event, following either route can result in success, although admittedly one path may take longer than the other. In hindsight I wish that I had made more right decisions during graduate school although I know that I have learned from this process.

I would like to thank my graduate advisor Dr. Brian Grady who has allowed me the room to explore while maintaining my focus on the finish line. I thank Dr. Grady for always being available for discussions, for his advice and encouragement, and for his understanding over extraneous circumstances outside of the work place. I would also like to thank my graduate committee members Drs. Scamehorn, O'Rear, Bumm, and Kendrick for being willing to participate in this process and for their advice and technical guidance along the way. I would like to give Dr. O'Rear special thanks for his kindness in allowing me to use the atomic force microscope.

There have been many people in the lab that have helped me to this point through many technical discussions and making the work place a fun environment. I will undoubtedly omit some names but thanks to Berlin Genetti, Xin Wei, Keith Farrell, Aaron Lowe, Andrew McGrew, Maricel Marquez, and Jessica John. Also I thank the many friends that I met during graduate school.

When getting married and graduating from college with a business degree in 1995, I would have never imagined that eight years later I would be about to defend my thesis in chemical engineering. I want to thank my wife Sharon for all of her support and encouragement along the way. She has always believed in me and in my abilities. Without her none of this would have been possible. I want to thank her for the most special gift that anyone can receive-- our beautiful baby Madeline. Although making a scientific discovery in the laboratory can be exhilarating, it pales in comparison to witnessing the creation of life. The birth of our daughter will undoubtedly remain my most poignant memory of graduate school. I dedicate this dissertation to my wife and to our daughter.

Table of Contents

CHAPER 1. SURFACTANTS AND ELECTRICALLY CONDUCTING POLYMERS 1

I. SURFACTANTS 1

A. INTRODUCTION 1
B. MICELLE FORMATION 4
1. Factors Affecting the cmc in Aqueous Solutions *6*
a) Electrolyte 6
b) Surfactant Structure 7
(i) Hydrophobic Group 7
(ii) Hydrophilic Group 8
(iii) Counterion Type 9
c) Addition of Organic Molecules 10
(i) Class I Compounds 10
(ii) Class II Compounds 11
d) Temperature 12
2. Empirical Equations for cmc Determination *13*
C. SURFACTANT SHAPE TRANSFORMATIONS 14
D. SURFACTANT ADSORPTION AT THE SOLID/LIQUID INTERFACE 18
1. Electrical Double Layer Theory *18*
2. Surfactant Adsorption Mechanisms *21*
3. Atomic Force Microscopy for probing Surfactant Film Morphology at the Solid/Liquid Interface *27*

II. ELECTRICALLY CONDUCTING POLYMERS 31

A. INTRINSICALLY CONDUCTING POLYMERS (ICPS) 31
1. Doping *32*
2. Polyaniline *34*
3. Polypyrrole *36*
B. ELECTRICALLY CONDUCTING COMPOSITE MATERIALS 37

III. ADSORBED SURFACTANT AGGREGATES AT THE LIQUID/SOLID INTERFACE FOR THIN FILM POLYMERIZATIONS – ADMICELLAR POLYMERIZATION 39

IV. SURFACTANT AGGREGATES FOR THE SYNTHESIS OF 1-D NANOSTRUCTURES OF ELECTRICALLY CONDUCTING POLYMERS 43

A. 1-D Π-CONJUGATED POLYMER NANOSTRUCTURES SYNTHESIZED USING "SOLID" TEMPLATES 44
B. 1-D Π-CONJUGATED POLYMER NANOSTRUCTURES USING MOLECULAR INTERACTIONS AS "SOFT" TEMPLATES 49

V. REFERENCES 55

CHAPTER 2. EXPERIMENTAL 63

I. CMC DETERMINATION IN THE PRESENCE OF SURFACTANT ADSORBING INORGANIC PARTICULATES 63

A. MATERIALS 63
B. ADSORPTION ISOTHERM GENERATION 64
C. CMC DETERMINATION 65
D. SODIUM ION DETERMINATION 68

II. SYNTHESIS AND CHARACTERIZATION OF POLYANILINE AND POLYPYRROLE THIN FILMS ON ALUMINA PARTICLES 69

A. MATERIALS 69
B. ADSORPTION ISOTHERMS OF SDS AND SDBS ON ACIDIC ALUMINA 69
C. POLYMERIZATION OF ANILINE AND PYRROLE ON ALUMINA 71
D. CONTACT CONDUCTIVITY MEASUREMENTS 73
E. WEIGHT FRACTION OF ORGANICS ON THE SURFACE OF THE ALUMINA 75
F. WETTING BEHAVIOR MEASUREMENTS 75
G. XPS EXPERIMENTS 78

III. ADSORBED SURFACTANTS AS TEMPLATES FOR THE SYNTHESIS OF MORPHOLOGICALLY CONTROLLED POLYANILINE AND POLYPYRROLE NANOSTRUCTURES ON FLAT SURFACES: FROM SPHERES TO WIRES TO FLAT FILMS 78

A. PANI SYNTHESIS ON HOPG AND MODIFIED HOPG 78
B. PPY SYNTHESIS ON HOPG 80
C. SPM IMAGING 81

IV. REFERENCES 84

CHAPTER 3. CMC DETERMINATION IN THE PRESENCE OF SURFACTANT ADSORBING INORGANIC PARTICULATES 85

I. OVERVIEW 85

II. RESULTS AND DISCUSSION 89

III. CONCLUSIONS 98

IV. ACKNOWLEDGEMENTS 98

V. REFERENCES 99

CHAPTER 4. SYNTHESIS AND CHARACTERIZATION OF POLYANILINE AND POLYPYRROLE THIN FILMS ON ALUMINA PARTICLES 101

I. OVERVIEW 101

II. RESULTS AND DISCUSSION 102

A. ADSORPTION ISOTHERMS OF SODIUM DODECYL SULFATE AND SODIUM DODECYLBENZENE SULFONATE ON ALUMINA 102
B. POWDER CONDUCTIVITY OF PPY AND PANI COATED ALUMINA 103
C. LOSS IGNITION OF POLYMER MODIFIED ALUMINA 107
D. WETTING PROPERTIES OF MODIFIED ALUMINA PARTICLES 110
E. CHARACTERIZATION OF POLYMER FILMS BY X-RAY PHOTOELECTRON SPECTROSCOPY (XPS) 113
1. Polyaniline 113
2. Polypyrrole 120

III. CONCLUSIONS 124

IV. ACKNOWLEDGEMENTS 125

V. REFERENCES 126

CHAPTER 5. ADSORBED SURFACTANTS AS TEMPLATES FOR THE SYNTHESIS OF MORPHOLOGICALLY CONTROLLED POLYANILINE AND POLYPYRROLE NANOSTRUCTURES ON FLAT SURFACES: FROM SPHERES TO WIRES TO FLAT FILMS 128

I. OVERVIEW 128

II. RESULTS AND DISCUSSION 133

A. POLYANILINE 133
B. POLYPYRROLE 144

III. CONCLUSIONS 151

IV. ACKNOWLEDGEMENTS 152

V. REFERENCES 153

CHAPTER 6. ATOMIC FORCE MICROSCOPY STUDIES OF POLYMER FILMS SYNTHESIZED IN THE PRESENCE OF SURFACTANT 155

A. POLYANILINE SYNTHESIS ON HIGHLY ORIENTED PYROLYTIC GRAPHITE USING SODIUM SULFONATE SURFACTANTS 155

B. PANI SYNTHESIS ON SILICON DIOXIDE USING SODIUM SULFONATE SURFACTANTS 160

C. PANI SYNTHESIS ON MICA USING SODIUM DODECYL SULFATE 163

II. REFERENCES..... 167

CHAPTER 7. CONCLUSIONS AND RECOMMENDATIONS 168

I. CONCLUSIONS 168

II. RECOMMENDATIONS AND FUTURE WORK 169

A. THIN FILM MODIFICATION OF ALUMINA PARTICLES WITH POLYANILINE AND POLYPYRROLE..... 169

B. SYNTHESIS OF MORPHOLOGICALLY CONTROLLED FILMS ON FLAT SURFACES170

List of Figures

Figure 1.1. Surfactant molecule showing headgroup and tail areas.....2

Figure 1.2. Surfactant Properties in Relation to the cmc.....2

Figure 1.3. Packing Parameter and Surfactant Morphologies in Solution.....16

Figure 1.4. Stern model of electrical double layer.....20

Figure 1.5. Stern model showing sign reversal by adsorption of counter ions in the Stern layer.....20

Figure 1.6. Schematic of zeta potential of quartz in dodecylammonium acetate.....23

Figure 1.7. Schematic representation of adsorption density of sodium dodecylsufonate on alumina (pH 7.2, ionic strength 2 x 10^{-3}M).....23

Figure 1.8. Adsorption of sodium dodecyl sulfate on alumina (pH 6.5, 0.1M NaCl).....25

Figure 1.9. Bilayer model of adsorption onto hydrophilic solid surfaces.....26

Figure 1.10. Possible adsorbed surfactant morphologies on hydrophilic surfaces.....28

Figure 1.11. Possible adsorbed surfactant morphologies on hydrophobic surfaces.....28

Figure 1.12. Structural formula of polyaniline.....35

Figure 1.13. Structural formula of polypyrrole.....35

Figure 1.14. Schematic of the admicellar polymerization process.....40

Figure 1.15. Solid template method for the fabrication of 1-D conducting polymer structures.....48

Figure 1.16. SEM image of polyaniline nanotubes (92 nm average diameter), synthesized in the presence of β-naphthalene sulfonic acid. 51

Figure 1.17. FE-SEM image of polypyrrole nanotubes (95 nm diameter), synthesized by reverse microemulsion polymerization using surfactant molecules as templates.....51

Figure 1.18. A schematic of the reverse microemulsion technique identifying four stages. In the first stage, reverse micelles form in an apolar solvent. These speherical micelles are then transitioned into cylindrical micelles by the addition of iron chloride in a second stage. Pyrrole then partitions around the cylindrical structure before being polymerized in the third step. Finally, the surfactant is removed, leaving Ppy nanotubes.....54

Figure 2.1. Membrane filters for cmc determination.....67

Figure 2.2. Schematic of contact conductivity measuring device. Particles are pressed between two electrodes and kept in place with an insulating jacket.....74

Figure 2.3. Schematic of the apparatus to measure the wetting behavior of particles.....77

Figure 2.4. Schematic representation of the components making up an AFM head.....83

Figure 3.1. Cmc determination of SDS in the presence of alumina particles using conductivity measurements.....90

Figure 3.2. Cmc determination of SDS by ultracentrifuge membranes.....90

Figure 3.3. Cmc determination of SDS using surface tension.....93

Figure 3.4. Cmc determination of SDS using capillary rise.....93

Figure 3.5. Surfactant concentrations found for adsorbed, micelle, and free SDS in the presence of alumina substrate.....97

Figure 3.6. Surfactant concentrations found for adsorbed, micelle, and free SDS in the presence of titania substrate.....97

Figure 4.1. Adsorption isotherms for SDS and SDBS measured on acidic alumina.....105

Figure 4.2. Contact conductivities of PAni and PPy modified alumina particles as a function of monomer concentration.....105

Figure 4.3. Loss ignition measurements of modified alumina particles.....109

Figure 4.4. Contact conductivities of PAni and PPy modified alumina particles as a function of weight percent of organics.....109

Figure 4.5. Wetting behavior of PPy modified alumina particles.....112

Figure 4.6. Wetting behavior of PAni modified alumina particles.....112

Figure 4.7. High-resolution XPS N1s fitted spectra of An56.....114

Figure 4.8. High-resolution XPS S2p fitted spectra of An56.....119

Figure 4.9. High-resolution XPS N1s fitted spectra of Py80.....122

Figure 4.10. High-resolution XPS S2p fitted spectra of Py80.....122

Figure 5.1. Illustration of the process to fabricate morphologically controlled nanostructures of electrically conducting polymers on surfaces using surfactant templates. This particular schematic represents the proposed schematic of wire formation on (A) chemically treated HOPG and (B) HOPG.....132

Figure 5.2. 500 x 500 nm AFM images of PAni films on HOPG with 0 mM 1-dodecanol (A) and 0.5 mM 1-dodecanol (B). Both images shown at a height scale of 12 nm.....135

Figure 5.3. X-ray photoelectron spectroscopy of PAni wires on freshly cleaved HOPG. Three nitrogen environments can be observed by curve fitting.....137

Figure 5.4. X-ray photoelectron spectroscopy of HOPG before and after chemical treatment. (A) Carbon, (B) Nitrogen, (C) Oxygen, and (D) Sulfur.....139

Figure 5.5. 2 x 2 μm AFM images of PAni films on oxidized HOPG with 0 mM 1-dodecanol (A), 0.1 mM 1-dodecanol (B). 141

Figure 5.6. 2 x 2 μm AFM images of PAni films on oxidized HOPG with 0.1 mM of 1-dodecanol and 3 hours of polymerization.....142

Figure 5.7. X-ray photoelectron spectroscopy of PAni wires on chemically treated HOPG indicating curve fitting and the different nitrogen environments.....142

Figure 5.8. 1 x 1 μm AFM images of PPy films on HOPG Sodium 1-octanesulfonate (A), Sodium 1-decanesulfonate (B).....146

Figure 5.9. 1 x 1 μm AFM images of PPy films on HOPG Sodium 1-dodecanesulfonate (A), Sodium 1-decanesulfonate with 0.8 mM decanol (B).....147

Figure 5.10. Cross-sectional analysis of PPy films for C8 system indicating polymer film on the right side of the image and bare HOPG on the left side of the film edge (A). Height of the film measured between the markers for C8 (B) and C10 (C) with heights of 26 nm and 16 nm respectively.....149

Figure 6.1. AFM image of PAni film on HOPG synthesized using C8 sulfonate.....157

Figure 6.2. AFM image of PAni film on HOPG synthesized using C10 sulfonate.....157

Figure 6.3. AFM image of PAni film on HOPG synthesized using C12 sulfonate.....158

Figure 6.4. AFM image of PAni film on chemically treated HOPG synthesized using C8 sulfonate.....158

Figure 6.5. AFM image of PAni film on SiO2 synthesized using C8 sulfonate.....161

Figure 6.6. AFM image of PAni film on SiO2 synthesized using C10 sulfonate.....161

Figure 6.7. AFM image of PAni film on SiO2 synthesized using C12 sulfonate.....162

Figure 6.8. AFM image of PAni film on mica synthesized using sodium dodecyl sulfate.....164

Figure 6.9. Optical micrograph of PAni film on mica indicating directional changes associated with steps in the surface. For reference the image is 100 x 75 microns.....164

Figure 6.10. Cross section of PAni film as synthesized in Figure 6.8. Some individual wire like structures are present with diameters on the order of 50 nm. Vertical height of the film appears to be ca. 12 nm.....165

Figure 6.11. N1s nitrogen environment of PAni film synthesized on the surface of mica. Deconvolution leads to peaks centered at 398.5, 399.6, and 401.38 with areas of 13.7, 46.7, and 39.6 % respectively. 166

List of Tables

Table 1.1. Cmc of SDS with added electrolyte.....7
Table 1.2. Constants for the relation log CMC = $A - BN$.....13
Table 4.1. Atomic concentrations of PAni films on alumina as determined by XPS.....114
Table 4.2. Atomic concentrations of PPy films on alumina as determined by XPS.....119

List of Equations

Equation 1 Free Energy of Micellization..... 4
Equation 1.2 CMC Determination as a function of added electrolyte..... 6
Equation 1.3 Relation for cmc determination..... 13
Equation 1.4 Packing Parameter..... 14
Equation 1.5 Volume of Surfactant Tail Group..... 15
Equation 1.6 Maximum Effective Length of Surfactant Hydrophobe..... 15
Equation 1.7 The Debye Length (Effective thickness)..... 19

Abstract

The underlying theme to this work is surfactant adsorption at the solid/liquid interface. More specifically, surfactant adsorption has been studied in relation to the critical micelle concentration (cmc) and to the applicability of adsorbed surfactant as a template for the synthesis of electrically conducting polymers. Measurement of the cmc of sodium dodecyl sulfate (SDS) in the presence of alumina and titania particles has been determined using ultracentrifuge membranes. Such membranes are able to allow individual SDS monomer to permeate while excluding aggregated SDS. Adsorbed SDS and sodium dodecylbenzene sulfonate (SDBS) have been used to fabricate thin films of polyaniline (PAni) and polypyrrole (PPy) respectively on the surface of alumina particles. Powder conductivities were found to reach ~ 10^{-1} S/cm exhibiting an eight order of magnitude increase over bare alumina (~ 10^{-9} S/cm). PAni and PPy films on alumina were characterized by loss ignition, wetting, and X-ray photoelectron spectroscopy (XPS) experiments. In addition, atomic force microscopy (AFM) was used to investigate the morphology of PAni and PPy films synthesized, in the presence of surfactant, on *flat surfaces*. Control over film morphology can be achieved by either the nature of the surfactant or the surface chemistry of the substrate. Shape transitions between spheres → cylinders → flat films were observed in direct relation to what has been previously observed in the bulk.

Chaper 1. Surfactants and Electrically Conducting Polymers

I. Surfactants

A. Introduction

Surfactants are a class of molecules that have applications in a wide variety of sectors of the chemical industry. Surfactants can be found in many household products, pharmaceuticals, detergents, motor oils, drilling muds, flotation agents, and many other applications. More recently, surfactant uses have reached high-technology areas such as biotechnology, microelectronics, and electronic printing. Due to the nanoscale dimensions of surfactant aggregates there are undoubtedly many new applications that are on the horizon.

A surfactant (***surface active agent***), when present at low concentrations in water, can adsorb at interfaces that might be present in the system. The interfacial activity of surfactants in water is due to their bi-polar nature, meaning that the molecular structure is composed of two parts; a hydrophobic and hydrophilic portion (Figure 1.1). The hydrophobic portion drives the molecule away from the solution whereas the hydrophilic group can adsorb to oppositely charged interfaces (in the case of charged surfactants).

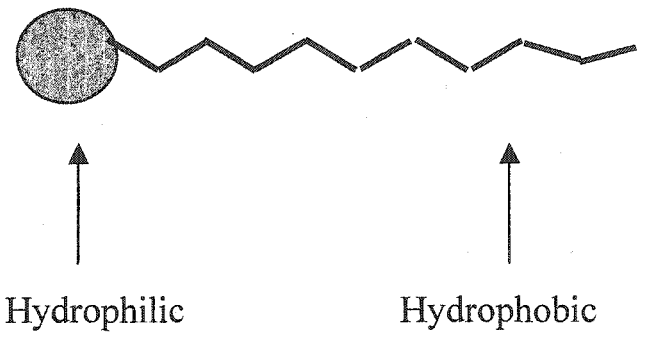


Figure 1.1. Surfactant molecule showing headgroup and tail areas

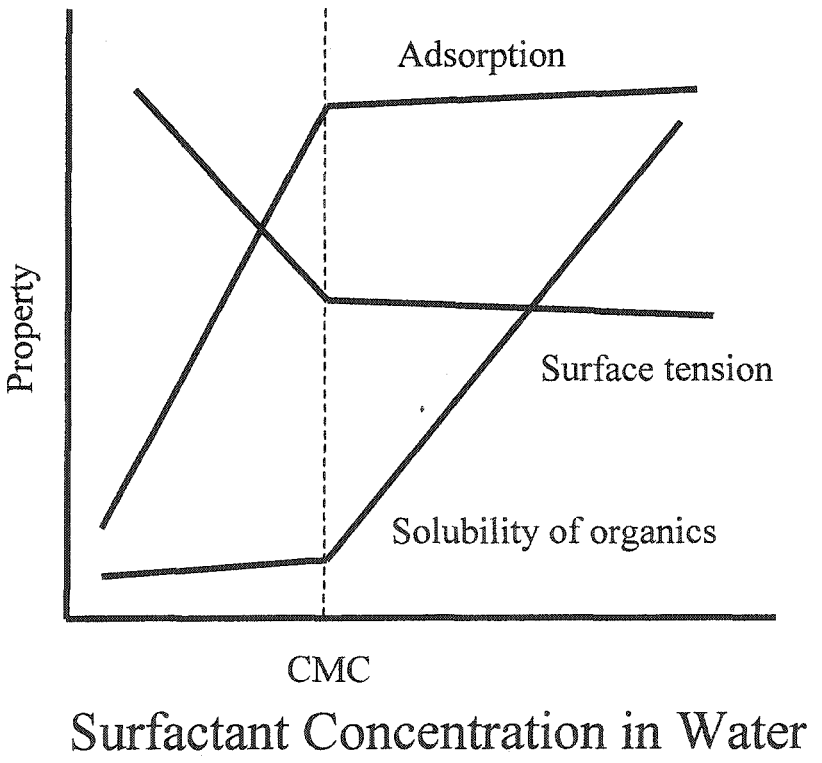


Figure 1.2. Surfactant Properties in Relation to the cmc

Alternatively, in the case of a nonpolar interface, the hydropobic tails can adsorb. When surfactants adsorb, they greatly affect the interfacial free energies of the interface. In general, when an interface is present in a solution and the concentration of surfactant is low, the surfactant can reside in three regions: in solution, at the solid/liquid interface, or at the surface of the liquid. Surfactants can be categorized into four main groups; anionic, cationic, zwitterionic, and nonionic representing negatively, positively, dual charged, and uncharged head-groups respectively.

In order to evaluate the performance of surfactants one must assess the amount of surfactant that is required to provide a change in the particular phenomenon under investigation. Additionally, one must assess the maximum change that the surfactant can cause irrespective of the amount required to produce this change. In the first case, this parameter is called the *efficiency* whereas the second instance is termed the *effectiveness*. In general the *efficiency* is the equilibrium concentration of surfactant in the liquid phase that is required to produce a predetermined amount of effect whereas the *effectiveness* is a determination of the maximum effect that the surfactant can produce without consideration to the amount required. It is not always the case that these two parameters change in parallel with each other.

B. Micelle Formation

Surfactant has the tendency to form aggregates due to its chemical nature i.e. one part of the molecule has an affinity for polar solvents whereas the other portion favors a non-polar environment. At low concentrations, surfactant exists as individual monomer in the bulk. Once a critical bulk concentration is reached, additional individual surfactant molecules no longer desire to exist as free molecules, rather they prefer to aggregate. The concentration at which surfactants begin to aggregate in the bulk is termed the critical micelle concentration (cmc).

Micellar solution properties can be predicted quantitatively by molecular thermodynamic theory.[1,2,3] The free energy of micellization (g_{mic}) is a measure of the free energy change when a surfactant monomer aggregates in a micelle. Five contributions determine g_{mic},

$$g_{mic} = g_{hc/mic} + g_{w/mic} + g_{\sigma} + g_{st} + g_{elec}$$

Equation 1 Free Energy of Micellization

where $g_{hc/mic}$ is the conformational restriction associated with hydrocarbon tails inside the micellar core; $g_{w/mic}$ is the free energy associated with removal of the surfactant hydrophobe from water to bulk hydrocarbon; g_{σ} which refers to the formation of an interface between the micellar core and water; g_{st} which

corresponds to steric repulsions between surfactant headgroups; g_{elec} refers to electrostatic interactions between surfactant headgroups. The major force associated with micelle formation is the removal of the surfactant hydrophobe from the aqueous medium ($g_{w/mic}$). This effect is referred to as the "hydrophobic effect".[4] Although above the cmc a driving force exists such that molecules aggregate, surfactant molecules also experience a loss of freedom by being confined in a micelle and, in the case of ionic molecules, experience charge repulsion between headgroups at the surface of the micelle.

The cmc for a particular surfactant is an important piece of information as it greatly influences phenomena such as detergency and solubilization. In addition, onset of the cmc has an effect on other physical properties of the system such as interfacial or surface tension although the micelle is not directly involved. Figure 1.2 represents a schematic of some surfactant properties as a function of concentration and indicates how these properties are affected by the cmc. Onset of the cmc can be measured by a number of techniques such as surface tension, conductivity, light scattering, refractive index, and capillary rise.[5]

1. Factors Affecting the cmc in Aqueous Solutions

There are many factors that influence the cmc of a surfactant. Some of these factors include, (a) the addition of electrolyte, (b) the structure of the surfactant, (c) the addition of organics to the system, and (d) the temperature of the system. A more detailed explanation of these factors will follow.

a) Electrolyte

The addition of electrolyte to aqueous surfactant systems causes a shift in the cmc. This change in cmc is more marked for anionic and cationic surfactants in comparison to zwitterionic and nonionic surfactants. In the case of ionic surfactants, the effect of electrolyte on the cmc can be determined by

$$\log CMC = -a \log C_i + b$$

Equation 1.2 CMC Determination as a function of added electrolyte

where a and b are constants that are dependent on the particular headgroup and temperature and C_i is the total concentration of counterions in solution (equivalent per liter).[6] The depression in cmc, owing to added electrolyte, is due mainly to a decrease in repulsion between headgroups in the micelle and also a decrease in the thickness

of the ionic atmosphere of the surfactant headgroup. For example, Table 1.1 shows the depression in the cmc of SDS as a function of added sodium chloride.

Surfactant	NaCl (M)	CMC (M)
$C_{12}H_{25}SO_4^-Na^+$ (SDS)	0	8.2×10^{-3}
$C_{12}H_{25}SO_4^-Na^+$ (SDS)	0.01	5.6×10^{-3}
$C_{12}H_{25}SO_4^-Na^+$ (SDS)	0.03	3.2×10^{-3}
$C_{12}H_{25}SO_4^-Na^+$ (SDS)	0.1	1.5×10^{-3}

Table 1 Cmc of SDS with added electrolyte[7]

b) Surfactant Structure

The structure of the surfactant plays a role in the cmc and can be evaluated by the hydrophobic group, hydrophilic group, and the nature of the counterion (for ionic surfactants).

(i) Hydrophobic Group

As the length of the hydrophobe increases (up to 16 carbon atoms) there is a reduction in the cmc. In general, and as a rule of thumb, the cmc is halved by the incorporation of a methylene group to a straight chain hydrophobe attached to a single terminal hydrophilic group.[7] In the case of zwitterionics and nonionics, incorporation of two methylene groups into the hydrophobe causes a decrease in the

cmc by a factor of one tenth (as opposed to one-quarter for ionics). A phenyl moiety incorporated into the hydrophobe with a terminal hydrophilic group is equivalent to three and one-half methylene groups. Increasing the hydrophobe above 16 carbon atoms does not have as drastic effect on the cmc. Once the hydrophobe chain exceeds 18 carbon atoms the cmc should remain virtually unchanged.[8] Adding methyl groups via branching causes about one-half the effect as adding carbon atoms to the straight chain.[9] The introduction of carbon-carbon double bonds into the hydrophobe generally causes an increase in the cmc with the *cis* isomer having a higher cmc than the *trans*.

(ii) Hydrophilic Group

In aqueous systems the cmc of ionic surfactants have much higher cmcs than nonionic surfactants with equivalent hydrophobic groups. For example, the cmc of a 12 carbon ionic surfactant is roughly two orders of magnitude higher than that of a 12 carbon nonionic (1×10^{-2} M Vs. 1×10^{-4} M respectively).[7] Zwitterionics have slightly lower cmcs than ionics with the same number of carbon atoms. Moving the hydrophilic group from a terminal position further toward the center of the hydrophobe tends to

increase the cmc as the hydrophilic group tends to act as a branch at the position of incorporation and methylene groups on the shorter portion of the chain appear to have half of their usual effect on the cmc.

(iii) Counterion Type

In aqueous solutions the cmc changes in parallel to the degree of binding of the counterion to the micelle. For instance, increased binding between the counterion and micelle results in a decrease in the cmc due to a reduction in the repulsive forces between headgroups at the surface of the micelle. The degree of binding increases with an increase in its polarizability and valence whereas it decreases with an increase in hydration radius. Therefore in aqueous medium and for anionic lauryl sulfate surfactants the cmc decreases in the following order: $Li^+ > Na^+ > K^+ > Cs^+ > Ca^{2+} > Mg^{2+}$. Conversely, the cmc is not a measure of the degree of binding of the counterion when comparing surfactants of different types. The reason for this is that the degree of counterion binding to a micelle also depends on the surface charge density of the micelle which in turn is dictated by the surface area occupied by the headgroup. Lower surface areas per headgroup result in a

greater degree of binding with respect to the counterion and micelle. Increasing the length of the hydrophobe, or increasing the bulkiness of the hydrophilic portion of the surfactant, in turn results in an increase in the surface area per headgroup.[10]

c) Addition of Organic Molecules

The addition of organics to aqueous systems of surfactants can have large effects on the cmc. Many times organics are present in surfactants due to being precursor molecules for synthesis or merely impurities. Therefore these organics must be removed if determination of the pure surfactant cmc is necessary. Typically organics cause changes in the cmc by either being solubilized into the micelle (class I materials) or by disrupting solvent-micelle or solvent-surfactant interactions (class II materials).

(i) Class I Compounds

Polar organics such as alcohols or amides are typical of molecules that fall into class I. These molecules tend to affect the cmc to a much larger extent at lower bulk concentrations than class II molecules. Shorter chain molecules tend to migrate to the inner portion of a micelle whereas longer chain molecules reside in the

outer portion of the core; therefore shorter molecules tend to have less effect on the cmc when compared to longer chain members. A maximum in depression is generally seen when the chain length is equivalent to that of the surfactant. Depression of the cmc is greater for straight-chain molecules than for branched molecules as straight chained molecules have a greater tendency to reside in the outer core whereas branched molecules would tend to be forced more into the interior. By the same token, hydrocarbons tend to have little effect on the cmc as they reside in the inner core.

(ii) Class II Compounds

Class II compounds alter the cmc of surfactants by modifying the interactions between the micelle and water or the surfactant and water. Affecting the structure of water, its dielectric constant, or its solubility parameter can do such modifications. Some typical examples of this class of molecule include urea, water soluble esters, ethylene glycol, and formamide. Molecules such as urea and formamide are known to increase the cmc of surfactants in the aqueous phase due to interruption of the water structure.[11] It has been proposed that disruption of the water structure leads to an increase in the degree of hydration of the hydrophilic group which

in turn opposes micellization. Also the surfactant hydrophobe is known to induce an ordering effect on water molecules surrounding the chain when exposed to water. This phenomenon has been termed the "iceberg effect". Since the process of micellization removes this ordering effect, the cmc is accompanied by an increase in entropy of the water. Therefore disruption of the ordered arrangement of water molecules surrounding the hydrophobe by class II molecules decreases the entropy increase on micellization, in turn increasing the cmc.

d) Temperature

The influence of temperature on the cmc of surfactants is somewhat complicated. Increasing the temperature tends to decrease the hydration of the hydrophilic group which in turn favors micellization, whereas an increase in temperature causes a disruption in the ordered water molecules surrounding the hydrophobe therefore opposing micellization. Therefore, a balance exists between these two opposing effects within a given temperature range. In general, the cmc tends to decrease until a minimum and then increases with higher temperatures. In general, the temperature at which this minimum occurs is 25°C for ionic surfactants,[12] and 50°C for nonionics.[13]

2. *Empirical Equations for cmc Determination*

Due to the importance of the cmc much research has focused on developing empirical equations relating the cmc to the molecular composition of the surfactant molecule. In the case of homologous straight-chain ionics, nonionics, and zwitterionics the following relation has been determined from experimental data[14]

$$\log CMC = A - BN$$

Equation 1.3 Relation for cmc determination

where A is a constant for a particular headgroup at a given temperature and B is a constant for a particular surfactant and N is the number of carbon atoms in the hydrophobe. Table 1.2 lists some of these values for typical surfactants as determined from experiments.

Surfactant Series	**Temp. (°C)**	***A***	***B***
Na carboxylates (soaps)	20	1.8	0.30
K carboxylates (soaps)	25	1.9	0.29
Na (K) *n*-alkyl 1-sulfates or -sulfonates	25	1.5	0.30
Na *n*-alkane-1-sulfonates	40	1.5	0.29
Na *n*-alkane-1-sulfonates	55	1.1	0.26
Na *n*-alkyl-1-sulfates	45	1.4	0.30
Na *n*-alkyl-1-sulfates	60	1.3	0.28
Na *n*-alkyl-2-sulfates	55	1.2	0.27

Na *p-n*-alkylbenzenesulfonates	55	1.6	0.29
Na *p-n*-alkylbenzenesulfonates	70	1.3	0.27
n-alkyltrimethylammonium bromides	25	2.0	0.32
n-alkyltrimethylammonium chlorides (in 0.1M NaCl)	25	1.2	0.33
n-alkyltrimethylammonium bromides	60	1.7	0.29
n-alkylpyridinium bromides	30	1.7	0.31
n-$C_nH_{2n+1}(OC_2H_4)_6OH$	25	1.8	0.49
n-$C_nH_{2n+1}(OC_2H_4)_8OH$	15	2.1	0.51
n-$C_nH_{2n+1}(OC_2H_4)_8OH$	25	1.8	0.50
n-$C_nH_{2n+1}(OC_2H_4)_8OH$	40	1.6	0.48
n-$C_nH_{2n+1}N^+(CH_3)_2CH_2COO^-$	23	3.1	0.49

Table 1.2 Constants for the relation log CMC = A- BN[7]

C. Surfactant Shape Transformations

The shape of a micelle is important and determines many solution properties such as solubilizing capacity of organics, viscosity, and cloud point. In 1976 Israelachvili et al. proposed the concept of the molecular packing parameter (g), which is a dimensionless number that can be used to predict the equilibrium size and shape of surfactant aggregates.[15] In this model, thermodynamic and molecular packing considerations give rise to the general formula

$$g = v / a_0 l_c$$

Equation 1.4 Packing Parameter

where v is the volume of the alkyl tail, l_c the maximum effective length of alkyl chains, and a_0 the cross-sectional area occupied by the hydrophilic group at the surface of the micelle (Figure 1.3). The volume of the surfactant tail and the maximum effective length are given by Tanford's[4] equations:

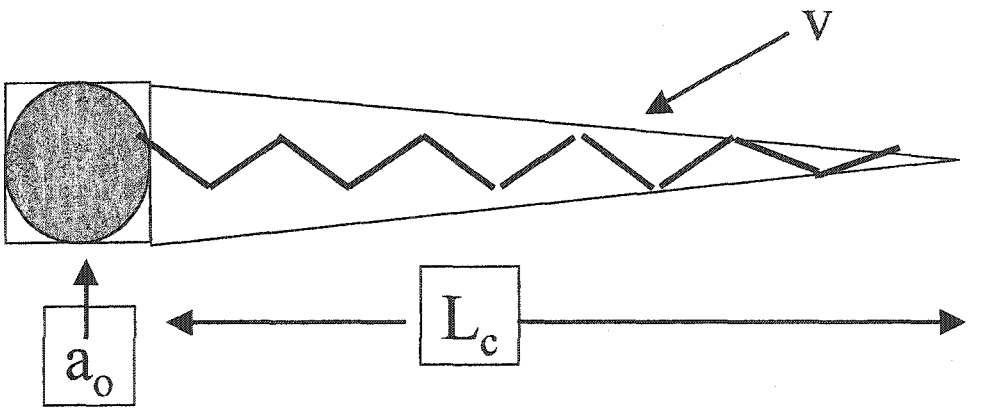
$$v = 27.4 + 26.9n \text{ Å}$$

Equation 1.5 Volume of Surfactant Tail Group

$$l_c \leq l_{\max} = 1.5 + 1.265n \text{ Å}$$

Equation 1.6 Maximum Effective Length of Surfactant Hydrophobe

where n is the number of methylene groups embedded in the micellar core. When the parameter lies within the ranges 0-1/3, 1/3-1/2, or 1/2-1 the favored aggregate morphology is spherical, cylindrical or a flat bilayer respectively (Figure 1.3). It has been pointed out recently that this model neglects the length of the surfactant hyrophobe as the ratio v_o/l_c is a constant and independent of tail length for common surfactants.[16]



Critical Packing Factor (Φ) $\Phi = v/a_o L_c$

$v = 27.4 + 26.9n$ Å^3

$L_c \leq 1.5 + 1.265n$ Å

Φ	Aggregate Structure
<0.33	(A) Spherical, Ellipsoidal Micelles
0.33-0.5	(B) Rod-like Micelles
0.5-1.0	(C) Vesicles; Bilayer Structures
1.0	(D) Planar Bilayers

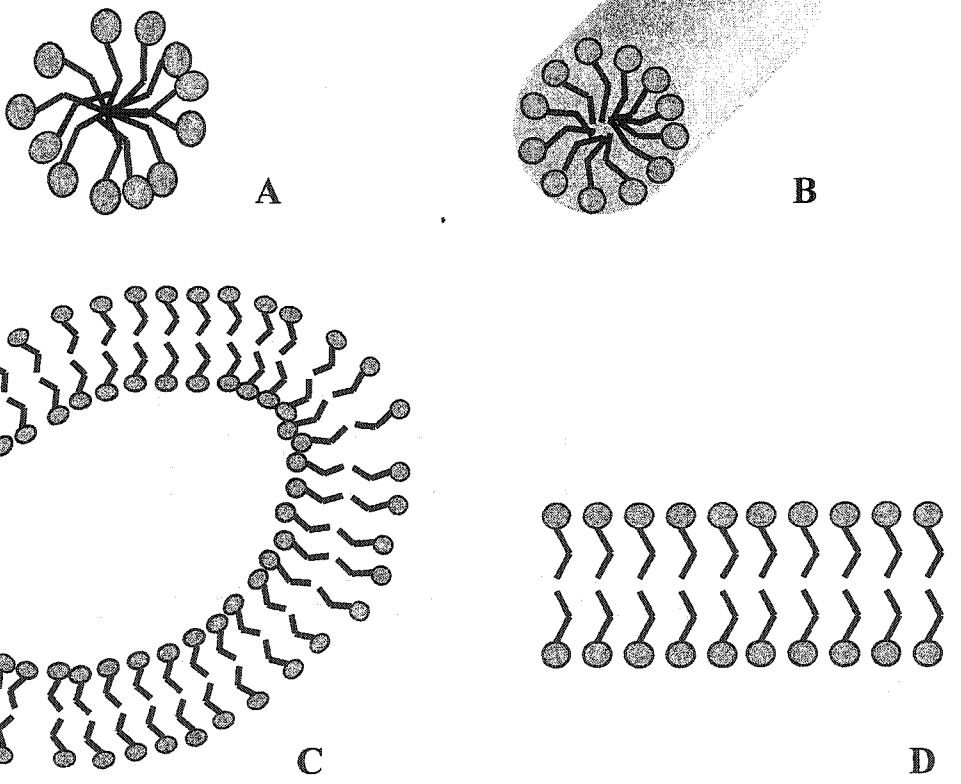


Figure 1.3. Packing parameter and surfactant morphologies in solution

Surfactants undergo shape transitions in solution from spherical to cylindrical aggregates as their concentration is increased. Transitions also occur due to many other influences. Surfactants with small head groups tend to favor formation of larger and less curved aggregates. Incorporation of co-adsorbing molecules such as long chain alcohols, are known to induce shape transformations (to lower curvature aggregates) due to alteration of the packing parameter.

In the case of ionic surfactants, shape transitions can be induced and controlled by the influence of certain counterions through the surface area shrinking effect.[17,18,19] For surfactants to assume spherical morphologies, the area occupied by the head group must be relatively large. Shape transformations from spheres to cylinders is induced if surfactant head groups are able to pack together more tightly. In order for head groups to reside in a closer proximity to one another, repulsive forces between head groups must by reduced. Therefore surfactants with a high degree of counterion binding may be able to overcome repulsive forces more easily as counterions can balance repulsive forces at the micellar surface. In the specific case of cationic surfactants, counterions such as salicylate,[20,21,22] thiocyanate,[23]and tosylate[22] have been shown to be effective in inducing phase transitions when bound to alkyltrimethylammonium and alkylpyridium surfactants.

D. Surfactant Adsorption at the Solid/Liquid Interface

As well as adopting organized aggregates in solution, surfactants also adsorb as aggregates at the solid/liquid interface. It is important to know the amount of surfactant adsorbed at an interface for applications such as foaming, detergency, and emulsification. Also the orientation of the molecules at the interface dictates the nature of the surface and we are also interested in the energy changes such as ΔG, ΔH, and ΔS as they give information regarding the mechanism of adsorption and the efficiency and effectiveness of the surfactant.

1. Electrical Double Layer Theory

In order to discuss the adsorption of surfactants at the solid/liquid interface, it is necessary to understand the electrical considerations of adsorption. An *electrical double layer* is the term given to the potential that exists across an interface due to an unequal distribution of charge between the two phases. To maintain charge neutrality in the system the net charge on one side of the interface must be balanced by the charge on the other side of the interface. An important piece of information is the rate of change of this potential as one moves away from the interface and into bulk solution.

Treatment of the region in contact with an interface can be visualized as two areas. The first area is composed of strongly bound counter ions adsorbed onto fixed sites on the charged surface. This region is called the Stern layer. The second region refers to a diffuse layer of counter ions that that are located further into solution away from the interface. Figure 1.4 represents a schematic of these regions and also shows how the potential drops off rapidly in the Stern layer and then more slowly in the diffuse portion. Counter ions can also change the sign of the potential that results from surface charges (Figure 1.5). Mathematical treatment with respect to the diffuse portion of the electrical double layer results in a term for the effective thickness ($1/\kappa$) of the layer.[24] The effective thickness, also called the Debye Length, refers to the distance from the charged surface in which the majority of the electrical interactions with the charged surface take place. An effective thickness can be described by

$$\frac{1}{\kappa} = \left(\frac{\varepsilon_r \varepsilon_o RT}{4\pi F^2 \sum_i C_i Z_i^2} \right)^{1/2}$$

Equation 1.7 The Debye Length (effective thickness)

where $\varepsilon_r = \varepsilon/\varepsilon_o$ = the relative static permittivity or dielectric constant of the solution (ε = the static permittivity of the solution and ε_o = the permittivity in vacuum), R = the gas constant, T = the absolute temperature, F = the Faraday constant, C_i = the molar concentration of any ion in the solution phase, and Z = the valence of the ions.

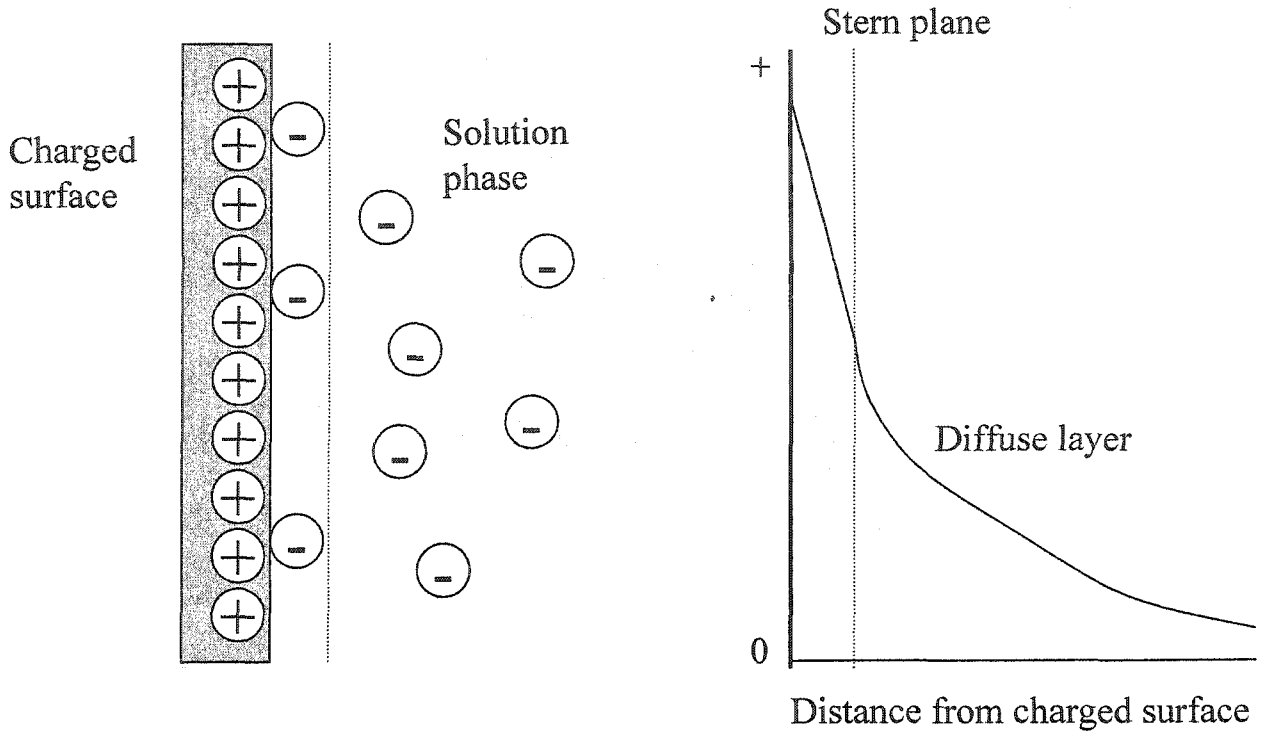


Figure 1.4. Stern model of electrical double layer.

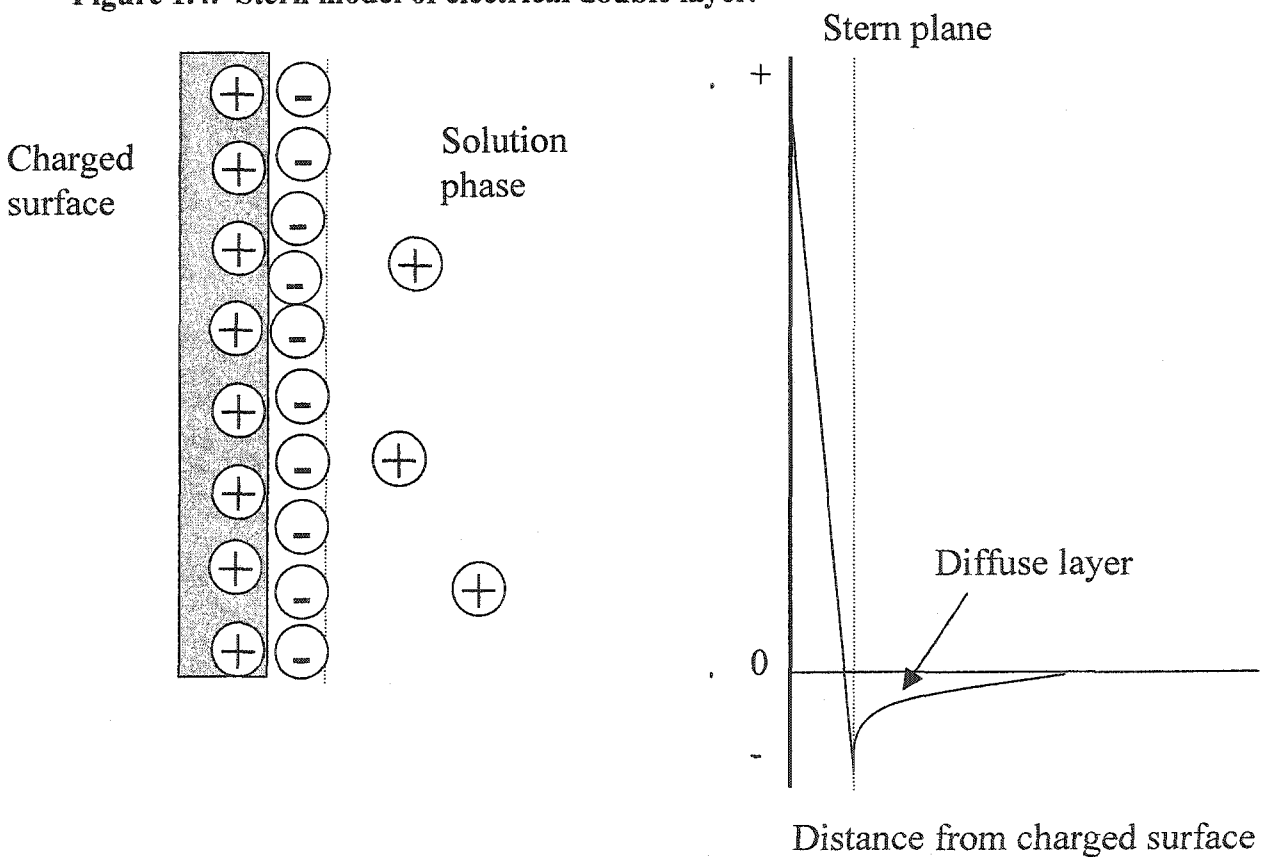


Figure 1.5. Stern model showing sign reversal by adsorption of counter ions in the Stern layer

In contrast to aggregation of surfactants in bulk solution, the introduction of a solid surface requires that interactions between surface and solution and between the hydrophilic and hydrophobic portions of the surfactant and surface must now be considered.

2. *Surfactant Adsorption Mechanisms*

Gaudin and Fuerstenau first investigated the morphology of adsorbed surfactant aggregates at the solid/liquid interface.[25,26] They investigated changes in zeta potential (ζ) of quartz in relation to dodecylammonium acetate at different pH values. Drastic changes in ζ were observed at the critical surfactant concentration, causing a change in sign (Figure 1.6). Inorganic electrolytes did not influence ζ in the same way. Results obtained by De Bruyn[27] showed an increase in surfactant adsorption at the same concentration at which changes in ζ occurred. Gaudin and Fuerstenau surmised aggregate morphology due to changes in ζ and termed this the *hemimicelle model.* Section A (Figure 1.6) represents a region in which concentration is below the critical surfactant concentration and surfactants adsorb individually on the surface of quartz due to electrostatic interactions. The proposed orientation of the surfactant molecules was deduced to be with charged head groups towards the surface and hydrophobic moieties protruding into solution. As surfactant

concentrations increase, adsorbed surfactant monomers tend to aggregate to reduce contact of hydrophobic tails with water (Figure 1.6, section B). Small aggregates of adsorbed surfactants are called hemimicelles. Further increases in surfactant concentration cause a shift in the sign of ζ and therefore what has been interpreted to be aggregation of a second layer of surfactant with reverse orientation to the hemimicelle. Somasundaran and Fuerstenau studied the adsorption of sodium dodecyl sulfonate on alumina at different pH levels and ionic strengths.[28] From this study three regions of the adsorption isotherm were identified (Figure 1.7) and therefore the same mechanism as for quartz was proposed. This model has been coined the *Reverse Orientation Model*.

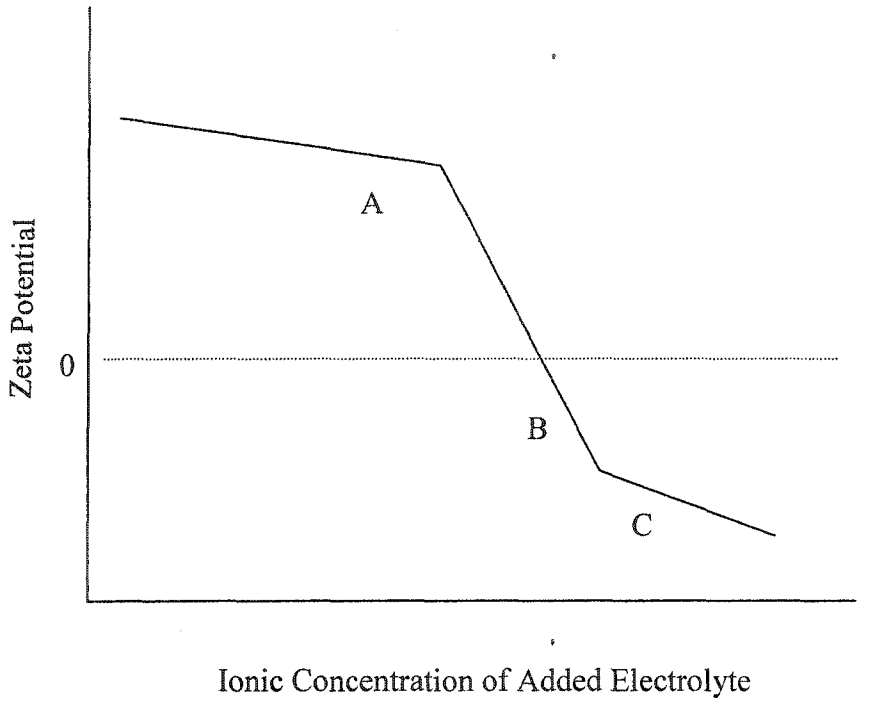


Figure 1.6. Schematic of zeta potential of quartz in dodecylammonium acetate

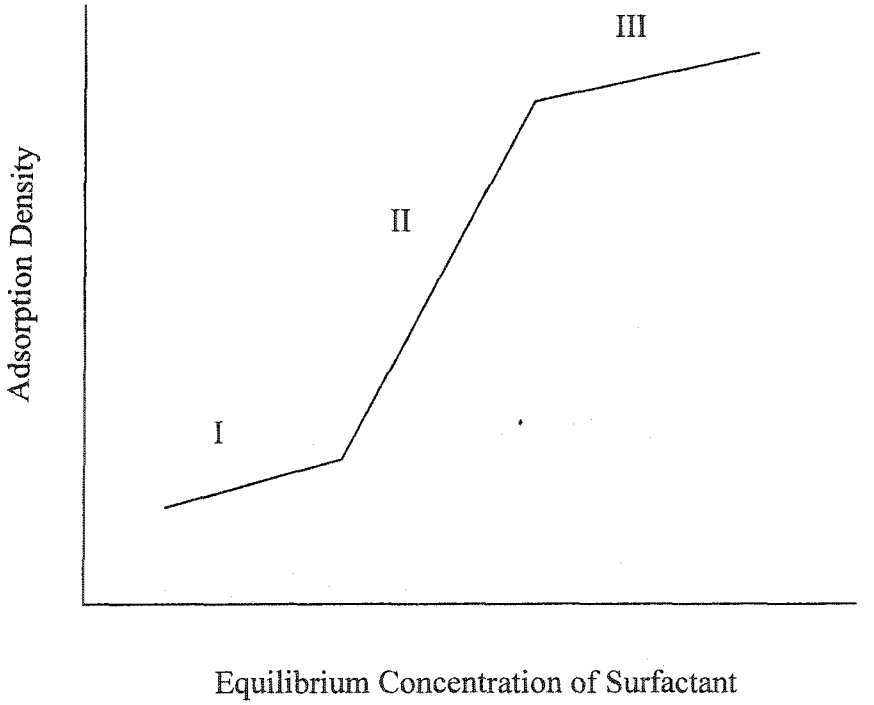
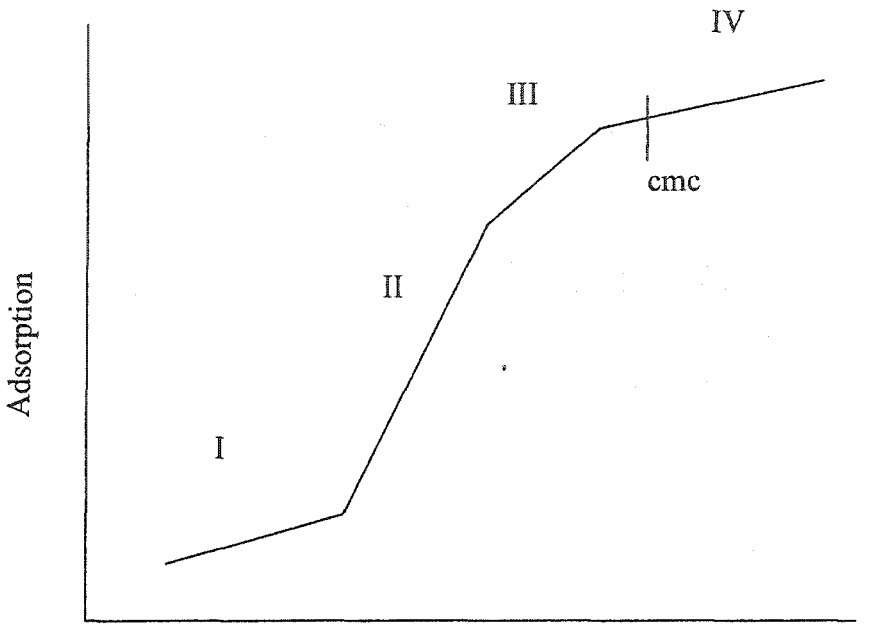


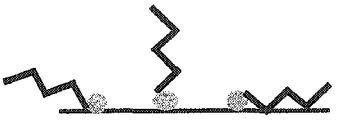
Figure 1.7. Schematic representation of adsorption density of sodium dodecylsufonate on alumina (pH 7.2, ionic strength 2 x 10^{-3}M)

Fluorescence probes were used to study the adsorption of sodium dodecyl sulfate adsorption on alumina by Chandar et al.[29] Probes enabled measurement of not only the adsorption but also the aggregation number of the hemimicelle. Four regions were observed on the isotherm (Figure 1.8). In region I, individual surfactant molecules adsorb by means of electrostatic interactions. Region II signifies the start of small size aggregates forming on the surface with a constant aggregation number although increasing number density. At the turning point from region II to III the zeta potential changes sign and surfactants begin to assume reverse orientations to hemimicelles. Region IV depicts complete bilayer coverage and zeta potential becomes more negative as more anionic head groups orient themselves towards the solution.

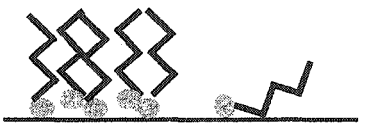
Scamehorn et al. and Harwell et al. developed a different mechanism, which they called the "bilayer model". In this approach the isotherm is broken up into four different regions (Figure 1.9). Region I represents individual sparsely adsorbed molecules. At the critical surfactant concentration, surfactant molecules form patches of bilayered aggregates (region II). In region III, surfactant bilayers are found to cover the majority of the substrate. Region IV signifies a plateau region in which bilayer coverage is complete and solution micelles begin to form.



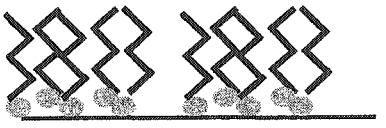
Region I:



Region II:



Region III:



Region IV:

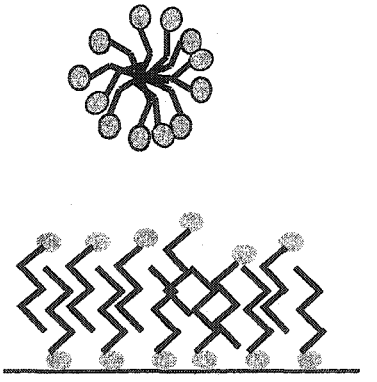
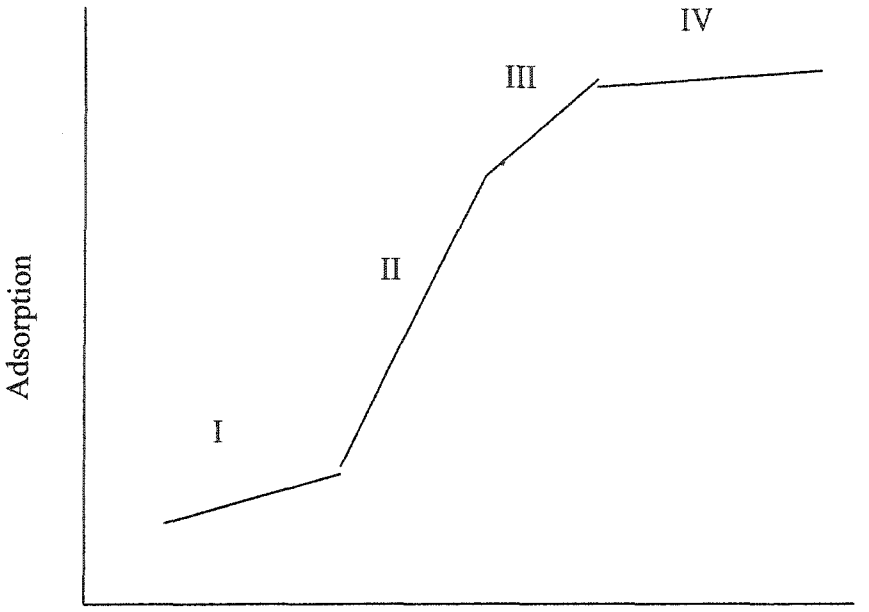


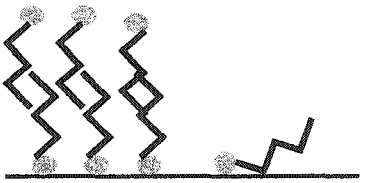
Figure 1.8. Adsorption of sodium dodecyl sulfate on alumina (pH 6.5, 0.1M NaCl)



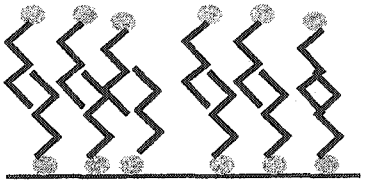
Region I:



Region II:



Region III:



Region IV:

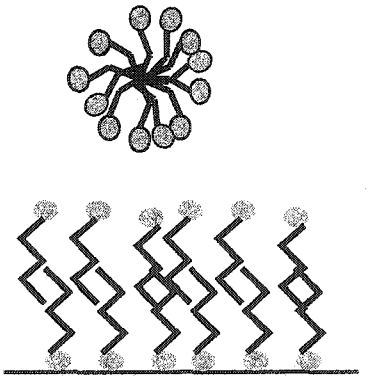


Figure 1.9. Bilayer model of adsorption onto hydrophilic solid surfaces

3. Atomic Force Microscopy for probing Surfactant Film Morphology at the Solid/Liquid Interface

Surfactant organization at solid/liquid interfaces has been extensively studied[30,31] due to practical implications in areas such as detergency, wetting, foams, emulsions, and floatation technologies. In 1995 Manne et al. provided a giant leap in our understanding of surfactant adsorption on solids by means of *in-situ* atomic force microscopy (AFM) experiments.[32] These studies indicated that surfactants often adopt periodic in-plane aggregates at the solid/liquid interface. There are some limitations inherent with these AFM studies in that one can only probe the adsorbed layer morphology on the solution side. One cannot interpret, from AFM images alone, the structure of the solid side adsorbed layer and therefore unequivocally elucidate the adsorbed structure for bi-layered aggregates. Additional *in-situ* studies delineating the structure of adsorbed surfactant aggregates have been carried out using other techniques such as ellipsometry,[33] fluorescence spectroscopy,[34] and neutron reflectivity.[35,36] A consistent picture has emerged from these investigations, implying that surfactants assemble at the surfaces of hydrophilic substrates as quasi two-dimensional analogues of morphologies observed in solution (Figure 1.10), whereas monolayers or hemi-micellar aggregates are the norm on hydrophobic surfaces (Figure 1.11).

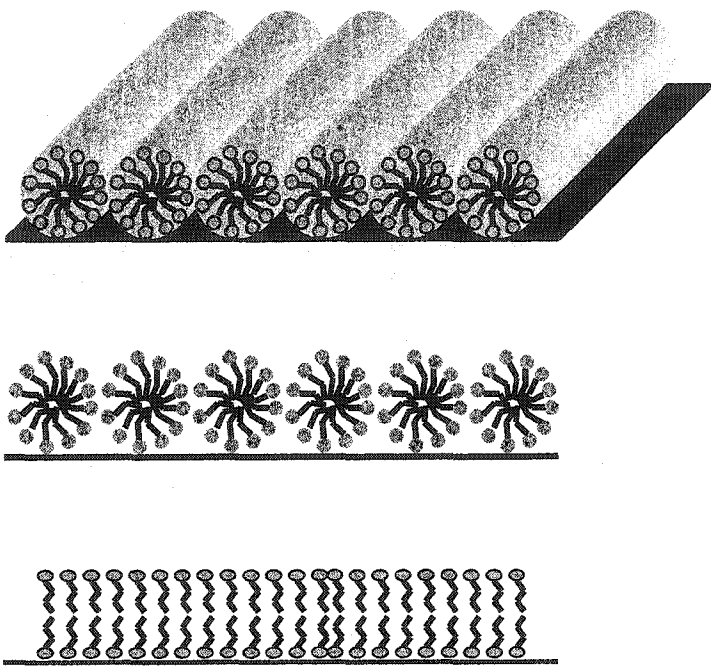


Figure 1.10. Possible adsorbed surfactant morphologies on hydrophilic surfaces

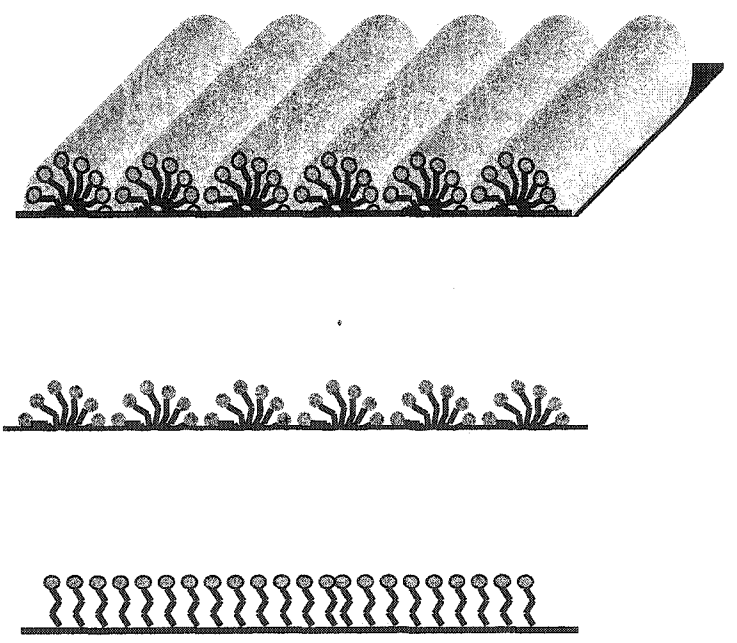


Figure 1.11. Possible adsorbed surfactant morphologies on hydrophobic surfaces

The hydrophobic model surface used for AFM investigations is typically highly ordered pyrolytic graphite (HOPG), while mica and silicon dioxide grown on single crystal silicon typically serve as hydrophilic model surfaces. All three provide *"atomically flat"* surfaces; mica and HOPG are used because one can create a fresh surface simply by cleavage; while silicon dioxide is used because of the ready availability of such surfaces due to their ubiquitous use in the semiconductor industry.

Crystalline graphite has been used to investigate the adsorption of cationic[37], anionic[38], zwitterionic[39], and non-ionic[40,41] surfactants via AFM. These studies showed that when alkyl chain lengths were equal to, or in excess of twelve carbon atoms, parallel lines, interpreted to be hemicylinders, were observed. In the specific case of sodium dodecyl sulfate (SDS), and at concentrations as low as 0.35 x critical micelle concentration (CMC), hemicylinders have been shown, by AFM, to form on graphite.[38] It has been proposed that the match between the centers of the hexagons in the graphite lattice (2.46 Å) and the distance between alternate methylene groups in the alkyl chain of the surfactant (2.51 Å) is responsible for such periodic structures on graphite.[42,43,44] Addition of small quantities of dodecanol to SDS/graphite systems induces a phase transition from hemicylinders to a planar adsorbed layer.[45] Hemicylinders

have also been reported on the hydrophobic crystal plane of MoS_2.[32] Conversely, non-crystalline graphite does not appear to induce hemicylindrical aggregate formation, rather ordinary monolayers with head groups oriented towards the solution have been observed for non-ionic[46,47] and ionic[48] surfactants.

Muscovite mica has been used extensively as a hydrophilic substrate for studying the adsorption of quaternary ammonium cationic surfactants. Variables such as alkyl chain length,[49,50] counterion type,[49] and head-group structure[49,51] have been shown to change the morphology of adsorbed micelles, mirroring tendencies observed in bulk solution. In one study, addition of alkali cations to a hexadecyltrimethylammonium/muscovite mica system caused the opposite sequence of shape transformations to that observed in bulk solution.[52] This behavior was attributed to the alkali cations occupying sites on the mica therefore reducing the availability of surface cations for surfactant and therefore increasing the aggregate curvature. Additionally, surfactants with larger head groups than trimethylammonium tend to form spheres rather than cylinders on mica,[49] and the same behavior is true for divalent or "asymmetric gemini" surfactants. Increasing alkyl chain length induces a change in micellar shape from spheres to rods in bulk systems and this same trend has been

observed for dodecyltrimetylammonium chloride and tetradecyltrimetylammonium chloride adsorbed on mica. More strongly bound counterions have been shown to stimulate cylinder formation on mica for dodecyltrimetylammonium bromide, when compared to the chloride species. Similarly the salicylate ion favors cylindrical aggregates even for large head group sphere-forming surfactants. In general, spherical, cylindrical, and bi-layer surfactant aggregates are proposed to be the norm for alkylammonium halide surfactants adsorbed on muscovite.[51,32,49,53]

II. Electrically Conducting Polymers

A. Intrinsically Conducting Polymers (ICPs)

In 1977 it was discovered that polyacetylene can be doped either chemically or electrochemically giving rise to an increase in conductivity of eleven orders of magnitude.[54] Since this discovery, many studies have been carried out to better understand and improve the conductivities and properties of this class of polymers.[55-57] The term commonly given to an organic polymer that exhibits electrical, electronic, optical, and magnetic properties of a metal is that of an intrinsically conducting polymer (ICP). Conducting polymers such as polyaniline and polypyrrole have attracted a great deal of interest as

potential chemical sensors,[58] single-molecular transistors,[59] electron emitting flat panel displays,[60] and other microelectronic devices.[61] Conducting polymers are attractive in many applications as their conductivity can be tuned by chemical manipulation of the polymer backbone, by selection of the dopant, by alteration of the doping degree, or by mixing with a matrix material producing a composite. In addition, conducting polymers offer advantages over metals and other semi-conducting materials due to their stability, ease of processing, and relatively low price.

1. *Doping*

Central to distinguishing conducting polymers from other polymers is the concept of doping.[62] Doping can take an insulating or semiconducting polymer with a small conductivity (10^{-10} to 10^{-5} S/cm) to a material having conductivity in the metallic regime (~ 1 to 10^{4} S/cm). Dramatic changes in the electronic, electrical, magnetic, optical, and structural properties are observed during this process. Polymer may be doped and undoped in a reversible process that does not harm the material. Doping is generally a redox process involving either the partial addition (reduction) or removal (oxidation) of electrons to or from the π-conjugated system in the polymer backbone. In the doping process, counter ions are incorporated into the polymer backbone to maintain charge neutrality. Doped polymers are

therefore salts. Although redox doping can be carried out for all conducting polymers, protonic acids can also be used to dope a limited number of conducting polymers.

Electrical conductivity in these polymers results from charge carriers created through doping. These charge carriers have the ability to move along the π-conjugated system. Hence, conjugated polymers are good conductors for two reasons. First, since every repeat unit along the polymer backbone is a potential site for a redox reaction, a high number of charge carriers can be created. Secondly, electrons are attracted to the nuclei of neighboring units therefore leading to charge carrier mobility along the backbone. Charge mobility can also take place in three dimensions through interchain electron transfer. Interchain electron transfer is not as efficient as intrachain transfer and hence leads to reduced charge carrier mobility which in turn reduces the conductivity. One way to reduce interchain transfer is to increase the orientation of individual chains. Therefore methods to increase the orientation of ICPs are of great interest.

2. Polyaniline

PAni can exist in three different oxidation states; leucoemeraldine, emeraldine, and pernigraniline referring to reduced, reduced/oxidized, and oxidized states respectively (Figure 1.12). Partially protonated emeraldine salt can be synthesized either electrochemically or chemically by the oxidation of aniline. Emeraldine salt can be treated with aqueous ammonium hydroxide to give the fully deprotonated emeraldine base form of PAni which, in a reversible process, can be protonated back to the salt.

Polyaniline (PAni) is an unusual polymer that has the capability of being doped by either redox or protonic acid mechanisms. Redox doping involves a change in the number of electrons in the polymer backbone whereas protonic acid doping does not. The first example of protonic acid doping was the treatment of polyaniline base with aqueous acids. Conductivity resulted in a nine to ten order of magnitude increase to produce the protonated emeraldine salt.[63,64] Protonic acid doping has since been shown effective for poly(heteroaromatic vinylenes).[65]

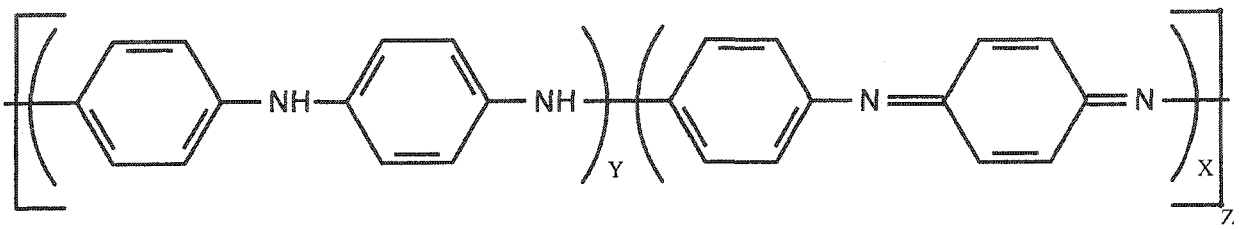


Figure 1.12. Structural formula of polyaniline:
when: x=(1-Y)=0 Leucoemeraldine (fully reduced)
x=(1-Y)=0.5 Emeraldine (half-oxidized)
x=(1-Y)=1 Pernigraniline (fully oxidized)

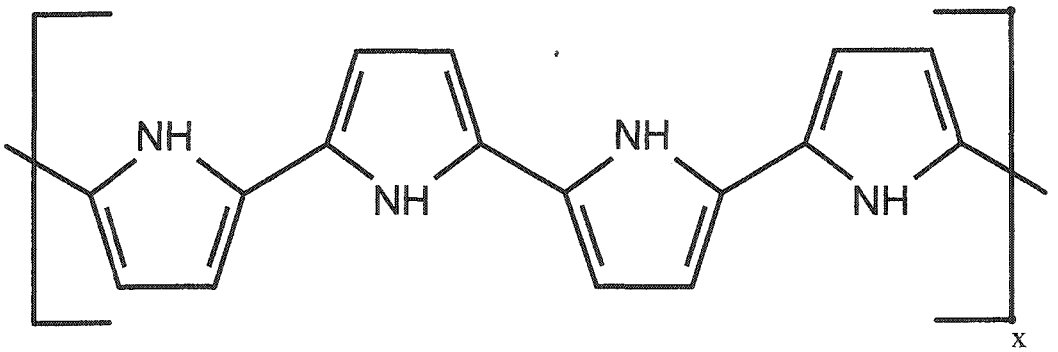


Figure 1.13. Structural formula of polypyrrole

Protonation of the emeraldine base form of PAni by aqueous acids leads to the emeraldine salt (conductive form). The positive charge in each repeat unit (from protonation) assumes a counterion to maintain charge neutrality. Typical counter ions are Cl^-, $DBSA^-$, or HSO_4^-. This transformation in conductivity is still not well understood. Although many experimental results have proven this phenomenon, no calculations are available to suggest that the emeraldine salt form is a lower energy state than the undoped state.

3. Polypyrrole

PPy (Figure 1.13) was first synthesized chemically in 1916 by the oxidation of pyrrole with peroxide.[66,67] In present day commercial applications, PPy is probably the most widely used ICP due to the long-term stability of its conductivity. Synthesis of PPy can be carried out either chemically or electrochemically. Conductive PPy can be synthesized directly in the presence of an oxidizing species such as iron (III) chloride or a persulfate salt. Under these conditions, oxidant salts serve as doping agents.

B. Electrically Conducting Composite Materials

The need to produce polymeric materials able to carry an electrical charge, as well as exhibit good mechanical properties, has led to the emergence of a class of materials called electrically conducting thermoplastic composites. In general, inherently conducting polymers (ICPs) have poor mechanical properties and therefore composite alternatives are commonplace. Polymer-matrix composites consist of filler material blended with a matrix polymer. Matrix polymer provides mechanical strength whereas fillers; which are typically low cost inorganic materials, add stiffness and reduce cost hopefully without sacrificing ultimate properties. In the case of conducting composites, conductive fillers are blended within an insulating polymeric matrix at loading fractions above the percolation threshold. Above the percolation threshold, conductive pathways have formed throughout the material able to transport charge. Such materials have advantages over other more traditional conducting materials in that they are lightweight, flexible, resist corrosion, absorb mechanical shock, offer control of conductivity, and are easily processible into complex parts.[68] Typical fillers currently used for conductive composites are powdered metals, carbon black, or ICPs.

In the past few years many investigators have attempted to improve the physical properties of PPy and PAni such as processability, stability and mechanical integrity. Recently PAni doped by organic acids, as opposed to typically used HCl, has been investigated to enhance processability and thermal limitations.[69] Therefore at present, ICPs have been used as filler material, as described earlier. Recently a three phase system of a homopolymer, "chaperone" polymer, and a π-conjugated polymer have been used to produce conductive materials with a 10 fold reduction in amount of π-conjugated polymer required to reach percolation.[70] Along with using conductive fillers, insulating fillers such as ceramics,[71] polymers,[72] alumina,[73] and glasses[74] have been modified with thin layers of conductive polymer to form conductive fillers. Surface modification of nickel flake with a thin layer of PPy has been carried out by a technique termed admicellar polymerization (AP).[75] In this study the conductivity of the composite material increased by three orders of magnitude above the percolation threshold.

III. Adsorbed Surfactant Aggregates at the Liquid/Solid Interface for Thin Film Polymerizations – Admicellar Polymerization

Solubilization and reaction within solution micelles has been studied for over 50 years. The knowledge that surfactants adsorb as aggregates at the solid/liquid interface has also been know for a long time. Since thin film fabrication of polymers onto a variety of substrates is attractive for many applications, a process in which adsorbed surfactant aggregates are used for the synthesis of adsolubilized monomer emerged in the 1980's. Adsolubilization is the term given to monomer that partitions into adsorbed surfactant aggregates and admicelle polymerization (AP) is the term given to the overall process. AP can be visualized as the surface analogue to emulsion polymerization.

AP can be represented by a four-step process, although in some cases some steps can be combined (Figure 1.14). Primarily, surfactants are used to form an adsorbed aggregate (typically a bilayer), at the surface of a hydrophilic substrate. Surfactant adsorption is then followed by the adsolubilization of a monomer into the adsorbed surfactant aggregate (surfactant adsorption and monomer adsolubilization can be performed in the same step). Polymerization of solubilized monomer is then carried out by means of a chemical initiator. After polymerization, the substrate is washed to remove excess material, i.e. surfactant, monomer, and initiator, leaving a thin layer of polymer.

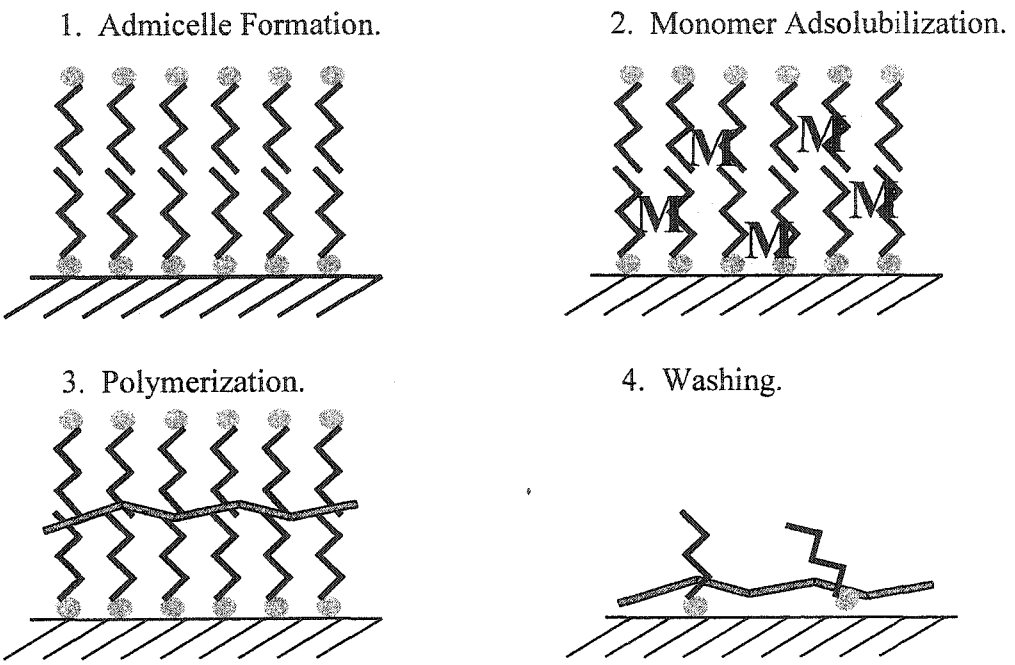


Figure 1.14. Schematic of the admicellar polymerization process.

Wu et. al. published the first two papers concerning AP.[76,77] In the first paper styrene was polymerized on alumina giving rise to a surface that was hydrophobic. Such a change in hydophobicity is one of the characteristic results of successful AP. In the second paper, kinetic measurements were made by measuring the concentration of monomer in solution and the amount of polymer on the surface. AP offers many advantages over existing methods of thin polymer film fabrication on substrates such as electrochemical synthesis[78] and layer-by-layer deposition.[79,80] A major advantage over electrochemical synthesis is that AP can be used to form thin films on non-conducting substrates and colloidal particles by careful selection of appropriate reaction conditions. Layer-by-layer deposition is limited to soluble polymers as a polymer is first dissolved in a solvent and then mechanically deposited onto a substrate by sequential induction and extraction through an interface. AP is not limited to soluble polymers.

Thin polymer films of polypyrrole (PPy) have been successfully fabricated on surfaces such as alumina,[81,82,83] mica,[83] and HOPG[84] using AP. AFM has been used to characterize the structure of PPy films synthesized on alumina,[83] mica,[83] and HOPG.[84] These studies show that thin (30-60 nm) PPy films, with high a degree of structural integrity, can be fabricated on a variety of substrates.

Thin films of PAni and PPy have been synthesized on alumina using sodium doedcyl sulfate (SDS) and sodium dodecylbenzene sulfonate (SDBS) as templates. These films showed an increase in eight orders of magnitude in conductivity in comparison to bare alumina. Thin PPy films have also been rendered on alumina by a similar procedure to admicelle polymerization although hexanoic acid was used as the surface-active species instead of surfactant.[85]

Chapters 5 and 6 show that the morphology of PPy and polyaniline (PAni) synthesized on highly oriented pyrolytic graphite can be controlled. The morphology of most interest is the analogue of the surfactant hemicylinders described previously, because of possible uses of these 1-Dimensional (1-D) nanotubes/wires of electrically conducting polymers as electronic junctions and other devices. To this end the following section is a brief review of other techniques currently available to synthesize 1-D nanotubes/wires of ICPs. Not surprisingly, surfactant molecules have a prominent role in most of these synthetic procedures.

IV. Surfactant Aggregates for the Synthesis of 1-D Nanostructures of Electrically Conducting Polymers

As the desire for smaller components heightens, techniques to fabricate materials and building blocks for materials that take advantage of the nanorealm continue to proliferate. Since the discovery of carbon nanotubes in 1991,[86] nanoscale objects fabricated from various compounds with various shapes have emerged. Although many synthetic techniques have surfaced to fabricate materials with nanoscale dimensions, there is a significant need to then arrange these materials into active and useful materials. Due to the requirement of smaller components for microelectronics, electrically conducting polymers have captured interest as materials of which nanoscale objects would be highly desirable. In addition, ICPs are known to increase in conductivity in conjunction with molecular alignment, therefore a number of techniques have arisen to synthesize 1-D nanostructures of conducting polymers. In the next few paragraphs techniques in which surfactants are used to synthesize 1-D nanoscale structures of electrically conducting polymers both in solution and on surfaces will be reviewed.

Since conventional lithographic techniques cannot be applied to produce conducting lines in the sub 100nm regime, the ability to render high quality 1-D wires of π-conjugated polymers with these dimensions is of great interest. Additionally, since the conductivity of π-conjugated polymers is dictated in part

by molecular alignment, and the radius of gyration of polymers is generally in the tens of nanometer range; 1-D nanostrutures of π-conjugated polymer would likely afford elevated conductivities. Although other methods do exist, techniques to fabricate 1-D nanostructures of conducting polymers evolve from the use of templates in the form of either solid materials or self-assembled molecules in solution. Both approaches have been successfully carried out using surfactant molecules as either a way to fabricate the solid template, or as promoters for self-assembly of monomer or polymer.

A. *1-D Π-Conjugated Polymer Nanostructures Synthesized using "Solid" Templates*

Given the high degree of order and periodicity of surfactant aggregates in solution and at interfaces, techniques using these structures as templates for ordered materials have surfaced. In 1992, Mobil researchers discovered that surfactant self-assembly in aqueous solutions of soluble silica resulted in the spontaneous co-assembly of silica-surfactant mesophases.[87] Subsequent removal of the surfactant renders imprints of the liquid-crystalline assembly in the form of an inorganic fossil. Following this discovery, pioneering work has been expanded to produce a wide compositional range of mesoporous solids in which the nanoscale pore size can be adjusted by a variety of surfactant systems.[88]

In order to render 1-D nanostructures of π-conjugated polymers one must have the ability to template the shape of the polymer product. Templates are typically in the form of preformed channels in solid materials or organized molecules in bulk solution. Representative materials used as solid templates are "track-etched" polymeric membranes, porous aluminas, and aluminosilicates such as MCM-41. Aluminosilicates are fabricated from the arrangement of silica/surfactant assemblies. Such materials all offer a narrow diameter confined channel in which 1-D structures can be synthesized.

In 1994 aluminosilicate MCM-41 templates were used to form polyaniline (PAni) nanofibers with diameters as small as 3 nm.[89] Figure 1.15 shows a generalized schematic of the template procedure. Since the discovery that the pores of membranes could be used to morphologically control the growth of 1-D polymer structures, polymeric nanotubes/fibers with controllable diameters have been synthesized using other nanoporous membrane materials.[90-93] Martin observed that when synthesizing PAni and PPy using the pores of track-etched polycarbonate membranes (not surfactant fabricated membranes), the polymer preferentially nucleates and grows on the pore walls.[94] This phenomenon can be explained in part by the polycationic forms of these polymers being solvophobically driven to the walls of the pores. This

driving force is coupled with electrostatic forces between the cationic polymer and the anionic sites on the pore wall. In general, when a "molecular anchor" exists for the material being deposited, hollow tubules are favored over solid fibers. Polyacetylene fibers synthesized within the pores of a template showed enhanced conductivities in comparison to bulk materials.[95] The reason for an elevation in conductivity of 1-D polymeric materials was found to be due to a superior molecular ordering of polymer chains owing to synthesis taking place in a confined environment.

Although membranes offer a route to 1-D nanostructures of conjugated polymers, a limitation inherent to the membrane synthesis technique is that post-synthesis steps are necessary to remove the polymer from the template. This process usually entails dissolving the template thereby releasing the polymer, which can unfortunately lead to damage or undesirable bundling of the product.[96]

In a similar technique, composite materials of conjugated polymer and silicas have been synthesized using a sol-gel based method. In this approach polymerizable diacetylenic surfactants are used as template molecules for the fabrication of conjugated nanofibers in the form of a polymer/silica nanocomposite material.[97-100] In this approach silica channels are formed and

packed with monomer simultaneously which in turn gives better filling of the channels as compared to post-loading approaches. More recently this same technique has been employed using pyrrole-containing surfactants which self-organize and are then polymerized to form PPy/silica nanocomposites.[101]

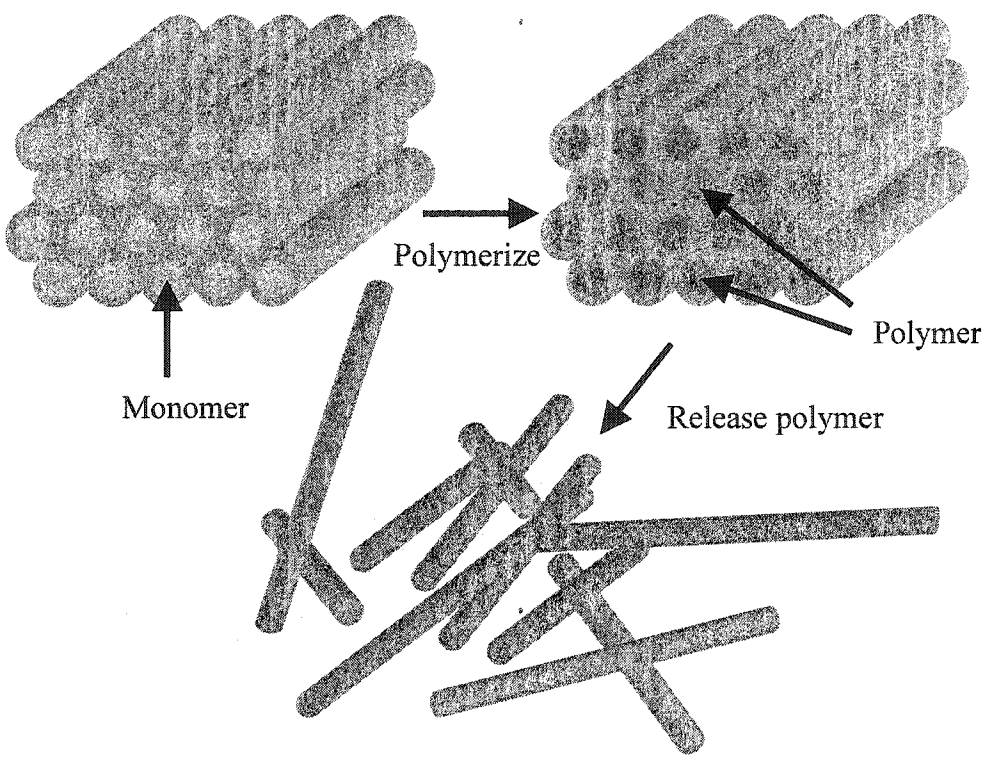


Figure 1.15. Solid template method for the fabrication of 1-D conducting polymer structures.

B. *1-D Π-Conjugated Polymer Nanostructures using Molecular Interactions as "Soft" Templates*

In a contrasting approach in which no solid support is required, 1-D polymer nanostructures can be fabricated by self-assembly. Through self-assembly, monomer aggregates with another molecule (usually a "surfactant-like" amphiphilic molecule) to form a cylindrical assembly which is subsequently polymerized retaining the fibril morphology in the polymer product. In 1999, Wan et al. developed a "template-free"[102] method to synthesize microtubes of PAni[103] and PPy[104] using β-naphthalene sulfonic acid (β-NSA) to control the polymer morphology and act as a dopant molecule. Subsequently, nanotubes of PAni with diameters in the range of 76 – 650 nm have been produced by this same technique and the formation mechanism has been attributed to a reaction between the basic aniline and acidic β-NSA to form an insoluble 1-D salt.[105] This salt then acts as a template in the formation of the PAni nanotubes/fibers (Figure 1.16). Interestingly in this work it was found that the diameter of the PAni structures could be controlled by the ratio of β-NSA to aniline. When the ratio was around 2, microtubules (diameter > 100 nm) were formed but when the ratio was reduced to ½ or ¼ nanotubes (diameter < 100 nm) were favored. Since then many other organic acids have been used to fabricate 1-D nanostructures of PAni. PAni nanotubes have been synthesized in the presence of D-10-camphorsulfonic acid,[106] (4-{n-[4-(4-

Nitrophenylazo)phenyloxy]alkyl}aminobenzene sulfonic acid),[107] azobenzenesulfonic acid,[108] 5-aminonaphthalene-2-sulfonic acid,[109] a sulfonated dendrimer PAMAM4.0[naphthyl(SO_3H)$_2$]$_{24}$ and hydrogensulfated fullerenol $C_{60}(OSO_3H)_6$.[110] In all cases the chosen molecule acts as a protonic acid dopant and templating agent.

In other work, surfactants along with various inorganic acids were used to form PAni nanostructures in which the morphology, size and electrical properties were dependent on the reaction conditions and dopant.[111] PAni nanofibers with diameters of 30 - 50 nm and lengths from 500 nm to several microns have been synthesized using camphorsulfonic acid at the interface between an organic and aqueous phase.[112] The dedoped nanofibers were shown to have much faster response to doping/dedoping than conventional undoped PAni films. In other work, organic acids such as β-NSA or p-toluenesulfonic acid, have been used to prepare Ppy micro/nanotubes with diameters of 50 – 2000 nm and high conductivities.[113] Once again the properties of the polymer can be controlled by the polymerization method and conditions, or by the dopant. In a surfactant based method, PPy nanotubes with diameters < 100 nm have been successfully fabricated by a technique that uses a reverse microemulsion (Figure 1.17).[114]

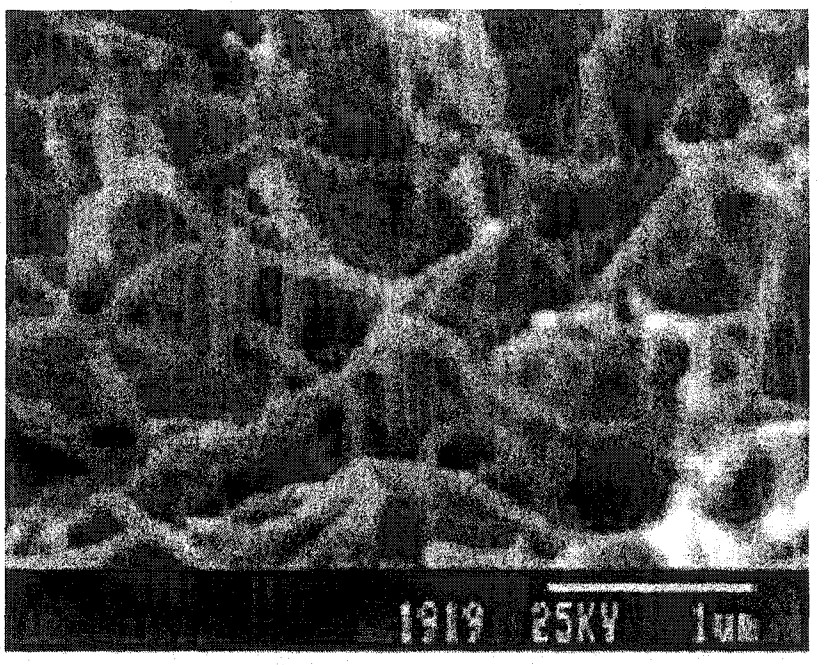


Figure 1.16. SEM image of polyaniline nanotubes (92 nm average diameter), synthesized in the presence of β-naphthalene sulfonic acid.[105]

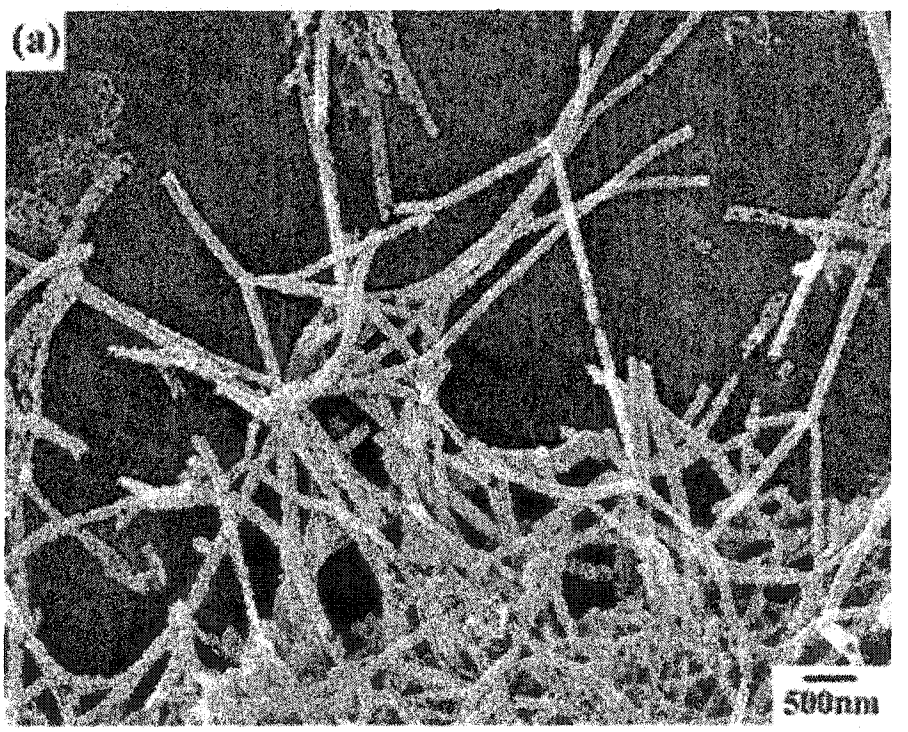


Figure 1.17. FE-SEM image of polypyrrole nanotubes (95 nm diameter), synthesized by reverse microemulsion polymerization using surfactant molecules as templates.[114]

The microemulsion method employs reverse micelles that form in apolar solvents with surfactant headgroups oriented away from the solvent. Upon addition of iron chloride, the morphology of the reverse micelles is transitioned into cylindrical micelles which can then be used as nanoreactors to carry out the controlled synthesis of a partitioned monomer (Figure 1.18). All of the aforementioned studies incorporate a polymerization step in the formation of the 1-D structure.

Preformed polymers have also been shown to self-assemble into hierarchical structures, including nanoscale polymeric cylindrical structures due to molecular interactions such as hydrogen bonding and recognition.[115] Comb-shaped polymers are a class of polymer that consists of amphiphilic molecules that are either covalently or physically bonded to the polymer backbone. Interactions between the polymer backbone and appendage molecules control the self-assembled structure. Conjugated polymers, or rigid polymers, can be decorated with amphiphiles to form so called "hairy rod" polymers, which in turn form self-organized structures. For example, high molecular weight dedoped PAni has been doped with camphorsulfonic acid (CSA) and then mixed with 4-hexylresorcinol (Hres). Hydrogen bonding between all three molecules induces self-organization into PAni cylinders with a repeat distance of 3.5 nm.[116-118] The conductivity of this material has been investigated and

found to increase by 2 orders of magnitude when cylindrical structures were present. Once again this elevation in conductivity has been attributed to the confinement of PAni chains within the cylinders.

Here we have endeavored to give an overview of techniques currently available to synthesize 1-D nanostructures of electrically conducting polymers in which surfactants are used. The drive for the fabrication of 1-D nanostructures of conjugated polymers continues to thrive with many approaches being reported recently in the literature. There is still the need for simple techniques that not only produce high quality nanomaterials with controllable dimensions and therefore properties, but also to then arrange these building blocks into architectures to make viable components or products. The field of nanotechnology is still in its infancy although has made huge strides over the last few years. The opportunities are endless for making exhilarating discoveries and inventing new devices and technologies based on materials having these dimensions.

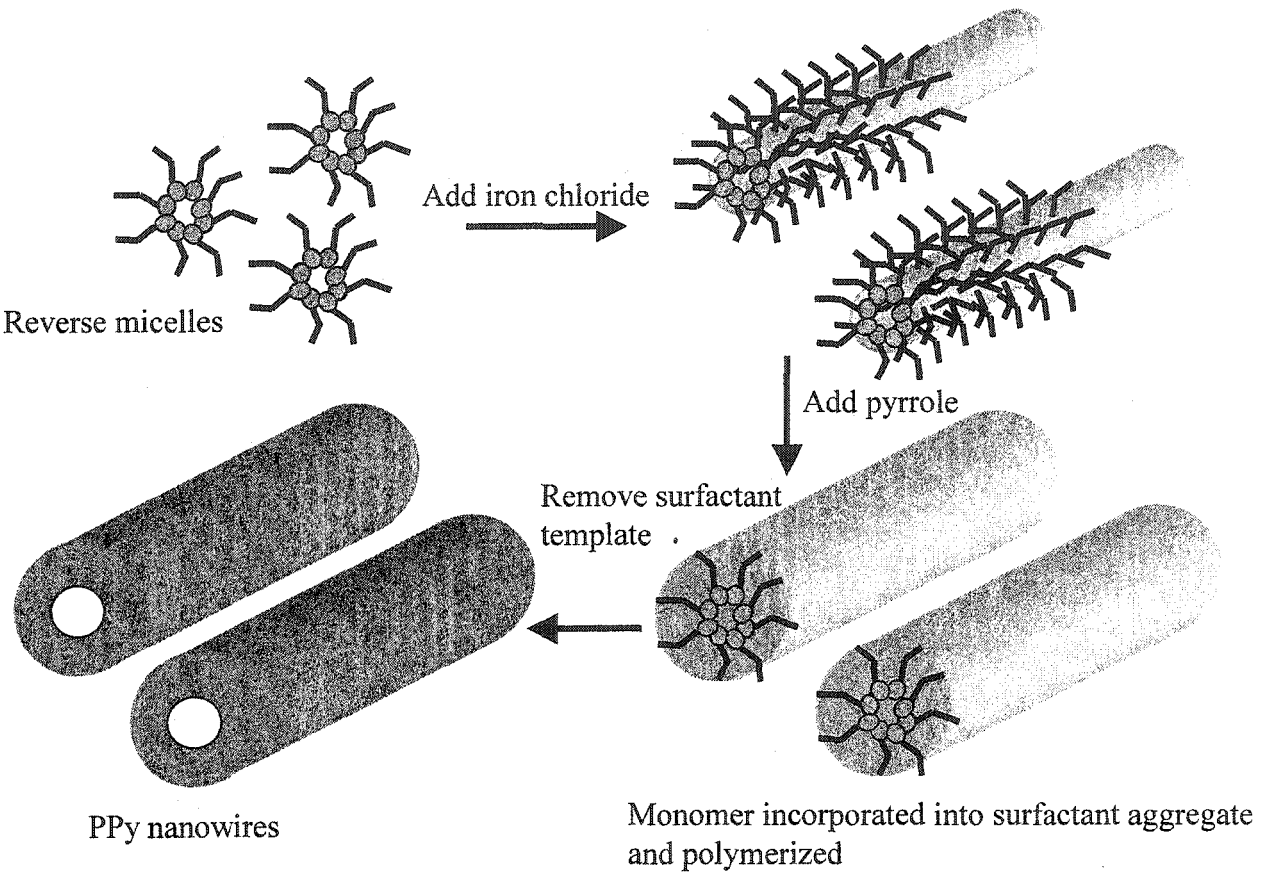


Figure 1.18. A schematic of the reverse microemulsion technique identifying four stages. In the first stage, reverse micelles form in an apolar solvent. These speherical micelles are then transitioned into cylindrical micelles by the addition of iron chloride in a second stage. Pyrrole then partitions around the cylindrical structure before being polymerized in the third step. Finally, the surfactant is removed, leaving Ppy nanotubes.

In Chapter 2, experimental details will be discussed for subsequent Chapters. Chapter 3 concerns work in which the cmc has been measured in the presence of surfactant adsorbing inorganic particulates. In Chapter 4, adsorbed surfactant aggregates are used in the synthesis of thin films of polypyrrole (PPy) and polyaniline (PAni) on the surface of alumina particles. Chapter 5 reports the use of adsorbed surfactant templates in the synthesis of morphologically controlled PPy and PAni films on highly oriented pyrolytic graphite (HOPG). In an extension to this work, Chapter 6 involves additional experiments in which PPy and PAni films are synthesized on silicon dioxide, mica, and HOPG using surfactant templates. In Chapter 7, conclusions and recommendations are discussed.

V. References

[1] Puvvada, S.; Blankschtein, D. J. *J. Chem. Phys.* **1990**, 92, 3710.

[2] Briganti, G. Puvvada, S.; Blankschtein, D. J. *J. Phys. Chem.* **1991**, 95, 8989.

[3] Carale, T. R.; Blankschtein, D. J, *J. Phys. Chem.* **1992**, 96, 459.

[4] Tanford, C. '*The Hydrophobic Effect: Formation of Micelles and Biological Membranes*', *2nd ed.*; Wiley-Interscience: New York, **1980**.

[5] Mukerjee. P.; Mysels, K. J. *Critical Micelle Concentrations of Aqueous Surfactant Systems*, NSRDS-NBS 36, U.S. Dept. of Commerce, Washington DC, **1971**.

[6] Corrin, M. L.; Harkins, W. D. *J. Am. Chem. Soc.* **1947**, 69, 684.

[7] Rosen M. J. *Surfactants and Interfacial Phenomena*, 2nd Ed., Wiley: New York, 1989.

[8] Greiss, W. *Fette Seifen*, Anstrichm **1955**, 57, 24, 168, 236.

[9] Götte, E.; Schwuger, M. J. *Tenside* **1969**, 3, 131.

[10] Zana, R. J. *J. Colloid Interface Sci* **1980**, 78, 330.

[11] Schick, M. J.; Gilbert, A. H. *J Colloid Sci.* **1965**, 20, 464.

[12] Flockhart, B. D. *J. Colloid Sci.* **1961**, 16, 484.

[13] Crook, E. H.; Fordyce, D. B.; Trebbi, G. F. *J. Phys. Chem.* **1963**, 67, 1987.

[14] Klevens, H. B. *J. Am. Oil Chem. Soc.* **1953**, 30, 74.

[15] Israelachvili, J.; Mitchell, D. J.; Ninham, B. W. *J. Chem. Soc. Faraday Trans. 2* **1976**, 72, 1525.

[16] Nagarajan, R. *Langmuir* **2002**, 18, 31.

[17] Underwood, L; Anaker, E. W.; *J. Colloid Interface Sci.* **1985**, 106, 86.

[18] Sepulveda, L.; Cortes, J. *J. Phys. Chem.* **1985**, 89, 5322.

[19] Bijma, K.; Blandamer, M. J.; Engberts, J. B. F. N. *Langmuir* **1998**, 14, 79.

[20] Kern, F.; Zana, R.; Candau, S. *Langmuir* **1991**, 7, 1344.

[21] Rehage, H.; Hoffmann, H. J. *J. Phys. Chem.* **1988**, 92, 4712.

[22] Kaler, E. W.; Herrington, K. L.; Murthy, A. K.; Zadadzinski, J. A. N. *J. Phys. Chem.* **1992**, 96, 6698.

[23] Hoffmann, H.; Bayer, O.; Ulbricht, W.; Thurn, H. *Adv. Colloid Interface Sci.* **1986**, 26, 177.

[24] Adamson, A. W. *Physical Chemistry of Surfaces*, 3rd ed., Interscience, New York, **1976**, pp. 197ff.

[25] Gaudin, A. M.; Fuerstenau, D. W. *Trans. AIME* **1955**, 202, 66.

[26] Gaudin, A. M.; Fuerstenau, D. W. *Trans. AIME* **1955**, 202, 958.

[27] De Bruyn, P. L. *Trans. AIME* **1955**, 202, 291.

[28] Somasundaran, P. Fuerstenau, D. W. *J. Phys. Chem.* **1966**, 70, 90.

[29] Chandar, P.; Somasundaran, P.; Turro, N. J. *J. Coll. Interface Sci.* **1987**, 117, 31.

[30] Tiberg, F.; Brinck, J.; Grant, L. *Curr. Op. Colloid Interface Sci.* **2000**, 4, 411.

[31] Warr, G. G. *Curr. Op. Colloid Interface Sci.* **2000**, 5, 88.

[32] Manne, S.; Gaub, H. E. *Science* **1995**, 270, 1480.

[33] Tiberg, F.; Landgren, M. *Langmuir* **1997**, 9, 927.

[34] Levitz P.; Van Damme, H.; Keravis, D. *J. Phys. Chem.* **1984**, 88, 2228.

[35] Lee, E. M.; Thomas, R. K.; Cummins, P. G.; Staples, E. J.; Panfold, J.; Rennie, A. R. *Chem. Phys. Lett.* **1989**, 162, 196.

[36] Cummins, P. G.; Staples, E,; Panfold, J. *J. Phys. Chem.* **1990**, 94, 3740.

[37] Manne, S.; Cleveland, J. P.; Gaub, B. E.; Stucky, G. D.; Hansma, P. K. *Langmuir* **1994**, 10, 4409.

[38] Wanless, E. J.; Ducker, W. A. *J. Phys. Chem* **1996**, 100, 3207.

[39] Ducker, W. A.; Grant, L. M. *J. Phys. Chem.* **1996**, 100, 11507.

[40] Patrick, H. N.; Warr, G. G.; Manne, S.; Aksay, I. A. *Langmuir* **1997**, 13, 4349.

[41] Holland, N. B.; Ruegsegger, M.; Marchant, R. E. *Langmuir* **1998**, 14, 2790.

[42] Groszek, A. J. *Proc. R. Soc. London Ser. A* **1970**, 314, 473.

[43] Yeo, Y. H.; Yackoboski, K.; McGonigal, G. C.; Thompson, D. J. *J. Vac. Sci. Technol. A* **1992**, 10, 600.

[44] Rabe, P.; and Buchholz, S. *Science* **1991**, 253, 424.

[45] Wanless, E. J.; Davey, T. W.; Ducker, W. A. *Langmuir* **1997**, 13, 4223.

[46] Fragneto, G.; Lu. J. R. McDermott, D. C.; Thomas, R. K. *Langmuir* **1996**, 12, 477.

[47] Tiberg, F. *J. Chem. Soc. Faraday Trans.* **1996**, 92, 531.

[48] Király, Z.; Findenegg, G. H. *J. Phys. Chem. B* **1998**, 102, 1203.

[49] Patrick, H. N.; Warr, G. G.; Manne, S.; Akşay, I. A. *Langmuir* **1999**, 15, 1685.

[50] Liu, J. F.; Ducker, W. A. *J. Phys. Chem. B* **1999**, 103, 8558.

[51] Manne, S.; Schäffer, T. E.; Huo, Q.; Hansma, P. K.; Morse, D. E.; Stucky, G. D.; Aksay, I. A. *Langmuir* **1997**, 13, 6382.

[52] Lamont, R. E.; Ducker, W. A. *J. Am. Chem. Soc.* **1998**, 120, 7602.

[53] Fujii, M.; Li, B.; Fukada, K.; Kato, T.; Seimiya, T. *Langmuir* **2001**, 17, 1138-1142.

[54] Chiang, C. K.; Fincher, C. R., Jr.; Park, Y. W.; Heeger, A. J.; Shirakawa, H.; Louis, E. J.; MacDiarmid, A. G. *Phys. Rev. Lett.* **1977**, *39*, 1098.

[55] MacDiarmid, A. G. *Angew. Chem. Int. Ed.* **2001**, 40(14), 2581.

[56] Shirakawa, H. *Angew. Chem. Int. Ed.* **2001**, 40(14), 2574.

[57] Heeger, A. J. *Angew. Chem. Int. Ed.* **2001**, 40(14), 2591.

[58] Kong, J.; Franklin, N. R.; Zhou, C.; Chapline, M. G. Peng, S.; Cho, K.; Dai, H. *Science* **2000**, 287, 622.

[59] Yao, Z.; Postma, H. W. Ch.; Balents, L.; Dekker, C. *Nature* **1999**, 402, 273.

[60] Normile, D. *Science* **1999**, 286, 2056.

[61] Skotheim, T. A.; Elsenbaumer, R. L.; Reynolds, J. H. Conducting Polymers in Microelectronics. Handbook of Conducting Polymers, 2nd ed.; Dekker: New York, 1998; Chapter 32, 921.

[62] (a) Chiang, C. K.; Fincher, C. R., Jr.; Park, Y. W.; Heeger, A. J.; Shirakawa, H.; Louis, E. J.; MacDiarmid, A. G. *Phys. Rev. Lett.* **1977**, *39*, 1098. (b) Chiang, C. K.; Drury, M. A.; Gau, S. C.; Heeger, A. J.; Louis, E. J.; MacDiarmid, A. G. *J. Am. Chem. Soc.* **1978**, 100, 1013.

[63] Chiang, J. C.; MacDiarmid, A. G. *Synth. Met.* **1986**, 13, 193.

[64] MacDiarmid, A. G.; Chiang, J. C.; Richter, A. F.; Epstein, A. J. *Synth. Met.* **1987**, 18, 285.

[65] Han, C. C.; Elsenbaumer, R. L. *Synth. Met.* **1989**, 30, 123.

[66] Angeli, A. *Gazz. Chim. Ital.* **1916**, 46, 279.

[67] Angeli, A.; Alessandri, L. *Gazz. Chim. Ital.* **1916**, 46, 283.

[68] Norman, R. H. *"Conductive rubbers and plastics" (Elsevier New York)* **1970**, p. 3.

[69] Byun, S. U.; Im, S. S. *J. Appl. Polym. Sci.* **1995**, 56, 425.

[70] Mezzenga, R.; Ruokolainen, J.; Fredrickson, G. H.; Kramer, E. J.; Moses, D.; Heeger, A. J.; Ikkala, O. *Science* **2003**, 299, 1872.

[71] Mehrotra, V.; Giannelis, E. P. *Solid State Commun.* **1991**, 77, 155.

[72] (a) Armes, J. P.; Aldissi, M.; Agnew, S. F.; Gottesfeld, S. *Langmuir* **1990**, 6, 1745. (b) Ruckenstein, E.; Chen, J.-H. *J. Appl. Polym. Sci.* **1991**, 43, 1209. (c) Simmons, M. R.; Charloner, P. A.; Armes, S. P. *Langmuir* **1998**, 14, 611.

[73] Cho, G.; Glatzhofer, D. T.; Fung, B. M.; Yuan, W. –L.; O'Rear, E. A. *Langmuir* **2000**, 16, 4424.

[74] Mehrotra, V.; Keddie, J. L.; Miller, J. M.; Giannelis, E. P. *J. Non-Cryst. Solids* **1991**, 136, 97.

[75] Genetti, W. B.; Yuan, W. L.; Grady, B. P.; O'Rear, E. A.; Lai, C. L. *J. Mater. Sci.* **1998**, 33, 3085-3093.

[76] Wu, J.; Harwell, J. H.; O'Rear, E. A. *Langmuir* **1987**, 3, 531.

[77] Wu, J.; Harwell, J. H.; O'Rear, E. A. *J Phys Chem* **1987**, 91, 623.

[78] (a) Berlot, I.; Labbé, P.; Moutet, J.-C. *Langmuir* **2000,** *16,* 5814. Shimoda, S.; Smela, E. *Electrochim. Acta* **1998,** *44,* 219. (b) Barr, G. E.; Sayre, C. N.; Connor, D. M.; Collard, D. M. *Langmuir* **1996,** *12,* 1395. (c) Kaplin, D. A.; Qutubuddin, S. *Polymer* **1993,** *36,* 1275. (d) Sasano, K.; Nakamura, K.; Kaneto, K. *Jpn. J. Appl. Phys. Part 2* **1993,** *32,* 863.

[79] Decher, G.; Hong, J. D.; Schmitt, J. *Thin Solid Films* **1992,** *210/211,* 831.

[80] Shimazaki, Y.; Mitsuishi, M.; Ito, S.; Yamamoto, M. *Langmuir* **1997,** *13,* 1385.

[81] Funkhouser, G. P.; Arévalo, M. P.; Glatzhofer, D. T.; O'Rear, E. A. *Langmuir* **1995**, 11, 1443.

[82] Cho, G.; Glatzhofer, D. T.; Fung, B. M.; Yuan, W. –L.; O'Rear, E. A. *Langmuir* **2000**, 16, 4424.

[83] Yuan, W. L.; O'Rear, E. A.; Cho, G.; Funkhouser, G. P.; Glatzhofer, D. T. *Thin Solid Films* **2001**, 385, 96-108.

[84] Yuan, W. L.; O'Rear, E. A.; Grady, B. P.; Glatzhofer, D. T. *Langmuir* **2002**, 18, 3343.

[85] Gyoujin, C.; Glatzhofer, D. T.; Fung, B. M.; Yuan, W.-L.; O'Rear, E. A. *Langmuir* **2000**, 16, 4424-4429.

[86] Iijima S. Helical microtubules of graphitic carbon. Nature **1991**, *354*, 56-58.
[87] Kresge, C.; Leonowicz, M.; Roth, W.; Vartuli, C.; Beck, J. *Nature* **1992**, 359, 710.

[88] (a) Hou, Q.; Margolese, D.; Ciesla, U.; Feng, P.; Gier, T. G.; Sieger, P.; Leon, R.; Petroff, P. M.; Schuth, F.; Stucky, G. *Nature* **1994**, 368, 317. (b) Firouzi, A.; Kumar, D.; Bull, L. M.; Besier, T.;Sieger, P.; Huo, Q.; Walker, S. A.; Zasadzinski, J. A.; Glinka, C.; Nicol, J.; Margolese, D.; Stucky, G. D.; Chmelka, B.F. *Science* **1995**, 267, 1138. (c) Tanev, P. T.; Pinnavaia, T. J. *Science* **1995**,

267, 865. (d) Antonelli, D. M.; Ying, J. M. *Angew. Chem. Int. Ed. Engl.* **1995**, 34, 2014. (e) Zhao, D.; Feng, J.; Huo, Q.; Nelosh, N.; Fredrickson, G.; Chmelka, B.; Stucky, G. D. *Science* **1998**, 279, 548.

[89] Wu, C.-G.; Bein, T. *Science* **1994**, 264, 1757.

[90] Martin, C. R. *Science* **1994**, 266, 1961.

[91] Parthsarathy, R. V.; Martin C. R. *Chem. Mater.* **1994**, 6, 1627.

[92] Cai, Z.; Lei, J.; Liang, W.; Menon, V.; Martin, C. R. *Chem. Mater.* **1991**, 3, 960.

[93] Martin, C. R.; Parthasarathy, R.; Menon, V. *Synth. Met.* **1993**, 55, 1165.

[94] Martin, C. R. *Science* **1994**, 266, 1961.

[95] Liang, W.; Martin, C. R. *J. Am. Chem. Soc.* **1990**, 112, 9666.

[96] Duchet, J. Legras, R.; Demoustier-Champagne, S. *Synth. Met.* **1998**, 98(2), 113.

[97] Aida, T.; Tajima, K. *Angew. Chem.* **2001**, 113(20), 3919.

[98] Aida, T.; Tajima, K. *Angew. Chem. Int. Ed.* **2001**, 40(20), 3803.

[99] Lu, Y.; Yang, Y.; Sellinger, A.; Lu, M.; Huang, J.; Fan, H.; Haddad, R.; Lopez, G. Burns, A. R.; Sasaki, D. Y.; Shelnutt, J.; Brinker, C. J. *Nature* **2001**, 410, 913.

[100] Yang, Y.; Lu. Y.; Lu. M.; Huang, J.; Haddad, R.; Xomeritakis, G.; Liu, N.; Malanoski, A. P.; Sturmayr, D.; Fan, H.; Sasaki, D. Y.; Assink, R. A.; Shelnutt, J. A.; van Swol, F.; Lopez, G. P.; Burns, A. R.; Brinker, C. J. *J. Am. Chem. Soc.* **2003**, 125, 1269.

[101] Ikegame, M.; Tajima, K.; Aida, T. *Angew. Chem. Int. Ed.* **2003**, 42, 2154.

[102] The term "template free" is a misnomer, as described below. A more precise term would be "hard-template free".

[103] Huang, J.; Wan, M. *J. Polym. Sci. Part A* **1999**, 37, 151.

[104] Shen, Y.; Wan, M. *J. Polym. Sci. Part A* **1999**, 37(10), 1443.

[105] Wei, Z.; Zhang, Z.; Wan, M. *Langmuir* **2002**, 18, 917.

[106] Zhang, L.; Wan, M. *Nanotechnology* **2002**, 13, 750.

[107] Qiu, H.; Wan, M. *J. Polym. Sci. Part A* **2001**, 39, 3485.

[108] Huang, K.; Wan, M. Synth. Met. **2003**, 135-136, 173.

[109] Wei, Z.; Wan, M. *J. Appl. Poly. Sci.* **2003**, 87, 1297.

[110] Qiu, H.; Wan, M.; Matthews, B.; Dai, L. *Macromolecules* **2001**, 34, 675.

[111] Zhang, Z.; Wei, Z.; Wan, M. *Macromolecules* **2002**, 35, 5937.

[112] Huang, J.; Virji, S.; Weiller, B. H.; Kaner, R. B. *J. Am. Chem. Soc.* **2003**, 125, 314.

[113] Yang, Y.; Liu, J.; Wan, M. *Nanotechnology* **2002**, 13, 771.

[114] Jang, J.; Yoon, H. *Chem. Commun.* **2003**, 6, 720.

[115] Ikkala, O.; Brinke, G. T. *Science* **2002**, 295, 2407.

[116] Kosonen, H.; Ruokolainen, J.; Knaapila, M.; Torkkeli, M.; Jokela, K.; Sermiaa, R.; Brinke, G. T.; Bras, W.; Monkman, A. P.; Ikkala, O. *Macromolecules* **2000**, 33, 8671.

[117] Kosonen, H.; Ruokolainen, J.; Knaapila, M.; Torkkeli, M.; Sermiaa, R.; Bras, W.; Brinke, G. T.; Ikkala, O. *Synth. Met.* **2001**, 121, 1277.

[118] Kosonen, H.; Valkama, S.; Ruokolainen, J.; Knaapila, M.; Torkkeli, M.; Sermiaa, R.; Monkman, A. P.; Brinke, G. T.; Ikkala, O. *Synth. Met.* **2003**, 137, 881.

Chapter 2. Experimental

I. CMC Determination in the Presence of Surfactant Adsorbing Inorganic Particulates

A. Materials

Al_2O_3 with surface area 97 m^2/g and nominally non-porous TiO_2, surface area 52 m^2/g were used as received (Degussa and Nikko Chemical respectively). Sodium dodecyl sulfate (SDS, 98%) was purchased from Aldrich and recrystallized once from 95% ethanol/5% water for cmc and atomic absorption (AA) measurements, but was used as received for adsorption isotherm measurements. The surfactant was not recrystallized for adsorption isotherm determination because the amount of surfactant adsorbed was sufficient so that the effect of impurities on the isotherm could be neglected for almost all adsorption levels. Recrystallized surfactant was used within two weeks after recrystallization. Cmc determination was not performed on the same solutions used to measure adsorption isotherms because the volume of liquid required to measure the isotherm would have changed the solids:liquid ratio in the centrifuge tubes, possibly skewing the results. Standard SDS solutions were prepared using deionized water from a Sybron/Barnstead PCS filtration system, with a pH that was adjusted to 3.5 by addition of HCl (EM

Science) so that the water was below the point of zero charge of each substrate.

B. Adsorption Isotherm Generation

Standard SDS solutions were prepared (10mM to 90mM) with deionized water adjusted to a pH of 3.5. No attempt was made to control pH after the addition of either surfactant or solid, consequently the pH rose in all cases, reaching a high of 8.3 for alumina at 90 mM surfactant concentration. For Al_2O_3 and TiO_2 0.8g of substrate was added to 25mL of surfactant solution and all isotherms were measured at 25°C. A solid-liquid contact time of 24 hours was allowed to ensure that equilibrium was reached; measurements on a number of systems with particulate solids including both systems described in this paper have shown that 5-10 hours is necessary to achieve equilibrium within the measurement error. The amount of surfactant in solution after adsorption, i.e. the equilibrium surfactant concentration, was measured using HPLC and the amount adsorbed was determined by subtracting this value from the known amount of surfactant originally in solution. A 0.2 μm syringe filter was used to remove particulate matter before HPLC, and this medium was tested with the full concentration range of standard solutions to ensure that

no SDS was removed from the solution by filtration. HPLC was performed on a Shimadzu Scientific Instrument (SCL-10A) with an in-line Alltech 320 Conductivity Detector. A Waters μBondpack C18 125 Angstrom 10μm 3.9x300mm column was used to isolate the surfactant. All HPLC data was collected and integrated by a Hewlett Packard 3396 Series III integrator. HPLC was performed with an 80:20 methanol:deionized water mobile phase at a flow rate of 1mL/min. A calibration curve for SDS solutions was determined by HPLC using the parameters above.

C. Cmc Determination

Samples were prepared directly in centrifuge bottles. 0.16 g and 5 ml of liquid were used, and hence the ratio (mass of metal oxide/volume of surfactant solution) was identical to the ratio used in adsorption isotherm measurements. After equilibrium was reached, the samples were centrifuged for approximately five minutes before ultrafiltration was commenced, in order to prevent the suspended particulates from interfering with the membrane. Membrane filters from Amicon Corporation (YM-3, with a nominal molecular weight cutoff of 3000 daltons) were then placed in the solution immediately prior to the final

centrifugation (Figure 2.1). The centrifuge used was a Beckman Accuspin FR at a speed of 3000 rpm. In this experiment, the relative centrifugal force (RCF) was 1700*g, which is well below the maximum rating of the filter. The samples were centrifuged for a given time as described in the text. The concentration of surfactant on the surfactant-poor side of the filter was determined by HPLC and was assumed to consist entirely of free surfactant. The implications of this assumption are described more fully in the text.

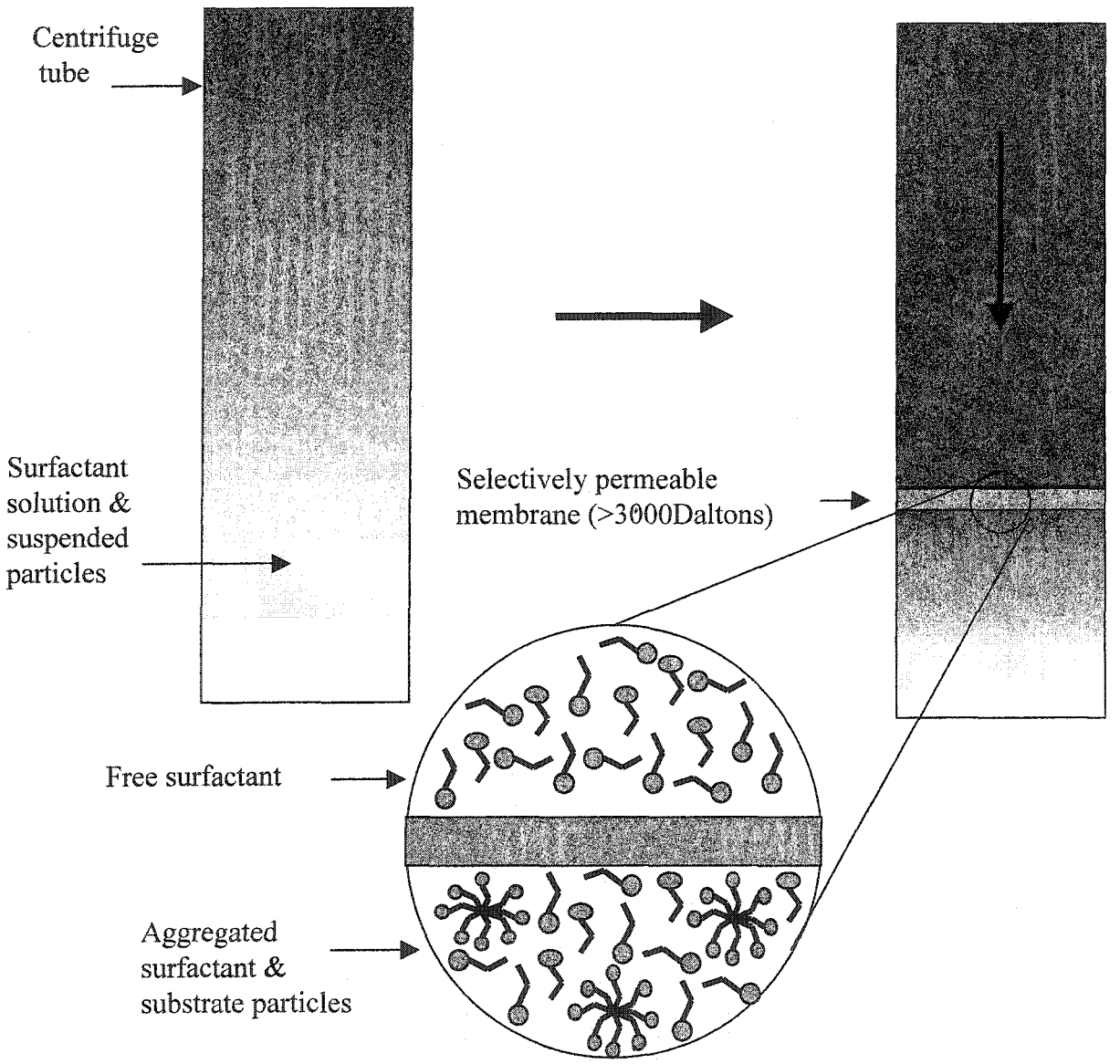


Figure 2.1. Membrane filters for cmc determination

D. Sodium Ion Determination

The total concentration of sodium ions present in a post-adsorption solution slightly above the plateau point of the isotherm was measured by a Varian Spectra AA-20 atomic absorption (AA) spectrometer. The solution was prepared using recrystallized SDS, and isolated from the solid by filtration using two different methods to ensure that solid would not interfere with the results. Both 0.2 micron syringe filters and ultracentrifugation filters were used; for the latter, the system was allowed to sit for one day so that equilibrium with respect to surfactant concentration was achieved on both sides of the membrane. The difference in the measured sodium ion concentration between these two methods was negligible, presumably indicating that little or no particulates passed through either filter. Recrystallized SDS in water was used to calibrate this instrument.

II. Synthesis and Characterization of Polyaniline and Polypyrrole Thin Films on Alumina Particles

A. Materials

Acidic alumina powder, activity grade I, ($155 m^2/g$) was used as received from Aldrich chemical company. Aniline (98%, Aldrich Chemical Company) was distilled under reduced pressure prior to use. Pyrrole (98%, Aldrich Chemical Company) was passed through a column of basic alumina before use. SDS was obtained from Aldrich chemical company (98%) and was used without recrystallization. Sodium dodecylbenzene sulfonate (SDBS) was used as received (tech. grade, Aldrich Chemical Company). Reagent grade ammonium persufate (98+%, Aldrich Chemical Company) and hydrochloric acid (37%, EM science) were also used as received. All solutions were prepared with nanopure (18.2 $M\Omega$-cm^{-1}) water.

B. Adsorption Isotherms of SDS and SDBS on Acidic Alumina

High Performance Liquid Chromatography (HPLC) was used to determine the amount of surfactant that was adsorbed to the surface of the alumina. In the case of SDS standard SDS (3-25 mM) solutions were prepared with deionized water adjusted to a pH of 3 with HCl. 0.8g of acidic alumina

was weighed in a 30 mL vial and 25 mL of the surfactant solution was added. No attempt was made to control pH after the alumina was contacted with the SDS solution. A solid-liquid contact time of 24 hours was chosen to ensure that equilibrium was reached; measurements on a number of systems with particulate solids including both systems described in this paper have shown that 5-10 hours is necessary to achieve equilibrium within the measurement error. The amount of surfactant in solution after adsorption, i.e. the equilibrium surfactant concentration, was measured using HPLC and the amount adsorbed was determined by subtracting this value from the known amount of surfactant originally in solution. A 0.2 μm syringe filter was used to remove particulate matter before HPLC, and this medium was tested with the full concentration range of standard solutions to ensure that no SDS was removed from the solution by filtration. HPLC was performed on a Shimadzu Scientific Instrument (SCL-10A) with an in-line Alltech 320 Conductivity Detector. A Waters μBondpack C18 125 Angstrom 10μm 3.9x300mm column was used to isolate the surfactant. All HPLC data was collected and integrated by a Hewlett Packard 3396 Series III integrator. HPLC was performed with an 80:20 methanol:deionized water mobile phase at a flow rate of 1mL/min.

Adsorption isotherms for the DBSA on acidic alumina were measured by preparing SDBS solutions (3-25 mM) at a pH of 3 adjusted with HCl. In a 30 mL vial, 1 g of acidic alumina was contacted with 15 mL of SDBS solution for 24 h.[1] Measurement of SDBS concentrations in solution were carried out in an identical fashion as for SDS although a Waters 486 Tunable Absorbance UV Detector was used at a wavelength of 258 nm to identify SDBS.

C. Polymerization of Aniline and Pyrrole on Alumina

In the case of aniline, a 16.7 mM solution of SDS was prepared and the desired amount of aniline added (5.6 – 226 mM). The pH of the solution was adjusted to 1.0 by the addition of HCl. All solutions were clarified at 40°C and then 1 L of the SDS/aniline was contacted with 40 g of alumina in a 2 L rounded bottom flask. Adsorption and adsolubilization (solubilization of the monomer into the adsorbed surfactant) was carried out at 40°C for 24 h with stirring. Room temperature (22 ± 1°C) ammonium persulfate (APS) solutions were prepared in order that a 100 mL charge would give a final aniline/APS ratio of 1:1. APS solutions were added dropwise to the stirred reaction vessel over a period of 30 minutes. Polymerization was allowed to take place for a total of 5 h

(including induction time) at 40°C. Proceeding polymerization, the particles were collected in 0.22 μm membrane filters, and then washed thoroughly with 4 L of water. Following washing, particles were dried in a vacuum oven at 50°C for 24 h. Modified particles ranged in color from pale green to black depending upon aniline concentrations.

Polymerization of pyrrole was carried out by preparing a solution of 24 mM SDBS with the desired amount of pyrrole (8 - 200 mM). HCl was added to the solution until a pH of 3.0 was obtained then 1L of the SDBS solution was contacted with 66.6g of acidic alumina in a 2 L rounded bottom flask. Adsorption/adsolubilization carried out for 24 h at room temperature (22 ± 1°C) with stirring. A 100 mL charge of a concentrated APS solution was added dropwise to the vessel over a period of 30 minutes to give a final pyrrole/APS ratio of 1:1. Polymerization was conducted for 5 h with stirring at room temperature (22 ± 1°C). Washing and drying was carried out in an identical fashion as for PAni samples.

D. Contact Conductivity Measurements

Powder conductivity of alumina particles was measured across a packed pellet of the material. In an attempt to carry out reproducible measurements, 0.2 g of the particles were compressed to a pressure of 1000 psi between two electrodes and the resistance measured by the apparatus detailed in Figure 2.2. A pressure of 1000 psi was used, as changes in resistance with increased pressure were small above that pressure indicating that the particles were well compressed. Apparent conductivity can be given by $\sigma = l/AR$; where l is the thickness of the pellet, A the cross sectional area of the electrodes and R the resistance.

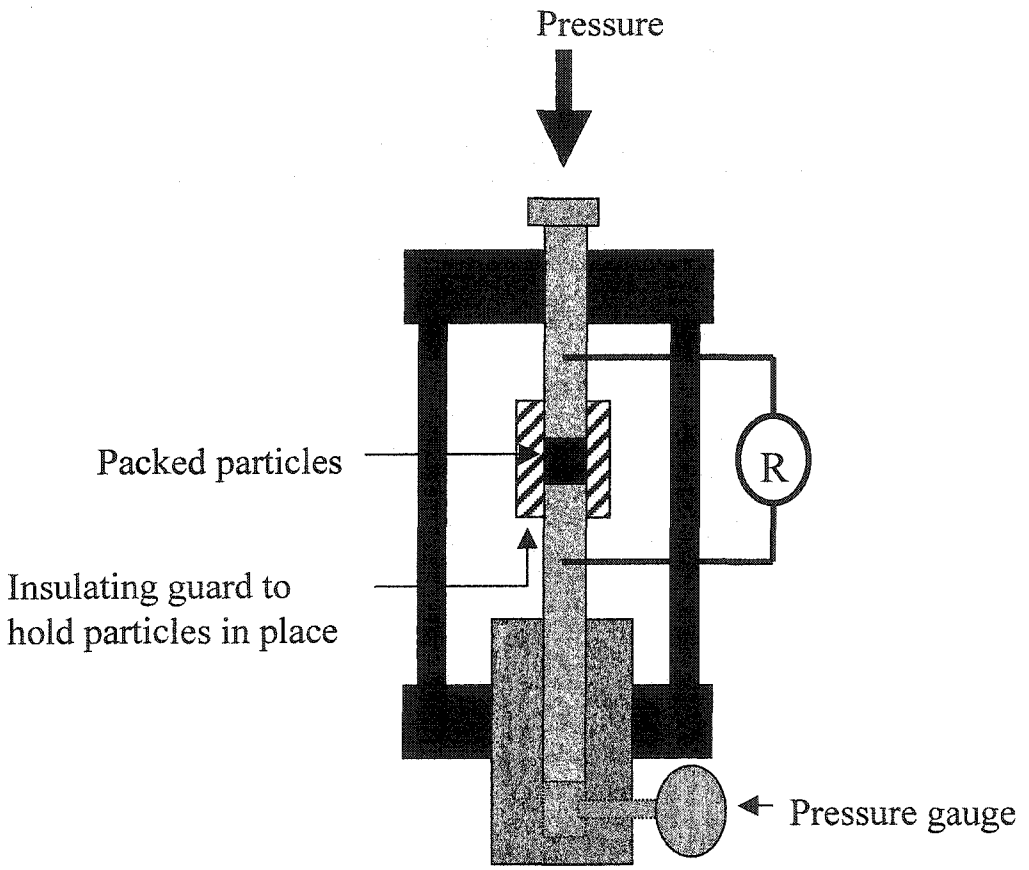


Figure 2.2. Schematic of contact conductivity measuring device. Particles are pressedbetween two elecrtodes and kept in place with an insulating jacket.

E. Weight Fraction of Organics on the surface of the Alumina

The weight fraction of polymer/surfactant was determined by a loss ignition. Vials were cleaned, dried and placed into a Lindberg Hevi-Duty furnace at 600°C for 1 h. Vials were then cooled in a dry environment before weighing. Approximately 0.2 g of the alumina powder was placed in each vial. The samples were then exposed to 600°C for 2 h in the furnace, at which point the polymer coating had been removed and the particles had the appearance of white alumina. All samples were then brought back to room temperature by placing them in a sealed container with desiccant. Samples were then reweighed in order to calculate the weight fraction of organics on the surface of alumina.

F. Wetting Behavior Measurements

The wettability of the particles with respect to different amounts of organic coating was determined using the Washburn Technique (Figure 2.3). A non-wetting plastic column was packed with approximately 15 g of material with minimal pressure (~100 psi in order to yield reproducible results). Methanol was placed into the tray on the balance (Sartorius BL210S) and the packed column was lowered until it first touched the surface of the liquid. Mass vs. time information was collected at one-second time intervals. As discussed in the Results and Discussion, this

technique could not be used for a quantitative assessment of the contact angle. Evaporation of methanol from the tray and slight wetting of the screen was accounted for in the results.

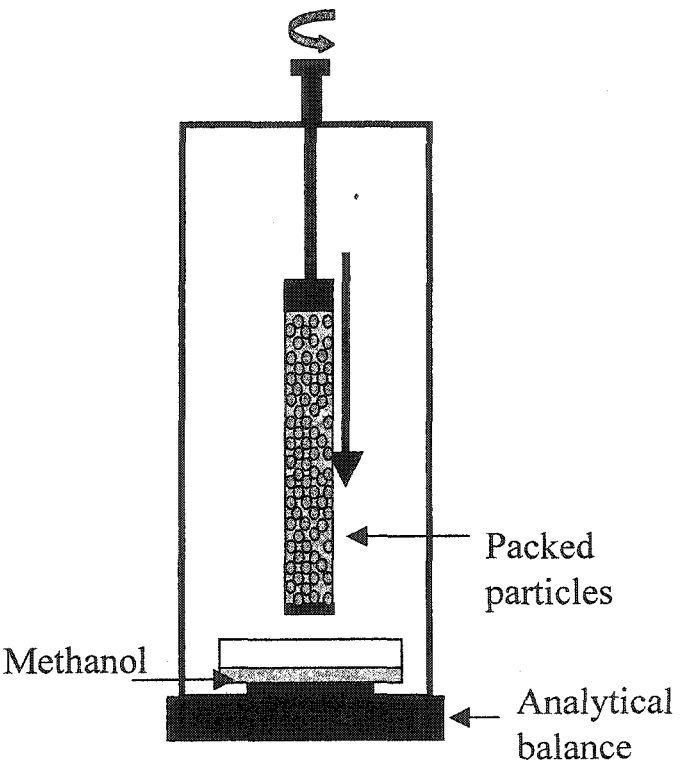


Figure 2.3. Schematic of the apparatus to measure the wetting behavior of particles.

G. XPS Experiments

XPS experiments were carried out on a Physical Electronics PHI 5800 ESCA System with a background pressure of approximately 2.0 X 10^{-9} Torr. The electron takeoff angle was 45° with respect to the sample surface. Spot sizes of 800 μm and pass energies of 23 eV were typically used for the analysis. Binding energies were corrected for surface charging by reference to the C1s line at 284.6 eV for hydrocarbon. A nonlinear Shirley-type background was used for the area analysis of each in conjunction with appropriate sensitivity factors. All curve fitting was performed with Voigt Amplitude curves using PeakFit® software from Systat Software. Each sample was analyzed in two areas and an average value of atomic concentration was calculated.

III. Adsorbed Surfactants as Templates for the Synthesis of Morphologically Controlled Polyaniline and Polypyrrole Nanostructures on Flat Surfaces: From Spheres to Wires to Flat Films

A. PAni synthesis on HOPG and Modified HOPG

An aqueous solution of 5.4 mM sodium dodecyl sulfate (SDS, 98% Aldrich Chemical Company, recrystallized once from 95% ethanol, cmc 8.1×10^{-3}M), and 5.4mM aniline (99% Aldrich, distilled under reduced pressure) was prepared at pH 2 using HCl (ACS plus grade, Fisher

Scientific). 1-dodecanol (98% Avocado Research Chemicals) was used as received. All solutions were prepared with 18.2 MΩ-cm^{-1} nanopure water in polypropylene (PP) vessels, stirred at 27 ± 1°C for 1 h and then used immediately. Although SDS was recrystallized once from 95% ethyl alcohol, almost certainly dodecanol remains as an impurity.[2] As low pH will also contribute to the hydrolysis of SDS, solutions were prepared and used in a timely manner to ensure reproducibility.

Advanced Ceramics, ZYB grade HOPG (12 x 12 mm) was cut into four pieces of approximately 5 x 5 mm on a band saw (ZYB grade HOPG was used to give a surface with fewer grain boundaries compared to ZYH HOPG). Thin sections of HOPG were cleaved with a razor blade exposing a fresh surface used for reaction. HOPG thin sections were not re-used for subsequent reactions because of contamination of underlying layers. Chemically modified HOPG was prepared by the treatment of a freshly cleaved graphite monochromator ZYB (5 mm x 5 mm Advanced Ceramics) with 5 mL of a 5.4 mM ammonium persulfate (APS, 98% Aldrich Chemical Company) at a pH of 2 adjusted with HCl for 3 hours at 22 ± 1°C in a polyethylene (PE) vial. The block was then briefly rinsed with nanopure water and dried for at least 12 hours in a dessicator prior to use.

Graphite substrates were contacted with 5 mL of the SDS/aniline solution for 5 h at 27 ± 1°C in PE vials. A final monomer/oxidant molar ratio of 1:1 was obtained by the addition of 100 μL of an APS solution with stirring for approximately 5 minutes the polymerization for the desired time interval.[3] Following polymerization, the substrate was rinsed thoroughly with pH 2 water (adjusted with HCl) and dried at room temperature in a dessicator for at least 12 h prior to imaging.

B. PPy Synthesis on HOPG

Sodium 1-octanesulfonate (99% Aldrich Chemical Company, cmc $1.6x10^{-1}$M), sodium 1-decanesulfonate (98% Avocado Research Chemicals Ltd., cmc $4.3x10^{-2}$M) and sodium 1-dodecanesulfonate (99% Avocado Research Chemicals Ltd., cmc $1.2x10^{-2}$M) were all used without further purification as were 1-octanol and 1-decanol (99% Avocado Research Chemicals Ltd.). Pyrrole (98% Aldrich Chemical Company) was filtered through a basic alumina column prior to use. 5.4/2.7 mM surfactant/pyrrole solutions were used in all cases prepared with 18.2 MΩ-cm^{-1} nanopure water in PP vessels. A fresh surface of HOPG was rendered by cleaving a thin section of graphite monochromator ZYH (5 mm x 5 mm Advanced Ceramics) as described previously. HOPG

substrates were then contacted with 5 mL of the surfactant/pyrrole solution for 2 h at 22 ± 1°C in PE vials. A final monomer/oxidant molar ratio of 1:1 was obtained by addition of 100 μl of an APS solution with stirring for approximately 5 minutes,[3] and oxidation carried out at 22 ± 1°C for 2 h. Following polymerization, the substrate was rinsed thoroughly with nanopure water and dried in a dessicator at room temperature for at least 12 h prior to imaging.

C. SPM Imaging

Scanning probe microscopy (SPM) is an imaging technique in which atomic resolution images can be acquired. SPM is a term that refers to many different acqusition modes although a common theme to all of these modes is that a probe is traversed above or in contact with the surface of a sample. Such modes are scanning tunneling microscopy (STM), tapping mode atomic force microscopy (TMAFM), contact mode atomic force microscopy (CMAFM), and lateral force microscopy (LFM). All of the above mentioned modes, with the exception of STM, are referred to as atomic force microscopy (AFM) as measurements are made due to interaction forces between the probe tip and sample. In STM, a tunneling current is applied between the tip and sample.

Figure 2.4 is a schematic representing an AFM head. There are five main components namely the laser diode, prism, probe, mirror, and photo-detector. A laser is directed through the prism onto the backside of the cantilever. The reflected beam from the cantilever hits a mirror which diverts it onto the photo-detector. Therefore small deflections of the tip by features on the surface being analyzed are detected by the photo-detector.

All AFM images in this work were collected on a Digital Instruments NanoScope III microscope, operated in tapping mode. MikroMasch Ultrasharp silicon nitride cantilevers were used with a backside aluminum coating and typical resonant frequencies of 325 kHz and force constants of 40 N/m. All scanning was performed under ambient conditions with typical relative humidity levels of around 30%. Images shown in Figure 5.2 were captured at a scan angle of 0^{o} with minimal engagement forces and relatively high scan rates (~15 μm/s). The wires appeared soft and easily distorted by lower setpoints. All other images were collected at a scan angle of 0^{o} and tip velocities of ~3 μm/s. No filtering of images was performed. AFM Calibration was carried out using grids with a pitch of 10 μm and depth of 180nm.

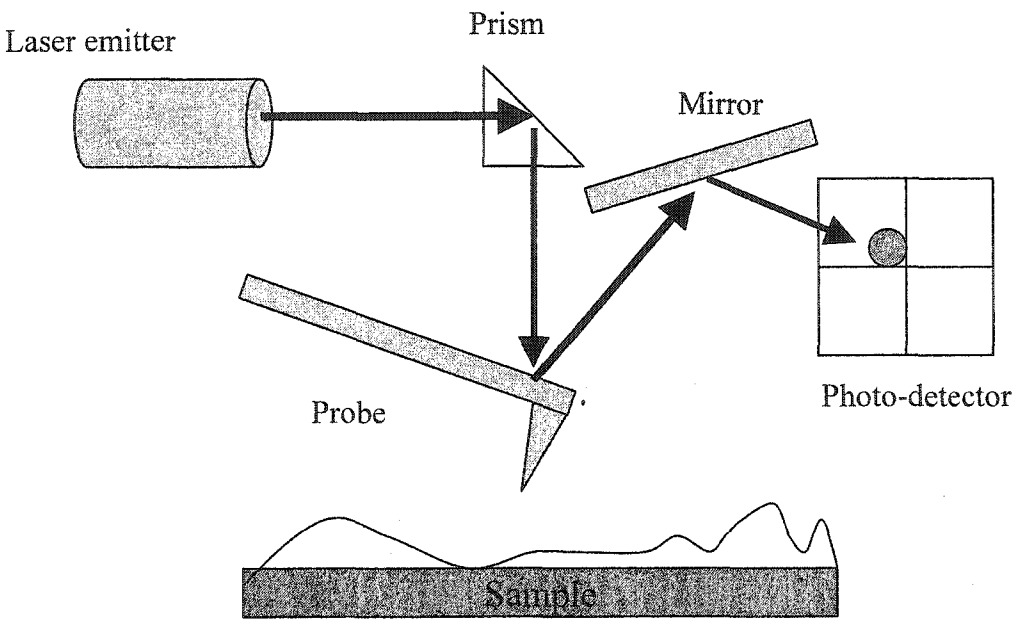


Figure 2.4. Schematic representation of the components making up an AFM head.

IV. References

[1] Different solid to liquid ratios were chosen for the SDBS system to facilitate sufficient adsorption on the surface of the alumina.

[2] Turner, S. F.; Clarke, S. M.; Rennie, A.R.; Thirtle, P.N.; Cooke, D. J.; Li, Z. X.; Thomas, R. K. Langmuir, **1999**, 15, 1017.

[3] Gentle stirring to ensure that color changes occurring during synthesis were homogeneous.

Chapter 3. Cmc Determination in the Presence of Surfactant Adsorbing Inorganic Particulates*

I. Overview

The cmc is a key thermodynamic quantity of surfactant-water mixtures. Knowledge of this quantity is crucial for both scientific and practical understanding of how a surfactant behaves. A great deal of research has been devoted to determining the cmc experimentally[1,2,3,4,5] and through predictive[6] techniques. However, in many applications involving surfactants, fine solid particulates are also present. With solid particulates present, determining the cmc experimentally is not straightforward because the solid can interfere with the measurement technique used to quantify the cmc.

When a solid particulate is present and the surfactant concentration is low, surfactant can reside in one of four environments: unassociated in solution, associated in solution, adsorbed at the solid-liquid interface, and adsorbed at the liquid-vapor interface. The total amount of surfactant at the latter interface is small for the solutions in this study; therefore for the purpose of this study this surfactant will be ignored. Although the physical and thermodynamic meaning of

---

* Carswell, A. D. W.; Lowe, A. M.; Wei, X.; Grady, B. P. *Colloids and Surfaces A: Physicochemical and Engineering Aspects* **2003**, 212, 147.

the cmc remains the same in the presence of particulates, three, rather than two, relevant environments must be considered.

Determination of the amount of surfactant in each environment requires measurement of the amount of surfactant located in two of the three environments; the amount in the third environment can be determined by difference. High Performance Liquid Chromatography (HPLC) can be used to measure the total amount of surfactant in solution, and by deduction, the amount at the solid-liquid interface calculated. The abscissa in these plots is the total surfactant concentration (i.e. both free and micellar surfactant) in solution after adsorption. In many cases, the concentration of surfactant in solution where the plateau adsorption is reached is assumed to be the cmc,[7] which is not necessarily true. In fact, this point could represent saturation of the surface of the solid with surfactant.[8] The purpose of the work described in this paper is to develop a method to distinguish between these two possibilities.

One of the simplest ways to distinguish between these possibilities is to measure the cmc with the solids present. Some of the most common methods to measure the cmc include surface tension,[7,9,10,11] light scattering,[4,12] and viscosity.[9] However, fine particulates confound measurement of the cmc. Brief descriptions of each method and possible complications are given in the following paragraphs.

Surface tension is one of the most common methods used to measure the cmc, because the method is easy to automate and the equipment can be relatively inexpensive. The cmc is determined to be the point at which a discontinuous change in slope occurs in a plot of surface tension vs. surfactant concentration. If surface tension is to be measured in the presence of particles, the particles either must quickly settle to the bottom of the solution or be removed by filtration, since the surface tension cannot be reliably measured in anything but a pure liquid. Settling is a significant problem, since the settling is a function of surfactant adsorption, which in turn is a function of surfactant concentration. For Al_2O_3 and TiO_2, settling did not occur, in a reasonable time frame, at concentrations near and above the cmc of SDS. Filtration is also problematic, preventing automation of the surface tension measurement. Further, impurities that might dissolve off the solid would very likely aggregate at the air/water interface, which in turn would confound the surface tension measurement.

Viscosity and light scattering are essentially impossible to perform in the presence of fine solid particulates. In the former, merely measuring the viscosity with settling particulates is non-trivial, and looking for the small change in viscosity at the cmc is extremely difficult since the influence of the solid on viscosity is much larger than that of the surfactant. This problem of settling is worse for light

scattering measurements than for surface tension, since almost any non-settling particles will scatter light much more intensely than a micelle.

A method probably could be developed to measure the cmc in the presence of particulates using surface tension and light scattering, however two other methods would require less effort and were judged to be more likely to be successful. First, conductivity is often used to measure the cmc. For conductivity to be successful, the solid, and in particular the surface coverage of the solid with surfactant, cannot significantly influence the conductivity. Although this assumption seems reasonable, results described later clearly show that the use of conductivity does not allow the determination of the cmc with sufficient accuracy.

Ultrafiltration membranes are able to exclude molecules above a specified molecular weight and have been used previously to measure the cmc in surfactant systems.[5,13,14,15] Using a centrifugal filtration technique that utilizes these membranes, the particulates can be forced to the bottom of the centrifugal filter, while allowing only a solution of free monomer to pass through the membrane. Micelle transfer across the membrane can be minimized by controlling centrifugation conditions, and the free surfactant concentrations on either side of the membrane will be essentially equivalent. The free surfactant concentration on the micelle-poor side of the membrane can be measured, and plotted vs. the total

concentration of surfactant in solution to determine the cmc easily and reproducibly.

II. Results and Discussion

Figure 3.1 represents data obtained from conductivity measurements of SDS solution with alumina particles. While there is a change in conductivity corresponding to the cmc, the concentration where this discontinuity in slope occurs is not clear. Data obtained from solutions containing titania particulates revealed similar vague turning points. Determining the cmc was difficult and we determined the error to be more than $1*10^{-3}$ M. Clearly conductivity does not allow for an acceptable level of accuracy for the solids tested in this study.

Experimental data for membrane filtration was first obtained from a SDS solution with no substrate present, in order to determine operating conditions for centrifugation. Figure 3.2 represents data obtained from a series of 15 minute centrifugations. An obvious discontinuity in slope is shown in this plot, which indicates the onset of micelle formation and therefore the cmc. The total surfactant concentration in solution corresponding to the plateau point in Figure 3.2 yields a cmc of $7.7*10^{-3}$ M. Longer and shorter centrifugation times were tested in order to validate that 15 minutes was the optimum operating time, at this centrifugation speed.

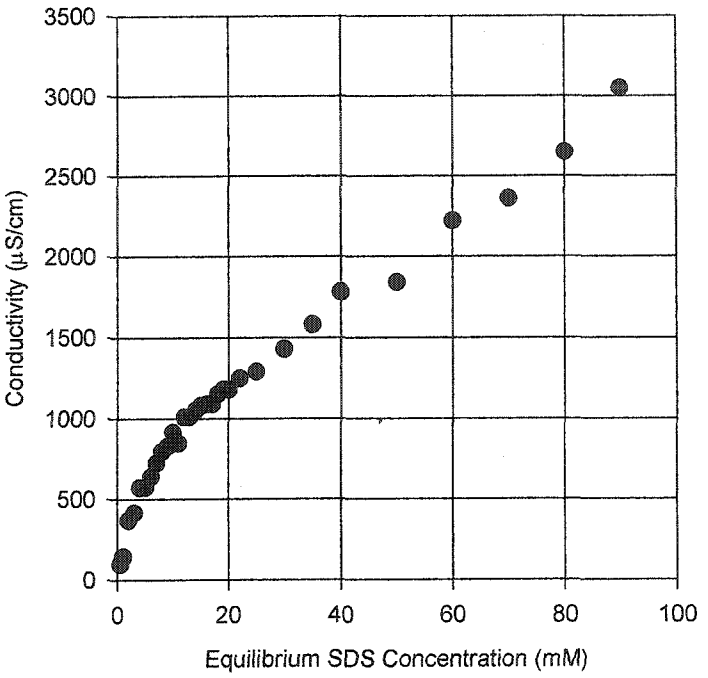


Figure 3.1. Cmc determination of SDS in the presence of alumina particles using conductivity measurements.

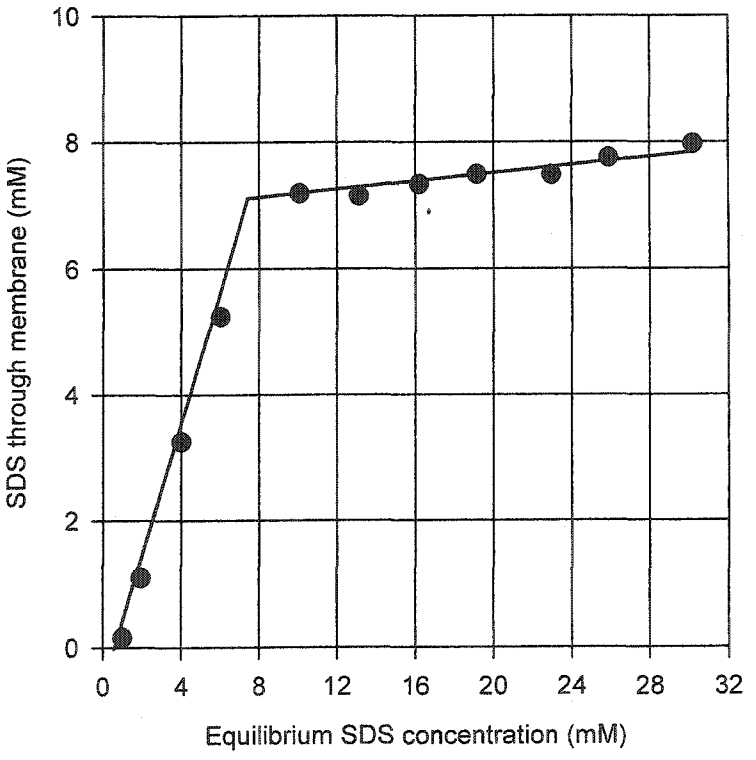


Figure 3.2. Cmc determination of SDS by ultracentrifuge membranes.

Measured cmcs, for pure SDS systems, at a variety of centrifugation times were compared to the cmcs measured by both surface tension and capillary rise. Cmcs measured by surface tension (Figure 3.3) and capillary rise (Figure 3.4) were determined to be $7.5*10^{-3}$ M and $7.6*10^{-3}$ M respectively. These values are both in good agreement with $7.7*10^{-3}$ M measured after 15 minutes of centrifugation as the statistical error in this number was measured as ±0.1 mM. Multiple trials were not performed to determine the experimental error. Although reproducible, this value is lower than the generally accepted value of 8.1×10^{-3} M for pure SDS,[16,17] indicating that SDS had degraded after purification or some dodecanol was still present in the SDS after one recrystallization.

The measured free surfactant concentration on the micelle-poor side of the membrane is actually less than the actual surfactant concentration in solution by as much as $1*10^{-3}$ M at concentrations below the cmc as shown in Figure 3.2. In theory, these two values should be identical, as SDS should only be in the form of monomers. In fact, the two were identical in studies of anionic surfactants using these types of membranes, although to our knowledge this situation has been found only in the presence of swamping electrolyte.[13,14] Two possible explanations exist for this discrepancy. One possibility is that the centrifugation time was not long enough to allow sufficient surfactant to pass through the membrane. The second possibility is that surfactant was entrapped by the filters.

The source of this discrepancy is unimportant in terms of cmc determination, since the cmc can easily be determined from the change in slope in the graph and by using surface tension and capillary rise we were able to show that the membrane is effective when used under our conditions.

Shorter centrifugation times were also chosen to minimize the amount of liquid passing through the membrane. If the diffusion rate of water across the membrane is higher then that of surfactant, the concentration of surfactant on the surfactant-rich side of the membrane will rise, and possibly will exceed the cmc at concentrations close to the cmc. In our experiments, roughly 1/5 of the liquid passed through the membrane to the surfactant-poor side. In the worst case scenario, i.e. no solids with no adsorption by the ultrafiltration membrane, a rise of 160 micromolar on the surfactant-rich side of the membrane would occur given the 800 micromolar difference at the cmc. This effect could have contributed to the difference of 400 micromolar between the measured cmc and the generally accepted value of 8.1×10^{-3} M. However, the possible worst-case increase in surfactant concentration on the surfactant-rich side of the membrane was only 70 micromolar with solids present. This difference is within the experimental error of the technique and can in no way explain difference in cmcs measured with and without solid as discussed below.

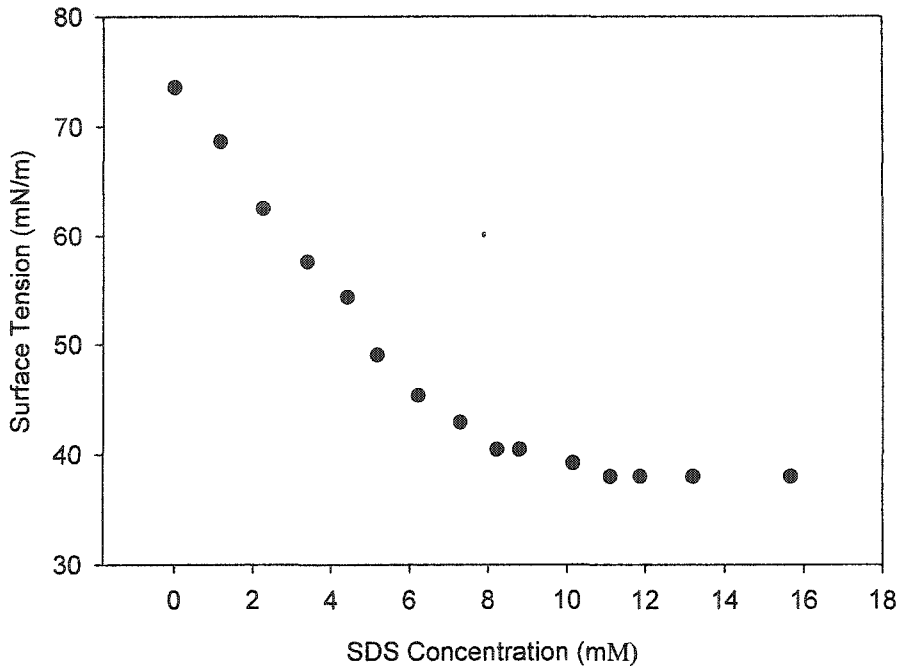


Figure 3.3. Cmc determination of SDS using surface tension.

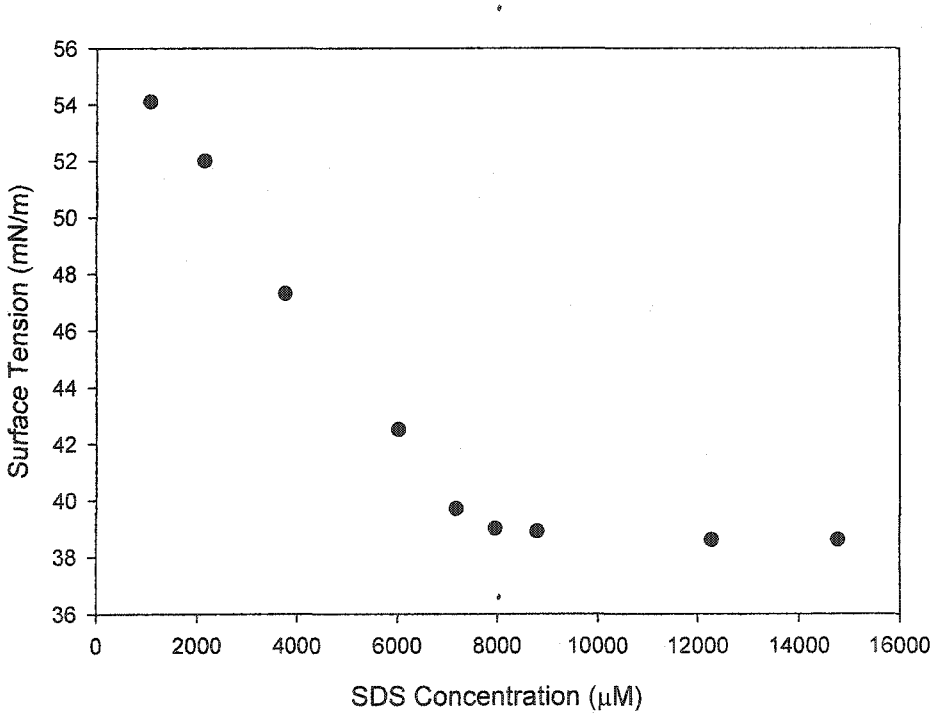


Figure 3.4. Cmc determination of SDS using capillary rise.

Data obtained from SDS solutions with alumina and titania are represented by Figures 3.5 and 3.6 respectively. Using the same procedure described previously, the cmcs of these systems were determined. The alumina-SDS system indicated a cmc of $6.3*10^{-3}$ M, while the titania-SDS system indicated $6.5*10^{-3}$ M. Both of these cmcs are significantly lower than the cmc of the surfactant/water mixture without solids present. Clearly, the cmc is lowered in the presence of these substrates.

One can imagine many possible reasons for the reduction in cmc. One possibility is pH; however, our measurements indicate that the pH rises with addition of solid, and above a pH of 4 there is virtually no change in the cmc for SDS.[18] Although impurities from SDS can influence the cmc,[17,19] trace organic impurities, i.e. dodecanol, will at least partially be adsorbed by the surface or solubilized by the admicelles, and hence the cmc would have been even be higher than the 7.7×10^{-3} M measured without solids. Perhaps impurities could be dissolving from the substrate causing the shift in cmc. In order to investigate this, each solid was contacted with water at a pH of 3.5 for 24 hrs. The water was then filtered away from the solid and used to prepare SDS solutions of which the cmc was measured using the membranes. For both solids, the cmc was roughly that measured previously, therefore water-soluble impurities were ruled out as being a cause of the reduced cmc. In a different test, the solids were washed with toluene

prior to measurement of the adsorption isotherm. The solids were then washed thoroughly with water and used to measure the adsorption isotherm. No shift was found in the isotherm, hence organic impurities on the surface of the solid are also almost certainly not the cause of the shift in cmc.

We attribute the decrease in cmc to introduction of electrolyte by the solid surface caused by the adsorption process. It is well known that the introduction of electrolyte can reduce the cmc of SDS.[20] AA measurements indicate that sodium ions dissociated during SDS adsorption, i.e. there were more sodium ions in solution than surfactant molecules, with the latter being determined via HPLC. In essence, cations on the surface of the solid (presumably aluminum or titanium) provided the necessary charge neutralization for the sulfate group of the surfactant, while to maintain charge neutrality in solution, an anion dissolved from the surface of the solid. The concentration of sodium ions unassociated with surfactant molecules was found to be 2.9mM and 1.5mM for alumina and titania respectively. Interestingly, the measured sodium ion concentration for the alumina system is approximately double that for the titania system corresponding well with the respective adsorbed amounts for these substrates. Assuming that only headgroups at the solid surface lose their sodium counterions and a bilayer structure, in both cases approximately ¾ of the headgroups contacting the solid surface have exchanged their sodium ions. Even though the excess sodium ion

concentrations are much different, the reduction in cmc for these two materials are close (1.4×10^{-3} M vs. 1.2×10^{-3} M), perhaps indicating that the nature(s) of the dissolving anion(s) may be different. An attempt was made to quantify the predicted drop in cmc with added electrolyte using a model presented elsewhere,[21] but these concentrations were outside the applicability of the model and extrapolating the model gave results which did not agree very well with these measured values.

The adsorption isotherms for these systems are also shown in Figures 3.5 and 3.6. Moles of surfactant, rather than the moles of surfactant per gram of oxide are shown to facilitate comparison with the amounts of surfactant in solution.[22] These graphs clearly indicate that the turning point of the isotherm occurs at the same concentration as the cmc. We were a bit surprised, since we felt that surface saturation was more likely to be the cause of the turning point of the isotherm vs. a decrease in the cmc. However, this result does not necessarily mean that the surface is not saturated with surfactant, since these two events could possibly occur at approximately the same surfactant concentration.

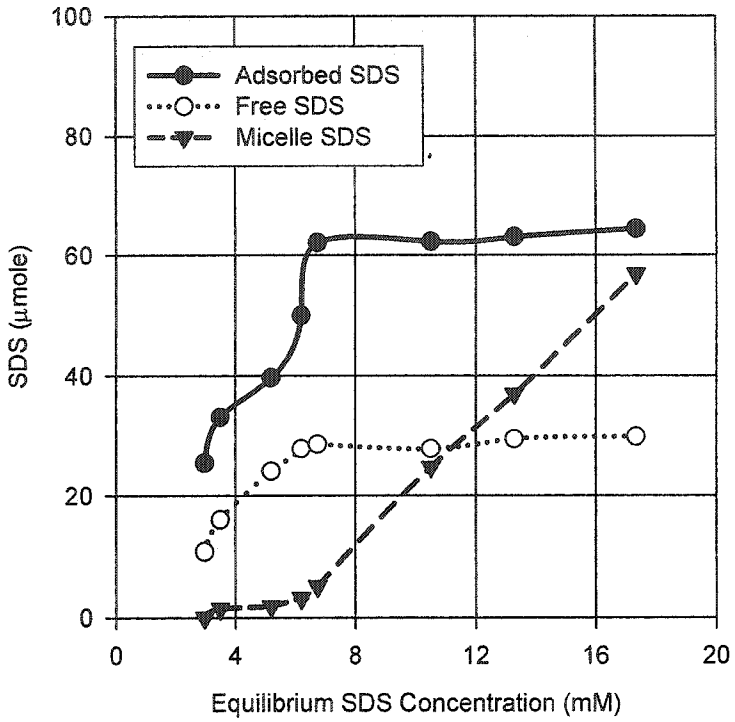


Figure 3.5. Surfactant concentrations found for adsorbed, micelle, and free SDS in the presence of alumina substrate.

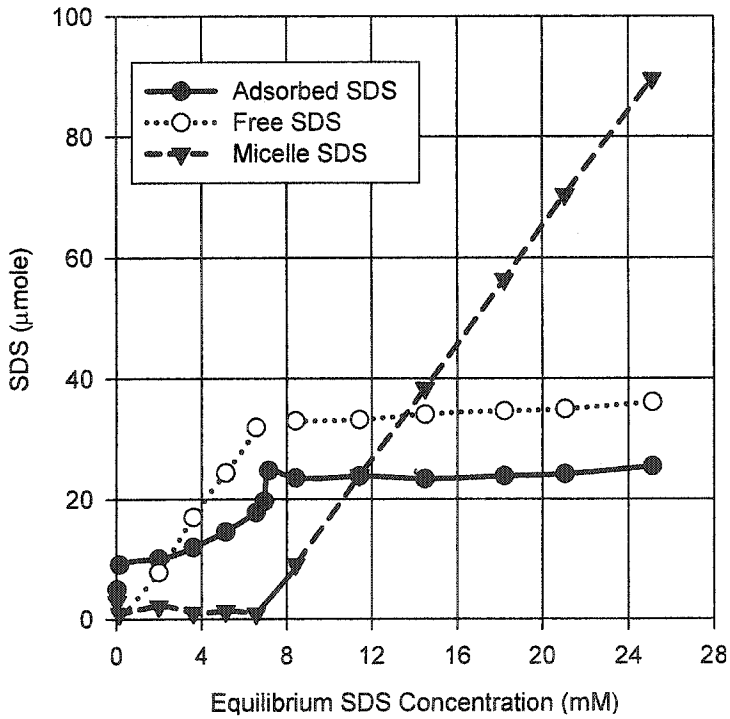


Figure 3.6. Surfactant concentrations found for adsorbed, micelle, and free SDS in the presence of titania substrate.

III. Conclusions

In summary, we have shown that ultrafiltration membranes can be used to measure the cmc of SDS in the presence of fine adsorbing particles. A reduction in the cmc was observed when SDS was adsorbed to both alumina and titania. The reason for this reduction has been attributed to sodium counter ions associated with the SDS being released into the bulk upon adsorption. In this study, the results suggest that the onset of the cmc coincides with the turning point observed in the adsorption isotherm. As we have only investigated two substrates here we can not say unequivocally that the two events always occur at the same concentration. However, if it is found that the cmc is always the same as the turning point of the isotherm, then this observation has implications for the thermodynamics of formation of self-assembled surfactant structures layers at the solid-liquid interface relative to the formation of self-assembled surfactant structures in solution.

IV. Acknowledgements

Support for this project was provided by the National Science Foundation (Grant CTS-9521985) and the NSF EPSCoR program (Cooperative agreement No. EPS 9720651). The authors thank Dr. John Scamehorn for interesting discussions and his insight into this work.

V. References

[1] Esposito, C.; Colicchio, P.; Facchiano, A.; Ragone, R. *J. Colloid Interface Sci.* **1998**, 200, 310.

[2] Abe, M.; Kato, K.; Ogino, K. *J. Colloid Interface Sci.* **1989**, 127, 328.

[3] Moroi, Y.; Motomura, K.; Matuura, R. *J. Colloid Interface Sci.* **1974**, 46, 111.

[4] Kato, T.; Iwai, M.; Seimiya, T. *J. Colloid Interface Sci.* **1989**, 130, 439.

[5] Asakawa, T.; Johten, K.; Miyagishi, S.; Nishida, M. *Langmuir* **1988**, 4, 136.

[6] Huibers, P.D.T.; Lobanov, V. S.; Katritzky, A.R.; Shah, D. O.; Karelson, M. *Langmuir* **1996**, 12, 1462.

[7] Brown, W.; Zhao, J. *Macromolecules* **1993**, 26, 2711.

[8] Besio, G. J.; Prud'homme, R.t K.; Benziger, J. B. *Langmuir* **1988**, 4, 140.

[9] Paxton, T. R. *J. Colloid Interface Sci.* **1969**, 31, 19.

[10] Piirma, I.; Chen, S.-R. *J. Colloid Interface Sci.* **1980**, 74, 90.

[11] Urban, P. C. *J. Dispersion Sci. Technol.* **1981**, 2, 233.

[12] Green, R. J.; Su, T. J.; Joy, H.; Lu, J. R. *Langmuir,* **2000**, 16, 5797.

[13] Osborne-Lee, I. W.; Schechter, R. S.; Wade, W. H. *J. Colloid Interface Sci.* **1983**, 94, 179.

[14] Osborne-Lee, I. W.; Schechter, R. S.; Wade, W. H.; Baraket, Y. *J. Colloid Interface Sci.* **1985**, 108, 60.

[15] Warr, G. G.; Grisser, F.; Healy, T. W. *J. Phys. Chem.* **1983**, 87, 1220.

[16] Elworthy, P. H.; Mysels, K.J. *J. Colloid Interface Sci.*, **1966**, 21, 331.

[17] Mysels, K. J.; *Langmuir*, **1986**, 2, 423.

[18] Rahman, A.; Brown, C. W. *J. Appl. Polym. Sci.* **1983**, 28, 1331.

[19] Georges, J.; Chen, J. W. *J. Colloid Interface Sci.* **1986**, 113, 143.

[20] Corrin, M. L.; Harkins, William D. *J. Am. Chem. Soc.* **1947**, 69, 683.

[21] Stellner, K.L.; Scamehorn, J.F. *JAOCS* 1986, 63, 566.

[22] If the same starting concentrations of impurities were present, then the adsorption isotherm measured would correspond exactly to the adsorption isotherm in the centrifugal filters because the ratio (mass of solid/volume of liquid) was identical. In our case the starting concentrations of impurities were probably different because recrystallized SDS was used only for CMC

determination; however, the effect of impurities on the isotherm can almost certainly be neglected since roughly half the surfactant is adsorbed to the solid substrate at the plateau concentration.

Chapter 4. Synthesis and Characterization of Polyaniline and Polypyrrole Thin Films on Alumina Particles*

I. Overview

Thin films of polyaniline (PAni) and polypyrrole (PPy) have been successfully synthesized on the surface of acidic alumina using sodium dodecyl sulfate (SDS) and sodium dodecylbenzene sulfonate (SDBS) as adsorbed templates. Thin polymer film formation in this fashion has been termed admicellar polymerization (AP) and can be viewed as the surface analogue to emulsion polymerization in which admicelles are used for polymerization as opposed to bulk micelles. The conductivity of modified alumina can be manipulated by controlling the amount of polymer on the surface. Contact conductivities of PAni and PPy modified alumina particles increased by as much as eight orders of magnitude with respect to bare alumina. Weight percent of the organic layer was evaluated by loss ignition measurements. Film uniformity was assessed with wetting and x-ray photoelectron spectroscopy (XPS) experiments. XPS was also used to analyze elemental compositions of the films and confirmed that surfactant molecules assumed the role as dopant.

* Carswell, A. D. W.; John, J.; Grady, B. P. *To be submitted*

II. Results and Discussion

A. Adsorption isotherms of sodium dodecyl sulfate and sodium dodecylbenzene sulfonate on alumina

A study concerning the solubilization locus of aniline-HCl in SDS micelles showed that the phenyl moiety resides within the hydrophobic region and the positively charged polar group at the surface of the micelle.[1] Due to this compatibility of aniline and SDS, SDS was used as the surfactant for PAni synthesis. A previous study suggested that the adsolubilization of pyrrole into SDS admicelles was limited without the addition of electrolyte,[2] therefore sodium dodecylbenzene sulfonate (SDBS) was chosen for thin film formation of PPy on alumina.

Adsorption of SDS and SDBS on acidic alumina was investigated in the absence of monomer and initiator as shown in Figure 4.1. From adsorption isotherms one can identify turning points at which adsorption of surfactant with respect to increased surfactant concentration in solution slows down reaching a plateau region. As onset of the plateau often occurs near or at the critical micelle concentration (cmc), we chose to carry out subsequent polymerizations at a surfactant concentration just prior to the turning point in order to maximize surfactant coverage on the

alumina. The goal is to maximize the propensity of monomer to partition into admicelles on the surface of the substrate, as opposed to bulk micelles in solution. In a previous study we measured the cmc of SDS in the presence of adsorbing substrates and showed that the turning point, and cmc, were the same for both substrates investigated.[3] Arrows in Figure 4.1 indicate points on the isotherm from which surfactant concentrations have been chosen for polymerization of PAni and PPy.[4] Surfactant concentrations were kept constant throughout all experiments whereas monomer concentrations were changed. Different monomer concentrations were chosen in order to evaluate the properties of the coated alumina with respect to surface coverage, and also to assess the ability to control surface coverage of polymer.

B. Powder conductivity of PPy and PAni coated alumina

Figure 4.2 shows contact conductivities of PAni and PPy coated particles as a function of monomer concentration. The number following designation of aniline (An) or pyrrole (Py) refers to initial monomer concentration in solution (mM), i.e. prior to adsolubilization and reaction, and will be used throughout the chapter. Both samples indicate that there is an initial abrupt increase in conductivity as monomer concentration increases, followed by a plateau type region in which conductivity tends to

level off. We believe that as more monomer is available in solution, coverage of polymer on the alumina becomes more uniform hence at some point a plateau in conductivity occurs corresponding to the point where the polymer film covers most or all of the alumina surface. Film uniformity will be more completely addressed later in the manuscript. Contact conductivities of PAni and PPy coated alumina are comparable at the highest monomer concentrations investigated, 1.19×10^{-1} and 8.94×10^{-2} $S.cm^{-1}$ respectively corresponding to an increase in conductivity of approximately eight orders of magnitude with respect to bare alumina (1.19×10^{-9} S/cm). Direct comparison of the conductivity of PAni and PPy coated particles, for a given monomer concentration, is not however appropriate as mass of substrate to volume of solution ratios are different for aniline and pyrrole experiments. Therefore, monomer available per unit surface area of solid is different in both cases. Different solid to liquid ratios were chosen in order to facilitate sufficient adsorption of the surfactant. A better comparison of contact conductivities between PAni and PPy would be to compare conductivity as a function of wt % of organics.

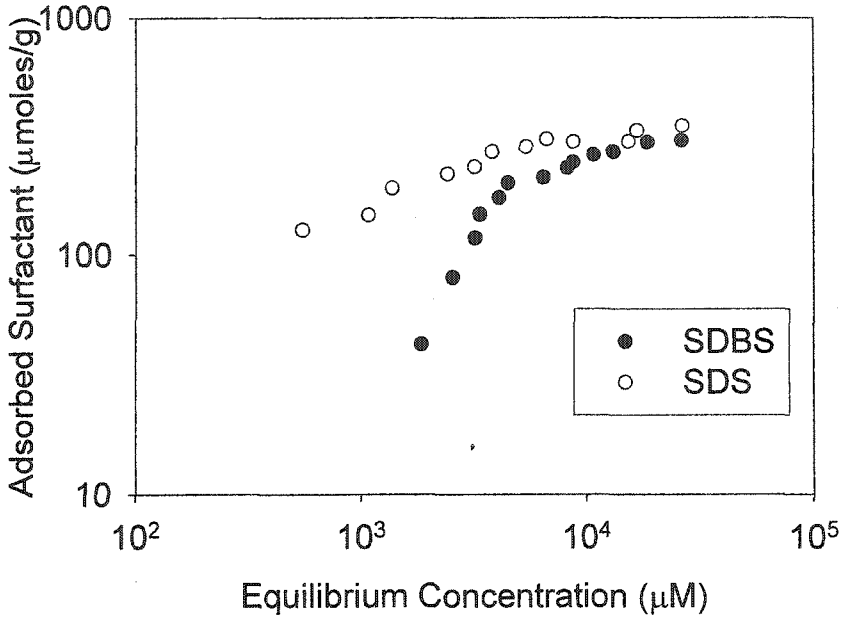


Figure 4.1. Adsorption isotherms for SDS and SDBS measured on acidic alumina.

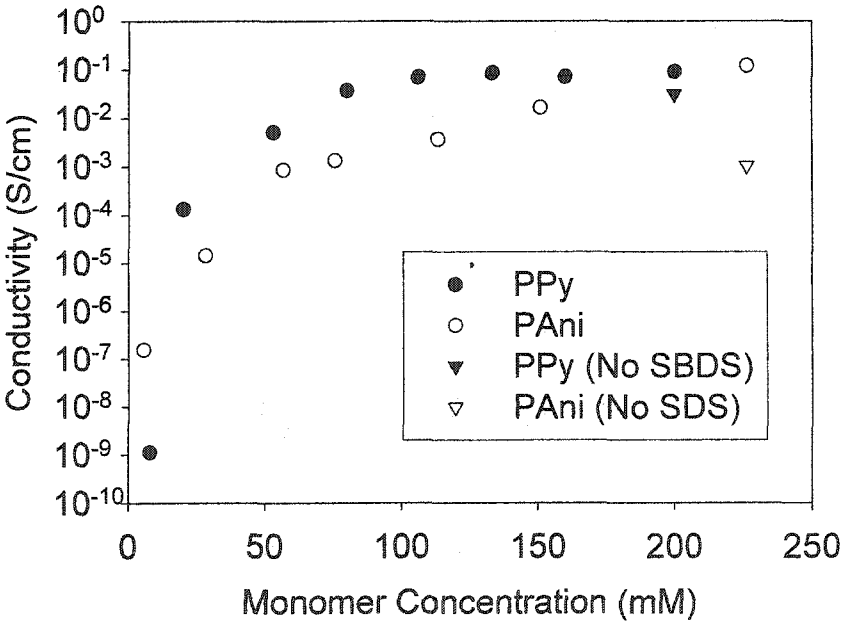


Figure 4.2. Contact conductivities of PAni and PPy modified alumina particles as a function of monomer concentration.

Both PPy and PAni were synthesized with the particulates in the absence of surfactant for the highest monomer concentration cases (Figure 4.2) using the same amounts of the other ingredients. PAni coated alumina has a contact conductivity two orders of magnitude less when SDS is not present (1.0×10^{-3} S/cm) whereas PPy coated alumina exhibits a lower although similar conductivity in the absence of surfactant (3.1×10^{-2} S/cm). Such a noticeable difference in the case of PAni indicates that surfactant may play a role in the integrity and therefore conductivity of the film although the amount of polymer on the surface must also be compared. Additionally, doping effects cannot be compared for the two cases as the dopant molecule and or levels will likely be different. Although PPy films do not show such drastic changes in conductivity with and without surfactant, there is still a three-fold increase when surfactant is present indicative of differences in the film. Again, more information regarding the amount of polymer on the surface of alumina is needed to better understand and compare results for films fabricated with and without surfactant present. To determine the amount of organics on the surface of the alumina, loss ignition was employed.

C. Loss ignition of polymer modified alumina

Figure 4.3 indicates that the amount of organic material on the surface of the alumina increases in a relatively linear fashion as more monomer is available in solution. Interestingly, the amount of PAni/SDS on the surface is much higher than that of PPy/SDBS for a given monomer concentration. As mentioned previously, solid to liquid ratios are different for the two systems, 40 and 67 g/l for SDS and SDBS respectively, therefore direct comparison is not justified. Loss ignition was also used to measure the amount of polymer present on the alumina in the absence of surfactant (Figure 4.3). Interestingly wt% of PPy is much larger than PAni which is in contradiction to what is observed when surfactant is present. Clearly, SDS appears to facilitate PAni film fabrication at the surface of alumina whereas SDBS does not. A possible explanation for this phenomenon may be a result of the point of zero charge (PZC) of alumina. Since PPy is polymerized at a higher pH than PAni, alumina may carry predominately negative charges on the surface. As doped PPy carries a positive charge, adsorption of PPy, i.e. absorption of the polymer from solution rather than adsorption of the monomer followed by subsequent polymerization, could be facilitated due to charge interactions. Due to the low pH at which PAni is synthesized, alumina will likely carry a positive charge which would not be conducive for adsorption of cationic

PAni. In any case, although more PPy is on the surface of alumina when no surfactant is present,[5] the film still has contact conductivities that are three times lower when compared to when surfactant is present. This result is not likely attributable to surface coverage as more polymer covers the surface of alumina when no surfactant is present. Therefore, surfactant appears to play role in the morphology of the polymer film, giving rise to an increase in conductivity although it is impossible to rule out the effects of different dopant ions and doping levels. Previous work has suggested that large surfactant-like dopants may cause polymer chains to adopt an expanded molecular conformation, which in turn may lead to enhanced charge transfer between polymer and dopant.[6,7] In contrast, lower conductivities of PAni films in the absence of surfactant are likely a result of lower surface coverage as evidenced by loss ignition.

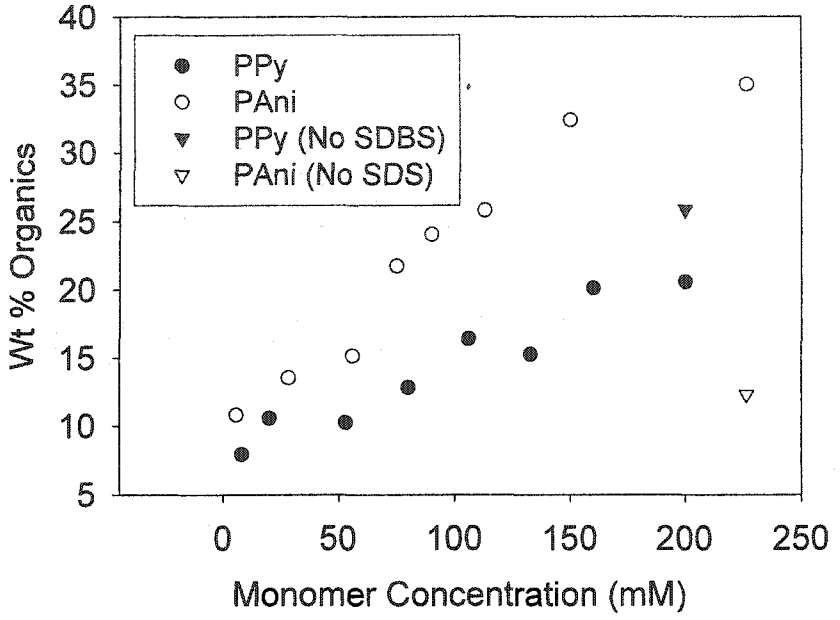


Figure 4.3. Loss ignition measurements of modified alumina particles.

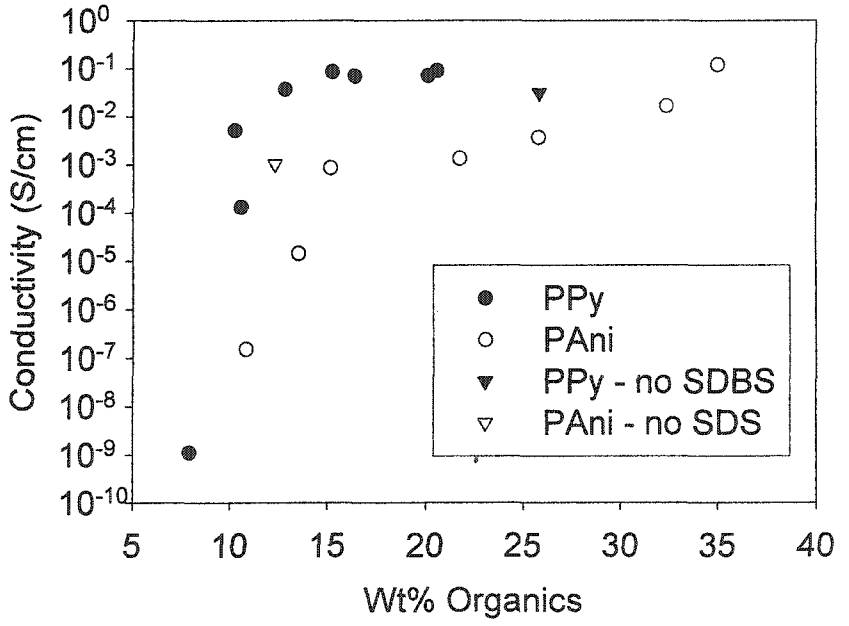


Figure 4.4. Contact conductivities of PAni and PPy modified alumina particles as a function of weight percent of organics.

As mentioned earlier, direct comparison of contact conductivities for PAni and PPy particles can be better assessed as a function of weight percent of organics (Figure 4.4). Both sets of data show an abrupt increase in conductivity, which levels off at around 15 wt% organics in both cases. Figure 4.4 shows that PPy films offer higher conductivities at much lower wt% organics indicative of either a more uniform film or an issue of doping degree. PAni and PPy films were both washed with copious amounts of water and since PAni can be undoped at neutral pH, one could assume that the doping degree of PAni films may be lower than that of PPy films.

D. Wetting properties of modified alumina particles

To qualitatively evaluate the fraction of the surface covered with polymer, we investigated the wetting behavior using the Washburn technique.[8] Typically a contact angle can be assessed, although in our case an absolute contact angle could not be measured due to charges along the polymer backbone. Since charges exist, we cannot neglect issues such as capillary rise due to osmotic effects.

Figure 4.5 represents mass uptake of methanol for a packed column of PPy coated alumina particles. AA represents bare acidic alumina and is

seen to wet most easily of all samples tested. Interestingly one may imagine that Py8 would follow AA as the sample that wets the second best. From Figure 4.5 it is obvious that this is not the case.[9] At low polymer coverage, a monolayer of adsorbed surfactant (with head groups toward the surface) will likely remain after washing and therefore there will be a large area of the surface covered by primarily hydrophobic surfactant tails. Samples Py20, Py80, and Py106 appear to wet to about the same degree, as do Py133, Py160, and Py200 (Figure 4.5). We do not understand the reason that Py53 does not seem to adopt the same trends as for other samples.

Figure 4.6 shows the wetting behavior of PAni coated alumina.[9] As observed for PPy particles, the exact same trend is evident with respect to An5.6 wetting more poorly in comparison to other samples with more monomer present. Again, surfactant hydrophobes probably render the surface hydrophobic. Samples An28.3 and An56.6 fall close to each other then there is a jump to An75.4. Samples An113.2, An150.9, and An226.4 all exhibit similar wetting. From these results it is obvious that wetting reaches a minimum amount for the last three or four samples in each system indicating that alumina is covered with polymer at this stage.

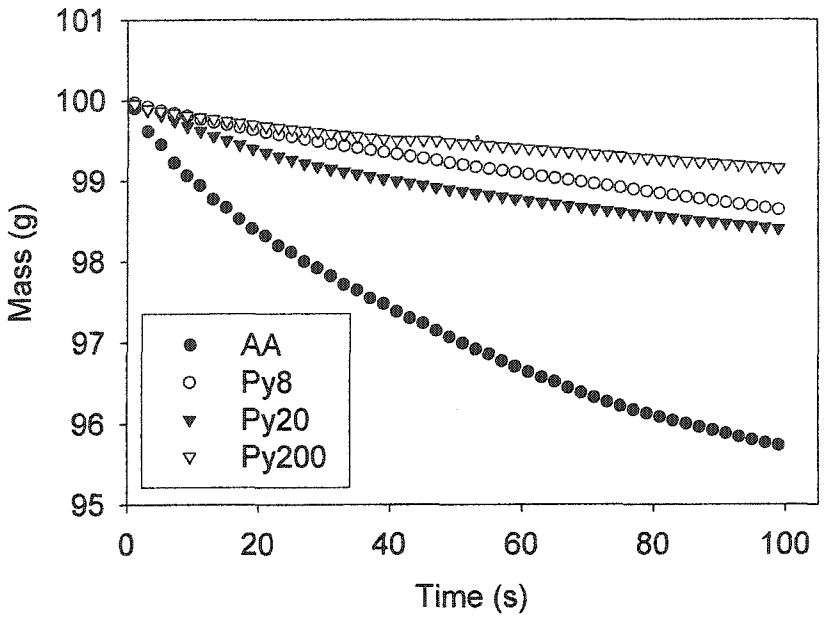


Figure 4.5. Wetting behavior of PPy modified alumina particles.

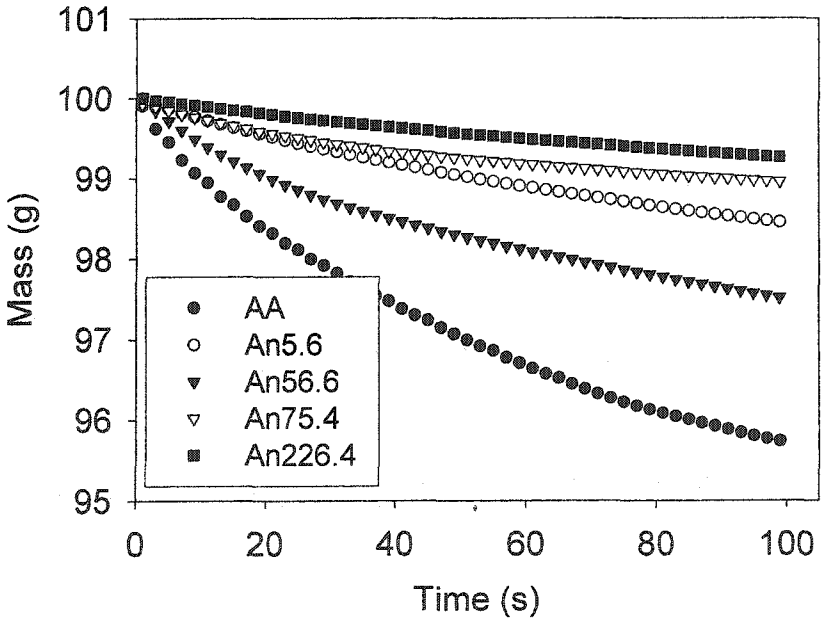


Figure 4.6. Wetting behavior of PAni modified alumina particles.

E. Characterization of polymer films by X-ray photoelectron spectroscopy (XPS)

XPS was used to further assess surface coverage and elemental composition of the polymer films. XPS is a surface specific tool that can be used to analyze atomic concentrations on a surface with penetration depths of 1 - 10 nm. In a recent study films of polystyrene fabricated on alumina by AP were characterized by XPS.[10] Samples below plateau conductivity were assessed along with the highest conductivity sample for both polymers. We will begin our discussion with alumina particles modified with PAni.

1. Polyaniline

Table 4.1 represents elements identified and atomic concentrations of those elements. As expected, atomic concentrations of Al and O tend to decrease as monomer concentrations rise and polymer film masks the surface of alumina. Conversely, concentrations of nitrogen and carbon increase as more polymer covers the surface of the alumina. Interestingly, alumina amounts measured for sample An75 are almost identical to those for An226 indicating that at a monomer concentration of 75mM surface coverage is complete. This observation is consistent with wetting experiments.

	C	N	O	Al	S	N^+/N_{total}	S/N^+
An6	21.7 ± 0.04	0.3 ± 0.04	51.5 ± 0.2	24.9 ± 0.1	1.5 ± 0.02	-	-
An56	64.5 ± 0.2	6.3 ± 0.01	20.7 ± 0.4	6.3 ± 0.1	2.2 ± 0.03	0.30	1.16
An75	76.2 ± 0.3	9.8 ± 0.1	11.1 ± 0.4	1.6 ± 0.007	1.3 ± 0.01	0.27	0.83
An226	74.6 ± 0.5	7.9 ± 0.06	13.7 ± 0.2	1.9 ± 0.06	2.1 ± 0.2	0.31	0.86

Table 4.1. Atomic concentrations of PAni films on alumina as determined by XPS.

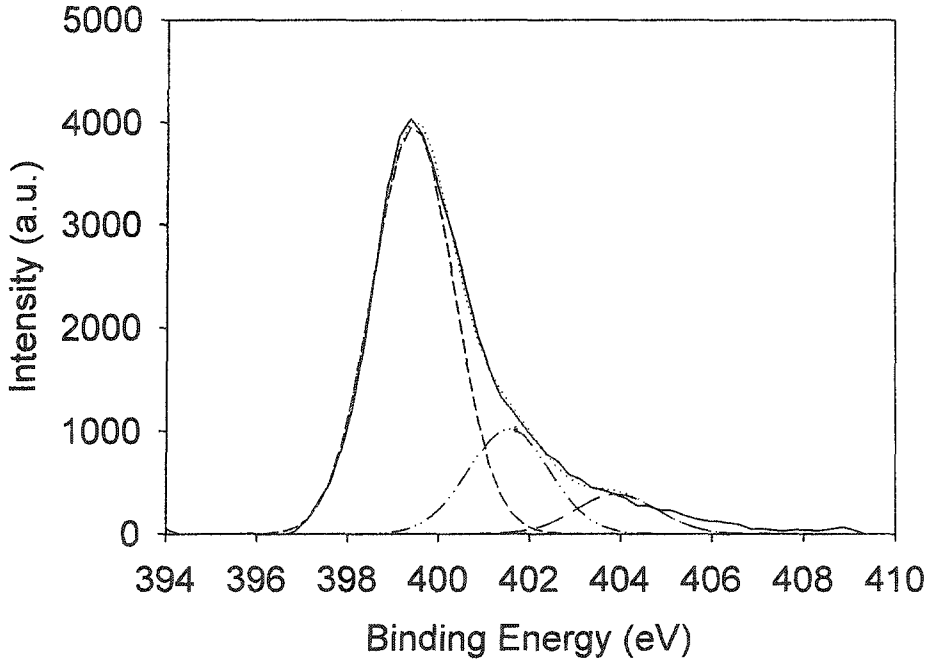


Figure 4.7. High-resolution XPS N1s fitted spectra of An56.

High-resolution XPS peaks associated with the N1s nitrogen line reveal the existence of three nitrogen environments. PAni has been investigated previously by XPS and found to exhibit three characteristic peaks with specific N_{1s} binding energies: <399, 399-400, and >400 eV representing –N=, –NH–, and –N+•– respectively.[11] Figure 4.7 shows the fitted N1s peak for An56. The lowest binding energy peak is not present i.e. –N= is not present. The region of the spectra constituting positively charged nitrogen, i.e. –N+•–, can be deconvoluted into two peaks. These two different environments are interpreted as polaron and bipolaron states respectively in order of increasing binding energy.[12] Numerical evaluation of positively charged nitrogen with respect to total nitrogen (N^+/N_{total}) gives the doping degree (Table 4.1). A doping degree of around 0.30 is found for all samples presenting a resolvable nitrogen peak; full doping would give a ratio of 0.5. As stated previously, PAni may be de-doped by copious washing with water during filtration therefore the measured doping degree may not be representative of the doping degree after polymerization. No attempt was made to re-dope samples by exposure to acidic conditions as the chemical composition of the film following synthesis is desired.

A point of interest is the lack of chlorine and sodium in any of the collected data. PAni is typically doped by chloride ions when synthesized under acidic conditions with HCl. An absence of chlorine indicates that PAni is doped by another anion whereas the lack of sodium indicates that sodium counterions associated with SDS are absent. The obvious supposition is that PAni is doped by the surfactant; the ratio of sulfur to positively charged nitrogen (Table 4.1) can be used to help explore this possibility. One can see that for An6, there is a large excess of sulfur with respect to nitrogen, indicating that a monolayer of adsorbed surfactant is likely present on the surface after washing, along with a small amount of polymer. Note that even in this case no sodium is present, which does not necessarily preclude adsorbed surfactant since we have shown in a previous paper that anionic surfactant can adsorb to alumina via an ion exchange mechanism which in turn releases sodium from the surface.[13] For sample An56, the amount of sulfur is slightly larger than that of N^+ consistent with positively charged nitrogen associating with a sulfur containing anion, with the remainder of sulfur perhaps representing surfactant adsorbed to the surface.[14] As the concentration of aniline is increased, S/N^+ ratios decrease to 0.83 and 0.86 for An75 and An226 respectively. The material may not be fully doped after washing, therefore

S/N^+ ratios slightly lower than unity are not inconsistent with the hypothesis that the surfactant is doping the polymer.

Due to sulfur being present in ammonium persulfate, it is necessary to validate that sulfur probed by XPS is indeed from SDS and not oxidant. If carbon atoms present in these films have only two origins: polymer and surfactant, the origin of sulfur can be determined. By assigning six carbon atoms for every nitrogen atom and twelve for every sulfur atom, an "accounted for" amount of carbon can be calculated. Results obtained are 19.8, 64.2, 74.4, and 72.6 which compare remarkably well to XPS determined values of 21.7, 64.5, 76.2, and 74.6. This calculation also shows that the level of sulfur or nitrogen contributions from the oxidant is essentially zero. Since all sulfur present appears to be due to surfactant, it is reasonable to deduce that the only anionic species able to dope the polymer is the dodecyl sulfate anion. Therefore, we find that SDS does indeed act as dopant in these PAni films. The slightly larger values of the measured carbon may result from the fact that dodecanol is almost certainly present in the film resulting from SDS hydrolysis.[15]

Analysis of S2p sulfur indicates the existence of two main peaks centered at ca. 168.6 and 169.7 eV. Sulfur at 168.6 eV can be attributed to sulfate[16]

whereas sulfur at 169.7 eV may be attributed to an oxidized form of sulfate. Figure 4.8 represents a fitted S2p peak for An56. Higher binding energy sulfur at 171.3 eV is evident for samples An75 and An226. Sulfur observed at higher energies may exist as a result of a positively charged environment. A positively charged environment could be a consequence of charge extraction associated with doping effects.[17]

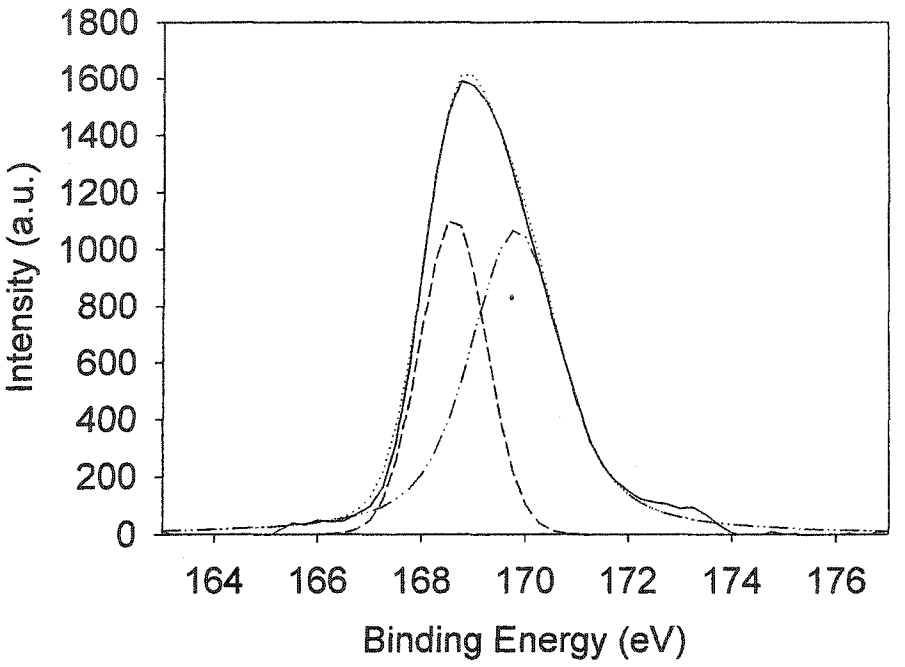


Figure 4.8. High-resolution XPS S2p fitted spectra of An56.

	C	N	O	Al	S	N^+/N_{total}	S/N^+
Py8	23.0 ± 0.3	0.8 ± 0.08	49.8 ± 0.3	25.4 ± 0.04	1.0 ± 0.02	0.44	2.84
Py20	61.4 ± 0.06	5.3 ± 0.2	22.6 ± 0.2	8.4 ± 0.3	2.3 ± 0.0	0.40	1.1
Py53	65.3 ± 0.3	7.3 ± 0.5	20.0 ± 0.02	5.1 ± 0.6	2.3 ± 0.1	0.40	0.79
Py80	71.3 ± 0.1	9.2 ± 0.4	15.3 ± 0.03	1.9 ± 0.4	2.3 ± 0.1	0.31	0.81
Py200	77.5 ± 0.6	5.8 ± 0.6	12.8 ± 0.06	1.0 ± 0.06	2.9 ± 0.04	0.26	1.9

Table 4.2. Atomic concentrations of PPy films on alumina as determined by XPS.

2. *Polypyrrole*

A similar analysis was carried out for PPy films (Table 4.2). Analogous trends of atomic concentrations with respect to monomer concentration are observed as for PAni coated alumina. Once again we see that the change in alumina content from Py80 to Py200 is small indicating that at 80mM of pyrrole, a uniform film is likely present. This observation is also confirmed by contact conductivity experiments as Py80 represents the starting point to plateau conductivity (Figure 4.2). Wetting experiments do not however verify this supposition, as there are still changes in wetting up to Py133. A possible explanation is a small difference in coverage, which wetting experiments can detect but contact conductivity experiments cannot. In parallel with PAni samples investigated, no measurable amount of chlorine or sodium is present on the surface after adsorption/polymerization of SDBS/pyrrole indicative that chloride does not participate as a dopant anion and that sodium ions associated with SDBS molecules are released during adsorption.

Three distinct N1s nitrogen environments can be observed for the PPy film. Assignments can be made for the peaks centered at ca. 400.1, 401.3, and 402.5 eV as –NH-,[18] N^+,[19,20] and N^{2+} [21] respectively. A representative spectra for sample Py80 is shown in Figure 4.9. The doping degree has

been evaluated for all samples and is shown in Table 4.2. Protonation levels of around 0.4 are observed for samples Py8, Py20, and Py53 although the doping degree is lowered to around 0.3 for samples Py80 and Py200. Lower doping levels measured for Py80 and Py200 may be a result of a lack of SDBS available, as surfactant levels are kept constant for all samples. Typical doping degrees observed for PPy are in the range of 0.25-0.33.[22] The higher protonation levels at low monomer contents may be due to the bulky nature of the dopant, which may induce a more expanded molecular conformation of polymer chains allowing for elevated charge transfer between polymer and bulky dopant.[23] S/N^+ ratios indicate for sample Py8 that there is more sulfur than protonated nitrogen which; as suggested previously is likely due to analysis of adsorbed SDBS and a small amount of polymer on the surface. With increasing pyrrole concentration, S/N^+ ratios fall to approximately 1, indicative that SDBS is acting as a dopant molecule. Surprisingly sulfur amounts measured for Py200 increase quite drastically giving a S/N^+ value of 1.9. The reason for this is not obvious although may be due to inefficient washing, leaving residual adsorbed surfactant. In a similar fashion to PAni films, we must investigate the origin of sulfur, as persulfate is also present.

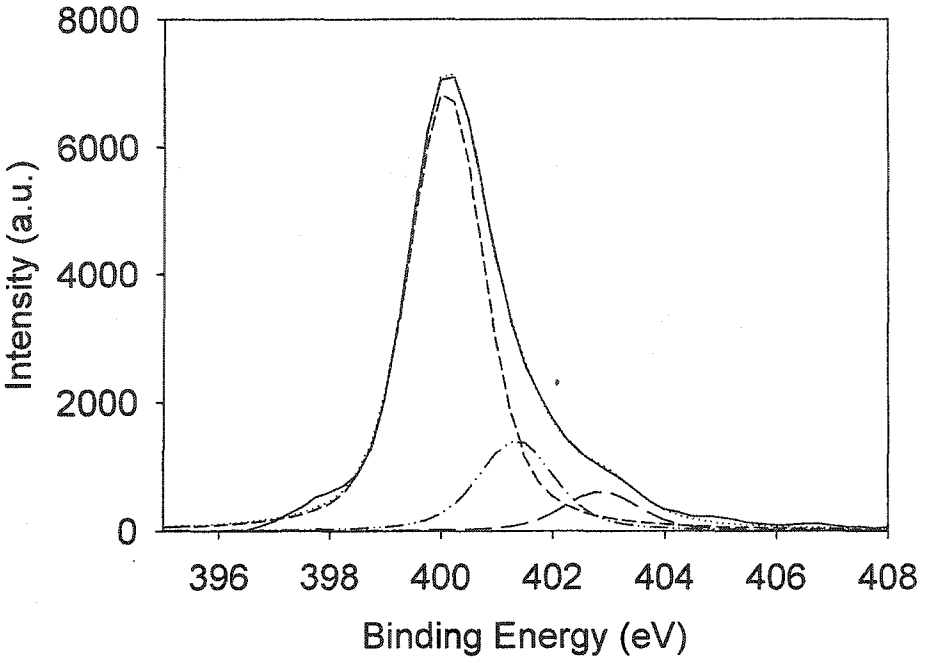


Figure 4.9. High-resolution XPS N1s fitted spectra of Py80.

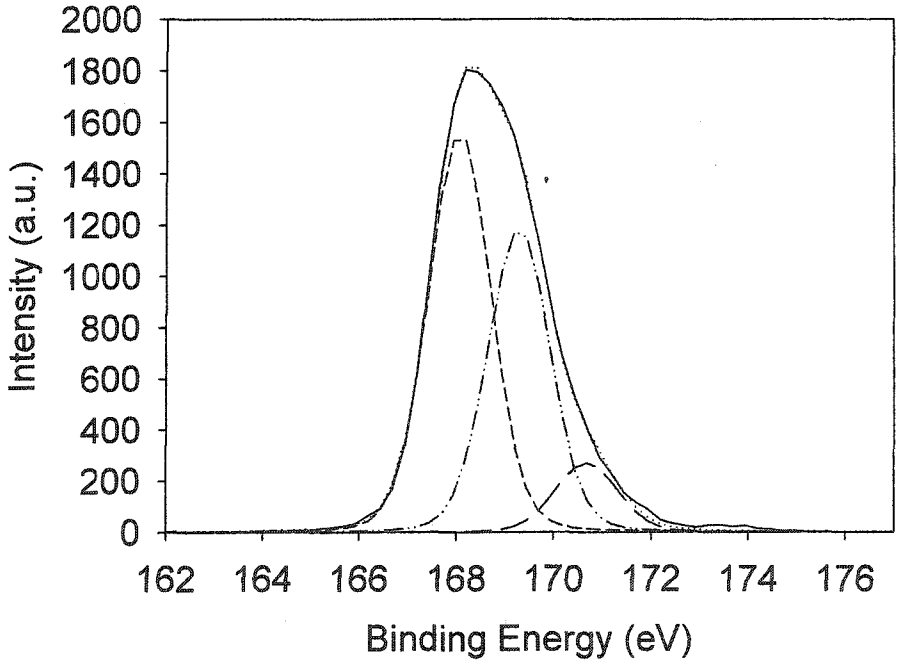


Figure 4.10. High-resolution XPS S2p fitted spectra of Py80.

Carbon contributions may arise from polymer and SDBS therefore we can use sulfur and nitrogen amounts by assigning 18 and four carbon atoms for every sulfur and nitrogen atom respectively. Calculations predict "accounted for" carbon as 21.2, 62.6, 70.6, 78.2, and 75.4 % in comparison to 23, 61.4, 65.3, 71.3, and 77.5 % as measured by XPS. Although "accounted for" and measured carbon amounts are not as close in comparison to PAni films, agreement is still good. A possible explanation for slight discrepancies in carbon amounts may be due to the purity of surfactant used. Technical grade SDBS was used without any further purification, therefore surfactants with a distribution of tail lengths and also possibly long chain alcohols may be present in the adsorbed layer.

Finally, high-resolution curve-fitted S2p sulfur spectra indicate the existence of two sulfur peaks for Py8, Py20, and Py53 whereas an additional higher binding energy peak is evident for Py80 and Py200. Figure 4.10 shows a fitted S2p peak for Py80. Peaks centered at 168.3 and 169 eV are characteristic of sulfonate[18] and an oxidized form of sulfonate[24] groups. Once again, XPS experiments reveal that sulfur is present as sulfonate and that surfactants dope the PPy film. Higher

binding energy sulfur (170.5 eV) can be attributed to sulfur experiencing a positively charged environment due to involvement as a dopant.[25]

In both cases surfactants are found to act as dopant molecules to the synthesized polymer films. As stated previously, bulky surfactant-like dopant molecules tend to cause morphological changes in the polymer chains, resulting in elevated conductivities.[26] Since polymer films show higher conductivity when surfactant is present, we believe that film morphology may be responsible for elevated conductivities although doping issues cannot be neglected.

III. Conclusions

Surfactants have been shown to produce highly conductive uniform films of PAni and PPy on the surface of acidic alumina by a simple low cost procedure. Contact conductivities of PAni and PPy coated alumina particles are 1.19×10^{-1} and 8.94×10^{-2} $S.cm^{-1}$ respectively representing an increase of approximately eight orders of magnitude in comparison to bare alumina, and significantly larger values then conductivities of samples coated with Pani and PPy synthesized without surfactant. When the weight percent of the organic film reaches approximately 15 wt%, the conductivity of PAni and PPy films reaches a plateau indicative of

uniform polymer coverage, a result confirmed by XPS and wetting experiments. Interestingly, loss ignition shows that SDS facilitates the amount of polymer on the surface of alumina whereas SDBS does not. However, in both instances contact conductivities of PAni and PPy films are higher when surfactant is present. XPS experiments reveal that surfactant acts as dopant to both PAni and PPy films resulting in higher conductivity particles in comparison to particles modified in the absence of surfactant. The most plausible explanation for these differences is that surfactant promotes morphological different films although dopant effects cannot be unequivocally ruled out.

IV. Acknowledgements

The authors would like to thank the National Science Foundation, Grant CTS-0210485, for financial support of this work. The authors would also like to thank Zhongrui Li from the University of Oklahoma, Department of Chemical Engineering and Materials Science for conducting XPS experiments.

V. References

[1] Kim, B. J.; Im, S. S.; Oh, S. G. *Langmuir* **2001**, 17, 565.

[2] Funkhouser, G. P.; Arévalo, M. P.; Glatzhofer, D. T.; O'Rear, E. A. *Langmuir* **1995**, 11, 1443.

[3] Carswell, A. D. W.; Lowe, A. M.; Wei, X.; Grady, B. P. *Colloids and Surfaces A: Physicochemical and Engineering Aspects* **2003**, 212, 147.

[4] Surfactant adsorption will likely change in the presence of monomer although the isotherm gives us a starting point.

[5] Wt% of organics measured in the absence of surfactant should consist of only polymer therefore the amount of polymer on the surface is much more when no surfactant is used.

[6] Kim, D. Y.; Lee, J. Y.; Kim, C. Y.; Kang, E. T.; Tan, K. L. *Synth. Met.* **1995**, 72, 243.

[7] Prissanaroon, W.; Brack, N.; Pigram, P. J.; Liesegang, J.; Cardwell, T. J. *Surf. Interface Anal.* **2002**, 33, 653.

[8] Washburn, E. W. *Phys. Rev.* **1921**, 17, 374.

[9] Data sets that overlapped each other were omitted from the plot to improve clarity.

[10] Wei, X.; Carswell, A. D. W.; Alvarez, W.; Grady, B. P. *J. Colloid Interface Sci.* **2003**, 264, 296.

[11] (a) Kim, B. J.; Oh, S. G.; Han, M. G.; Im, Ş. S. *Langmuir* **2000**, 16, 5841. (b) Kang, E. T.; Neoh, K. G.; Tan, T. C.; Khor, C. S. H.; Tan, K. L. *Macromolecules* **1990**, 23, 2918.

[12] Han, M. G.; Cho, S. K.; Oh, S. G.; Im, S. S. *Synth. Met.* **2002**, 126, 53-60.

[13] Carswell, A. D. W.; Lowe, A. M.; Wei, X.; Grady, B. P. *Colloids and Surfaces A: Physicochemical and Engineering Aspects* **2003**, 212, 147.

[14] There will be some error associated with curve fitting which will translate into numerical evaluation of N^+.

[15] Bethell, D.; Fessey, R. E.; Namwindwa, E.; Roberts, D. W. *J. Chem Soc. Perkin Trans. 2* **2001**, 9, 1498.

[16] Leontidis, E.; Kyprianidou-Leodidou, T.; Caseri, W.; Robyr, P.; Krumeich, F.; Kryiacou, K. C. *J. Phys. Chem. B* **2001**, 105,,4133.

[17] Neoh, K.G.; Kang, E. T.; Tan, K. L. *J. Phys. Chem. B* **1997**, 101, 726.

[18] Idla, K.; Talo, A.; Niemi, H. E-M.; Forsen, O.; Ylasaari, S. *Surf. Interface Anal.* **1997**, 25, 837.

[19] Pfluger, P.; Street, G. B.; *J. Chem. Phys.* **1984**, 80, 544.

[20] Ge, H.; Qi, G.; Kang, E. T.; Neoh, K. G.; *Polymer* **1994**, 35, 504.

[21] Joo, J.; Lee, J. K.; Bäck, J. S.; Oh, E. J.; Epstein J. *Synth. Met.* **2001**, 117, 45.

[22] Bredas, J. L.; Cornil, K.; Meyers, F.; Beljonne, *Handbook of Conducting Polymers (2nd edn),* Skotheim, T. A.; Elsenbaumer, R. L.; Reynolds, J. R. (eds) Marcel Dekker: New York, **1998**, 1-27.

[23] Kim, D. Y.; Lee, J. Y.; Kim, C. Y.; Kang, E. T.; Tan, K. L. *Synth. Met.* **1995**, 72, 243.

[24] Moulder, J. F.; Stickle, W. F.; Sobol, P. E.; Bomben, K. D. In *Handbook of X-ray Photoelectron Spectroscopy.* Chastain J (ed.). Perkin-Elmer: Eden Prairie, MN, 1992; 44-45.

[25] Neoh, K.G.; Kang, E. T.; Tan, K. L. *J. Phys. Chem. B* **1997**, 101, 726.

[26] Kim, D. Y.; Lee, J. Y.; Kim, C. Y.; Kang, E. T.; Tan, K. L. *Synth. Met.* **1995**, 72, 243.

Chapter 5. Adsorbed Surfactants as Templates for the Synthesis of Morphologically Controlled Polyaniline and Polypyrrole Nanostructures on Flat Surfaces: From Spheres to Wires to Flat Films*

I. Overview

Nanostructures of polyaniline (PAni) and polypyrrole (PPy) with controlled morphologies have been synthesized on atomically flat surfaces using adsorbed surfactant molecules as templates. Atomic force microscopy (AFM) has been used to investigate polymer film formation on highly oriented pyrolytic graphite (HOPG) and chemically modified HOPG. Morphological control over the resulting polymer film is possible by the addition of co-adsorbing molecules, manipulation of the length of the surfactant hydrophobe, or by changing the surface chemistry of the adsorbing substrate. Phase transitions between spheres, cylinders/wires, and featureless films have been observed which exactly parallel transitions between spheres, cylinders and flat layers in the adsorbed surfactant. Parallel arrays of PAni nanowires can be synthesized with alignment evident over large areas in a simple self-assembly technique in which fabrication and arrangement take place simultaneously. Such a technique in which one can engineer sub 100 nm ordered nanoscale π-conjugated polymer structures of a

* Carswell, A. D. W.; O'Rear, E. A.; Grady, B. P. *J. Am. Chem. Soc.* **2003**, 125, 14793.

desired shape by a simple self-assembly process present potential as templates, sensors, and microelectronic devices.

In addition to aggregation of surfactants at interfaces, aggregation of polymers at interfaces has also been extensively studied. Polymeric nanostructures, very different than those observed in bulk solution, have been observed to form on surfaces due to a combination of interfacial, intra-, and intermolecular forces.[1] Co-adsorption of surfactants and polymers on surfaces has been the focus of a number of studies, although the morphology of these adsorbed structures is much less explored. In one particular case nanoscale aligned strands of polymer did form; these were found for ethyl(hydroxyethyl)cellulose on the surface of graphite in the presence of surfactants.[2] However, to our knowledge, no other systems have shown such morphologies. Interactions between polymers and surfactants in the bulk have been extensively reviewed due to the relevance to many industrial applications.[3] In general, the addition of polymer to surfactant systems induces aggregation at a concentration (critical aggregation concentration, cac) well below the aggregation concentration (critical micelle concentration, cmc) for the surfactant-only system.

As well as synthesizing π-conjugated polymeric nanostructures in bulk solution, the ability to engineer ordered thin films of conducting polymers on flat surfaces is attractive in the fabrication of macromolecular electronic devices for

applications such as electro-optics, microelectronics and photonics.[4] Thin films of PPy have been successfully rendered on surfaces by a technique termed admicellar polymerization (AP) although to date no attempts have been made to control the morphology of the resulting polymer film. For many applications, spatial control of the deposition on the surface is desired. Typical routes to pattern surfaces with π-conjugated polymers include laser writing,[5] surface templated deposition,[6] screen printing,[7] photolithography,[8] and e-beam writing.[9] Limitations to these techniques include resolution, and possible damage of the polymer. As a result, a simple technique to pattern π-conjugated polymers with nanoscale dimensions is in great demand.

Although chemical vapor deposition has proven effective in rendering ordered nanostructures on surfaces, [10] this technique is not suitable for orienting polymeric materials. Ordered rod-like structures of polymerizable surfactants have been observed by AFM at the mica/water interface,[11] and polyelectrolyte ribbon-like structures have been observed at the graphite/water interface.[12] With respect to oriented conducting polymers on surfaces, there have been few reports in the literature. Sub-100 nm lines of conducting polymer have been "drawn" on surfaces using the tip of a scanning tunneling microscope,[13] and with the tip of an atomic force microscope in a direct-writing technique.[14] Oriented arrays of PAni

nanowires have been grown normal to surfaces by an electrochemical method in which no template is used.[15]

In this chapter a new way to pattern π-conjugated polymers with nanoscale dimensions on a solid surface is described, with some advantages over other processes. We show that by means of a three-step process, equilibrium adsorbed surfactant aggregates can be used as templates to synthesize organized polymer films on flat surfaces in which one has morphological control over the resulting polymer film. In the first stage monomer and surfactant is allowed to aggregate on the surface of the substrate; in the second stage an oxidizing agent is added to begin the polymerization reaction; and in the third stage the substrate is rinsed to remove excess ingredients. Figure 5.1 indicates a schematic representation of the process. Unique to our work is the fact that, in the case of the polymer nanowires, we can fabricate aligned arrays over large areas quickly in which orientation is dictated by the surface and alignment is parallel to the surface. The polymer structures have sub 100 nm features, are highly aligned, and are not trapped within a solid support.

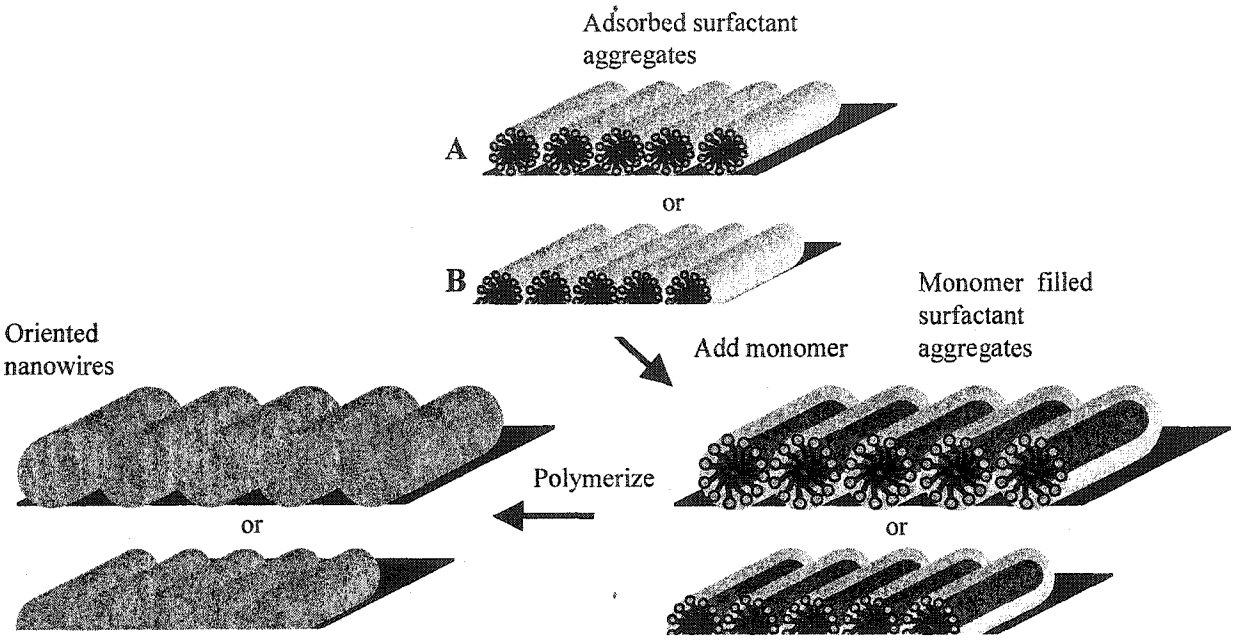


Figure 5.1. Illustration of the process to fabricate morphologically controlled nanostructures of electrically conducting polymers on surfaces using surfactant templates. This particular schematic represents the proposed schematic of wire formation on (A) chemically treated HOPG and (B) HOPG.

II. Results and Discussion

A. Polyaniline

In Figure 5.2A we show ordered arrays of PAni nanowires on HOPG using adsorbed SDS aggregates as a template. Orientation of the wires is maintained over large distances with directional changes seen at grain boundaries or steps inherent in the graphite surface. Such abrupt changes in orientation of SDS hemicylinders on HOPG have been observed previously.[16,17] separations, or cracks in the film, are observed along the long axis of the wires. These cracks are believed to form during drying and no attempts were made to try to stabilize these films during drying. A cross sectional view of the film (Figure 5.2A) identifies a distinct periodicity with a repeat distance of 16.7 ± 1.2 nm. Hemi-cylinder SDS aggregates adsorbed on HOPG have been shown to have diameters of approximately 6 nm although addition of 1-dodecanol causes the aggregates to swell to around 12 nm.[17] It is therefore likely that incorporation of aniline and aniline-HCl into adsorbed SDS aggregates causes a swollen aggregate to form. A recent study concerning the solubilization locus of aniline-HCl in SDS micelles showed that the phenyl moiety resides within the hydrophobic region and the positively charged polar group between negatively charged SDS headgroups at the surface of the micelle.[18] The incorporation of bulky phenyl groups within the hydrophobic core of the aggregate coupled with charge stabilization

at the surface of the aggregate could lead to an enlarged incipient structure. Height measurements have not been included due to geometric limitations of the tip and the fact that naked HOPG may not be exposed between the wires. PAni nanowires can be transitioned into a featureless PAni film by the addition of 1-dodecanol (Figure 5.2B). Cross-sectional analysis shows that the periodicity is lost and the roughness of the film is reduced, although the roughness is slightly larger (rms = 0.12 nm) than the roughness of the underlying graphite (rms = 0.07 nm). Additionally, no cracks are present in the film indicative of surface homogeneity. Addition of 1-dodecanol causes a change in aggregate packing parameter due to its smaller headgroup yet same length hydrophobe.

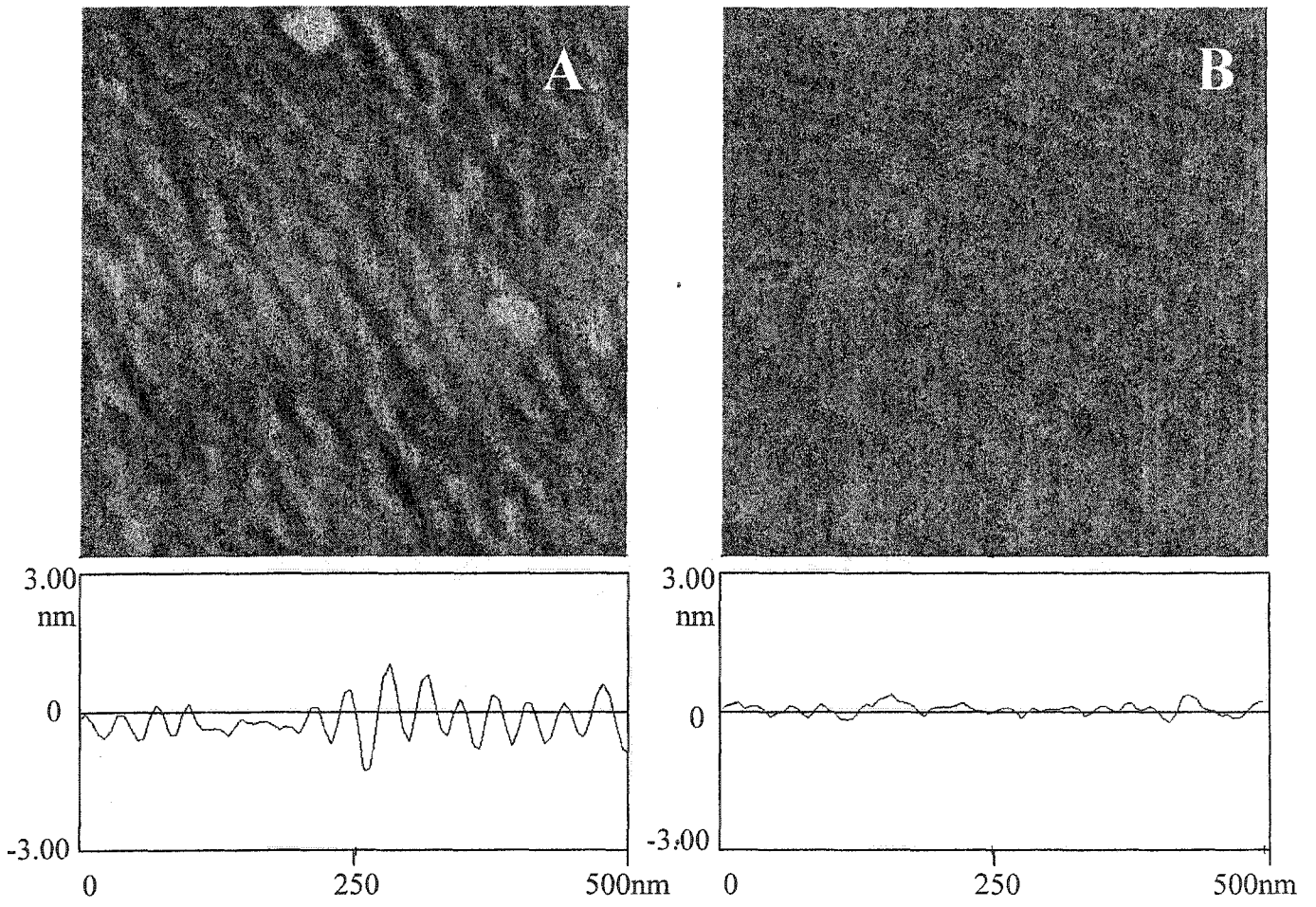


Figure 5.2. 500 x 500 nm AFM images of PAni films on HOPG with 0 mM 1-dodecanol (A) and 0.5 mM 1-dodecanol (B). Both images shown at a height scale of 12 nm.

Analysis of the chemical form of PAni can be ascertained by X-ray photoelectron spectroscopy (XPS) or sometimes called electron spectroscopy for chemical analysis (ESCA). PAni can be present in one of three oxidation states; leucoemeradine, emeraldine, and pernigraniline referring to reduced, reduced/oxidized, and oxidized states respectively. The particular form of PAni can be characterized by XPS by way of three different nitrogen environments with specific N_{1s} binding energies: <399, 399-400, and >400 eV representing –N=, –NH–, and –N+•– respectively.[19] Evaluation of the N_{1s} peak from XPS indicates that in both cases the polymer is in the emeraldine salt (conductive) form. Figure 5.3 represents spectra for the film shown in Figure 5.2A. Analysis of the area corresponding to positively charged nitrogen (>400 eV) suggests that two different species exist. These two different environments can be interpreted, in order of increasing binding energy, as polaron and bipolaron states respectively.[20] Evaluation of the relative area of the two peaks >400 eV with respect to total nitrogen (N^+/N) shows a doping degree of 0.45.[21] Ordered films of PAni should provide improved electrical properties and therefore evaluation of the conductivity of these films is currently under investigation.

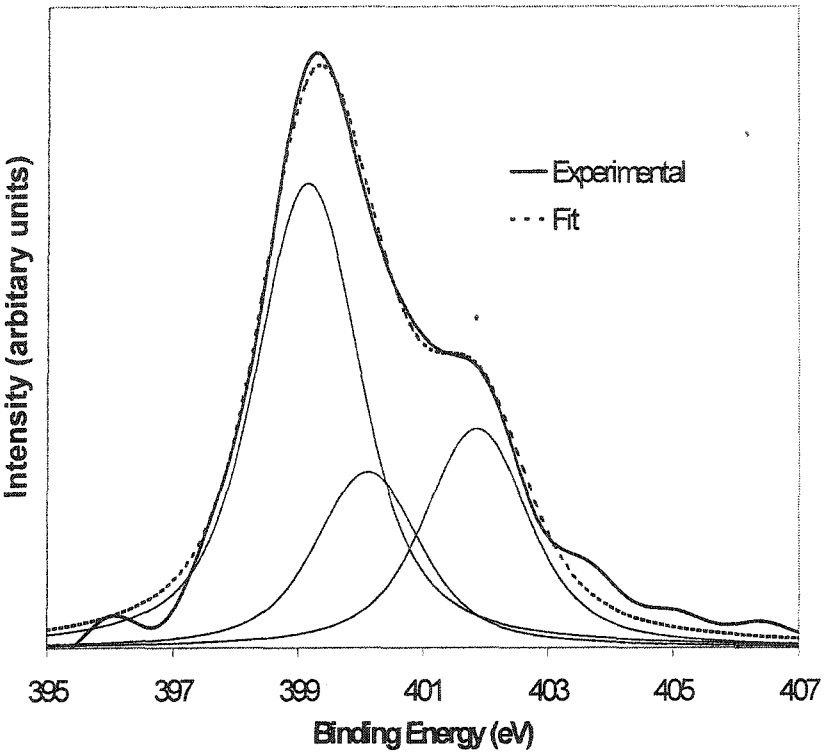


Figure 5.3. X-ray photoelectron spectroscopy of PAni wires on freshly cleaved HOPG. Three nitrogen environments can be observed by curve fitting.

In order to study PAni film formation on a less hydrophobic surface, chemical treatment of freshly cleaved HOPG was carried out by exposure to ammonium persulfate under acidic conditions prior to the addition of monomer and surfactant. Contact angle measurements show that the contact angle of the HOPG block with water changes from 90° to around 75° after surface treatment. XPS analysis of treated HOPG indicates peaks corresponding to specific binding energies associated with carbon, nitrogen, oxygen, and sulfur (Figure 5.4). A slight amount of oxygen is present in freshly cleaved HOPG (Figure 5.4C); possibly due to the sample being cleaved three days prior to analysis (the treated sample was treated and then also stored for three days before analysis). Since the binding energies for nitrogen, oxygen and sulfur are 402.2, 532.5, and 168.7 eV respectively we believe that the mode of surface modification is intercalation of ammonium persulfate ions into the graphene lattice. STM studies of the intercalation of various ions into HOPG have shown the existence of large periodic superstructures.[22]

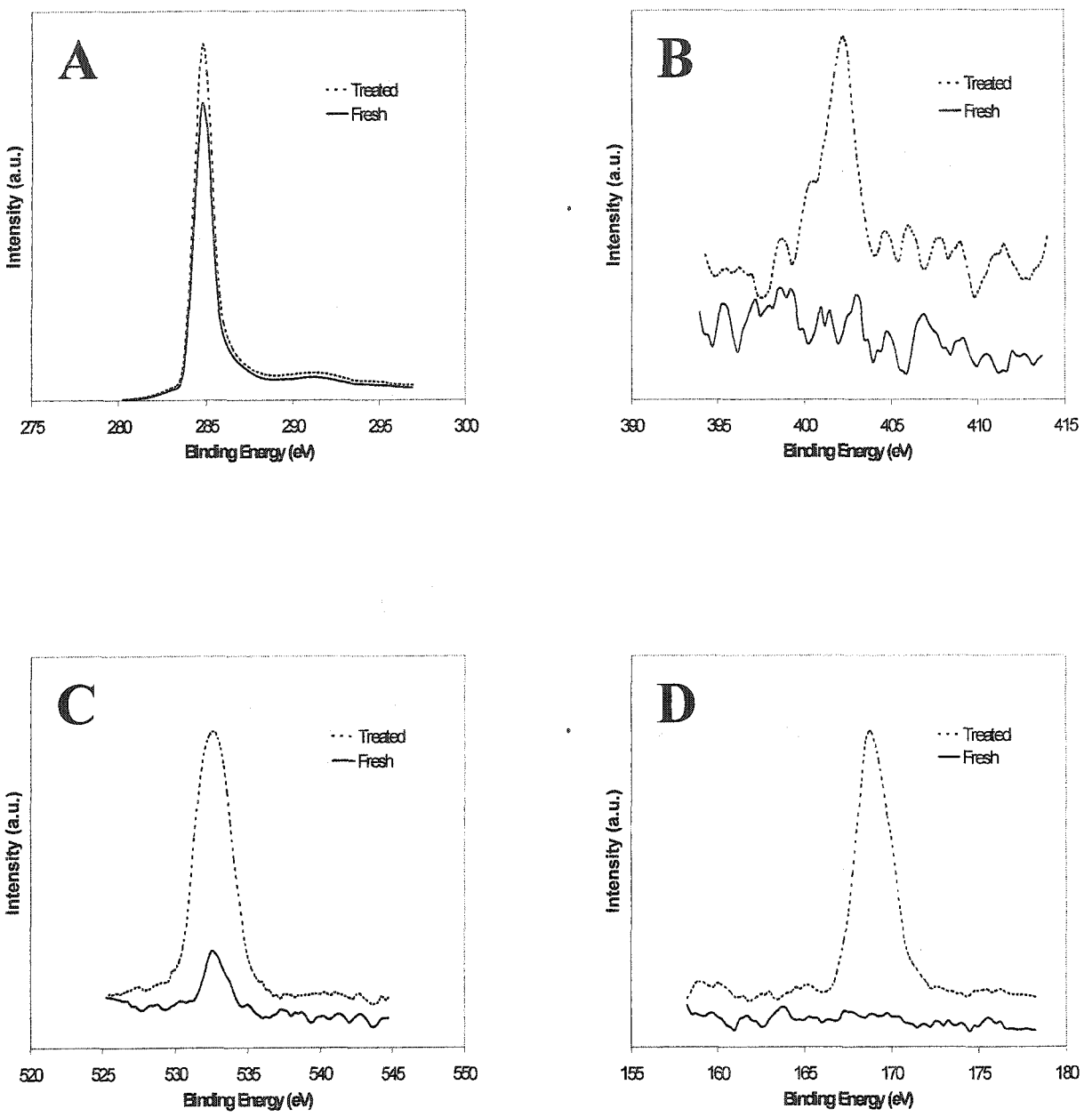


Figure 5.4. X-ray photoelectron spectroscopy of HOPG before and after chemical treatment. (A) Carbon, (B) Nitrogen, (C) Oxygen, and (D) Sulfur.

Following surface treatment of HOPG with ammonium persulfate, PAni synthesis was then carried out in an identical fashion as described previously. Resulting polymer films for the surfactant/monomer system (Figure 5.5A) contrast those synthesized on freshly cleaved HOPG (Figure 5.2A). Spherical PAni structures are fabricated with a diameter of 44.9 ± 2.6 nm covering the entire surface of the substrate. Many cracks are apparent in the film and appear to follow steps in the underlying graphite. Using the cracks as a reference point for the location of the underlying graphite we can measure a typical height of the film to be approximately 40 nm which corresponds well to the measured diameter indicating that the film morphology is indeed spherical. Addition of small quantities of 1-dodecanol causes the spheres to align into what looks like wires composed of connected spheres in a "pearl-necklace" like conformation (Figure 5.5B). Interestingly, increasing the reaction time from 1 h to 3 h, at the same 1-dodecanol concentration causes the globular texture of the wires to diminish, rendering well-formed PAni nanowires with a similar diameter of 44.5 ± 1.8 nm (Figure 5.6). Analysis by XPS indicates that PAni is in the conductive emeraldine salt form with a typical doping degree of 0.46 (Figure 5.7).[21] Featureless PAni films were not observed for this system at the highest 1-dodecanol concentrations investigated.

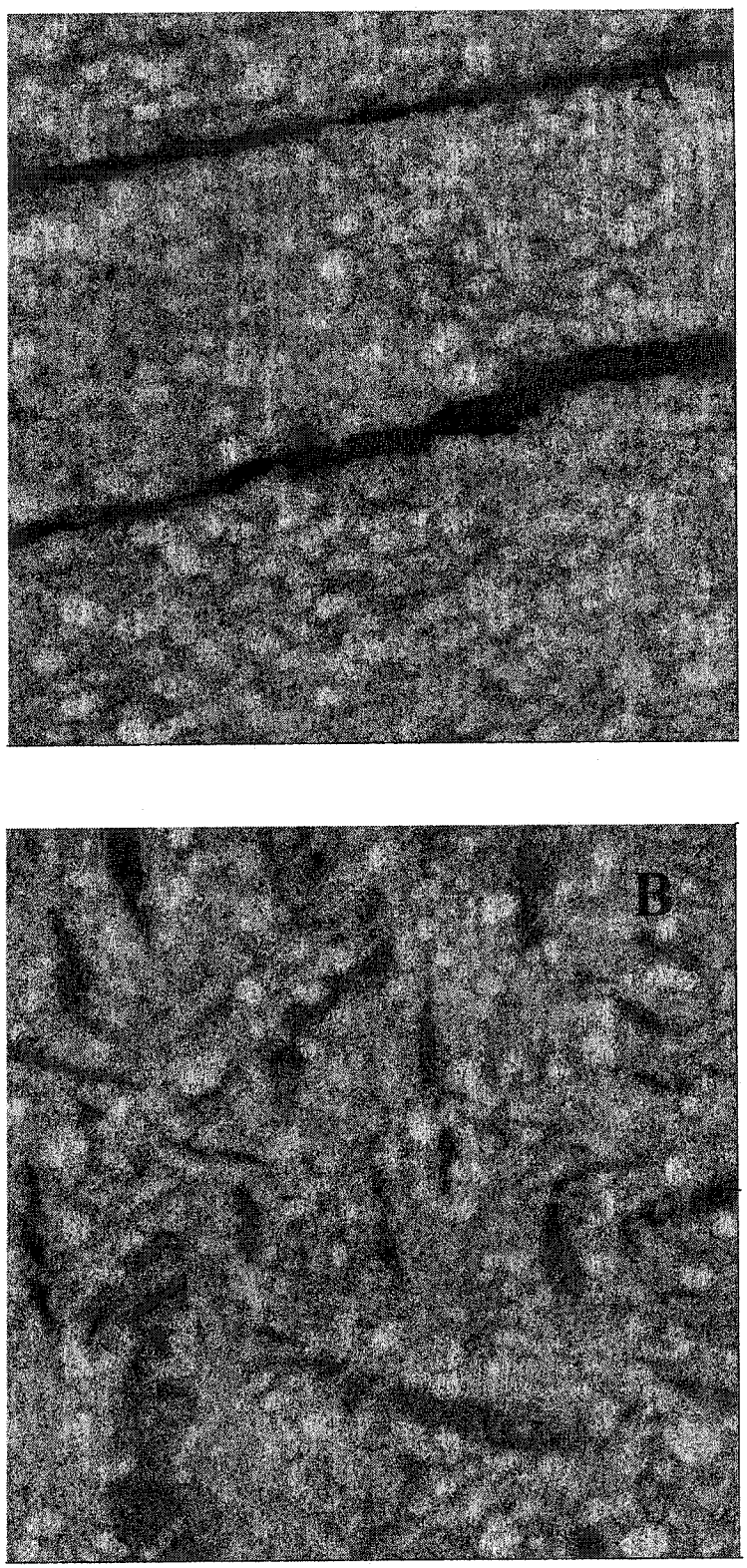


Figure 5.5. 2 x 2 μm AFM images of PAni films on oxidized HOPG with 0 mM 1-dodecanol (A), 0.1 mM 1-dodecanol (B).

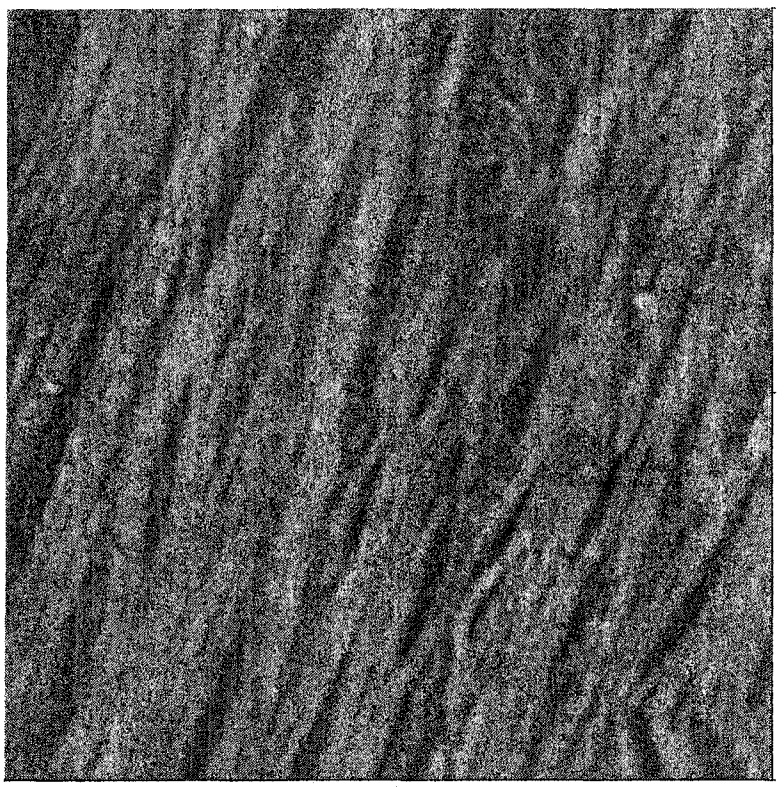


Figure 5.6. 2 x 2 μm AFM images of PAni films on oxidized HOPG with 0.1 mM of 1-dodecanol and 3 hours of polymerization.

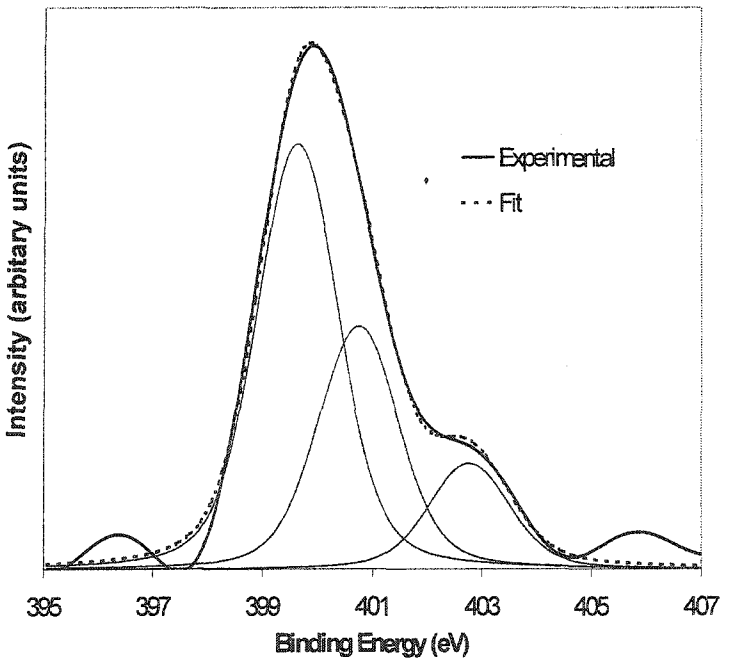


Figure 5.7. X-ray photoelectron spectroscopy of PAni wires on chemically treated HOPG indicating curve fitting and the different nitrogen environments.

Differences in film morphology with respect to surface treatment can be explained by a change in interaction between the surfactant and surface. For freshly cleaved HOPG the interaction between the surfactant and surface is primarily due to interactions between the tail group and surface, consistent with monolayer coverage. In the case of a less hydrophobic substrate, i.e. graphite chemically treated with ammonium persulfate, interactions between the head group and surface predominate leading to bilayer coverage, which in turn leads to features with larger dimensions (see proposed mechanism in Figure 1). Measurements of the height differences are consistent with this explanation; the height of the film shown in Figure 5.2A (periodicity of 16.7 nm) has been measured as 1.5 ± 0.4 nm, while Figure 5.6 (periodicity of 44.5 nm) has a height of 4.7 ± 1.9 nm. As mentioned previously, the tip is likely not contacting the surface of the graphite and almost certainly these height values are not quantitatively correct although this difference certainly represents a difference in polymer morphology.

If APS-treated graphite is soaked in water for a few hours prior to reaction, the results are the same as using freshly cleaved HOPG indicating that intercalated ions diffuse back out of the graphene lattice. Conversely, even though APS is present in reactions with freshly-cleaved HOPG, we believe that adsorption of surfactant occurs before addition of APS and therefore

retards (or at least slows down the kinetics of) APS intercalation and hence the surface is hydrophobic with respect to surfactant adsorption and subsequent polymerization.

B. Polypyrrole

In the studies of PAni described above, the morphology of the synthesized polymer was controlled by varying the template morphology using either the surfactant-surface energetic interaction or the addition of a co-adsorbing molecule. Another parameter we wished to examine was hydrophobe length, and further, we wished to determine whether the templating effect could be induced with a monomer other than aniline. Hence, three sodium 1-alkyl sulfonate surfactants were used; 1-octanesulfonate, 1-decanesulfonate, and 1-dodecanesulfonate. Sulfonate surfactants were used because the adsolubilization of pyrrole is somewhat limited in sulfate aggregates without the addition of electrolyte.[23] The disadvantage of this choice is that the adsorption of sodium sulfonate surfactants on atomically smooth surfaces has not been studied by AFM to our knowledge; therefore, the initial morphology of the surfactant aggregates in the absence of pyrrole is unknown.

In Figures 5.8 and 5.9 one can see the effect of varying the length of the hydrophobic moiety in the surfactant on PPy film formation. In Figure 5.8A

PPy spheres are observed for C_8 with a diameter of approximately 25.6 ± 2.8 nm. Increasing the length of the hydrophobe by two methylene groups to C_{10} creates a smaller spherical morphology (18.2 ± 1.9 nm) and a reduced film roughness indicated by the AFM cross section analysis (Figure 5.8B). A smaller spherical diameter in the case of C_{10} is somewhat counterintuitive although can be explained in terms of the critical micelle concentration (cmc). As the same concentration of surfactant is used in all cases, experimental conditions for C_{10} are closer to the cmc than for C_8 and hence the number density of spheres adsorbed on the surface is expected to be greater for the C_{10} surfactant, which in turn limits the size of polymer spheres. In contrast to spherical structures observed for C_8 and C_{10} hydrophobes, a featureless film is found in the case of C_{12} (Figure 5.9A). The transition from spherical to flat morphologies is predicted by the packing parameter of solution aggregates for an increase in length of the hydrophobe. Addition of 1-octanol to the C_8 system did not appear to affect the size or curvature of the PPy spheres as spheres with an average diameter of 27.5 ± 3.2 nm were observed at the highest concentration of 1-octanol investigated. However, 1-decanol did induce a phase transition to reduced curvature PPy films in the C_{10} system and subsequently to a featureless layer as evidenced by the cross section (Figure 5.9B).

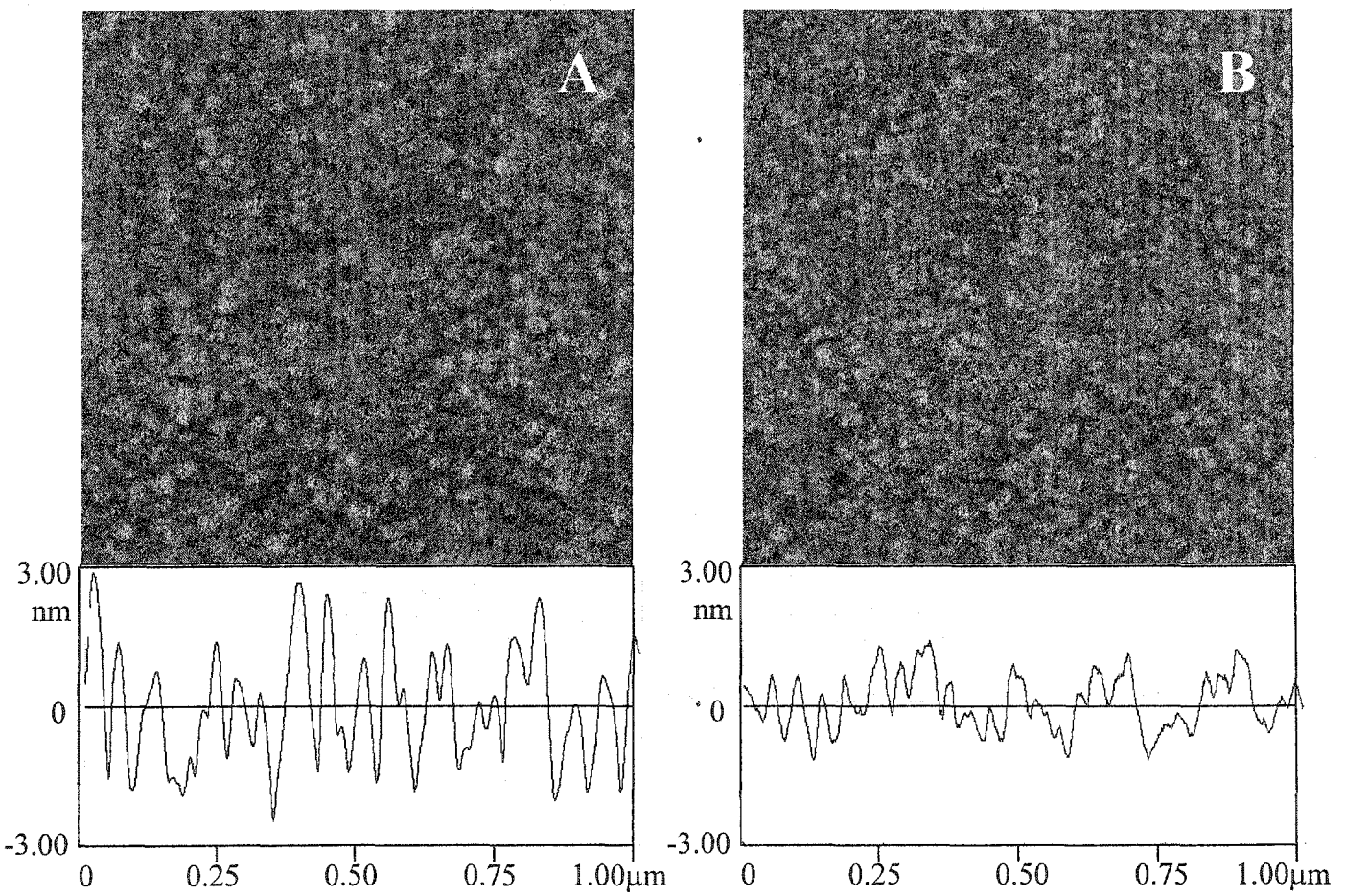


Figure 5.8. 1 x 1 μm AFM images of PPy films on HOPG Sodium 1-octanesulfonate (A), Sodium 1-decanesulfonate (B).

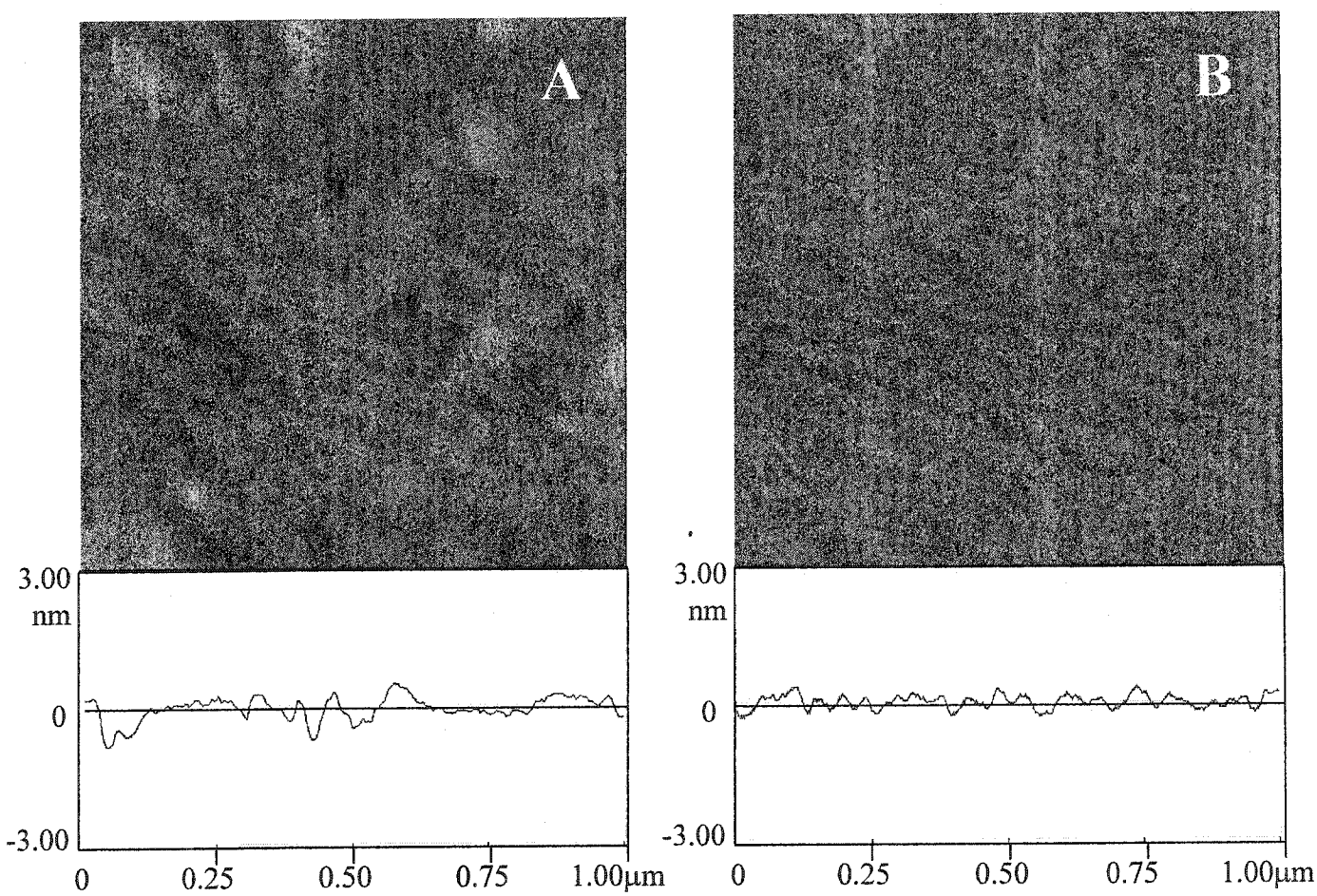


Figure 5.9. 1 x 1 μm AFM images of PPy films on HOPG Sodium 1-dodecanesulfonate (A), Sodium 1-decanesulfonate with 0.8 mM decanol (B).

Although films of PPy on HOPG appear to be spherical, one would expect that the films are hemi-spherical by considering the hydrophobicity of HOPG. The film thickness was measured by masking a portion of the HOPG from reaction. Surface masking was accomplished by trapping a bubble against the side of the vial and over a section of HOPG so that an edge was created across which one could measure the film thickness. Figure 5.10A represents the edge of the PPy film for the case of C_8. There is a slight disruption in film thickness at the edge of the bubble although the height can be estimated by placing cursors at selected points as shown in figure 5.10B. Multiple measurements indicate that the film thickness is very close to the measured diameter of the spheres (28 nm) indicating that indeed the film is composed of PPy nanospheres, not hemispheres. The same experiment was carried out for PPy films on HOPG in the case of C_{10} (Figure 5.8C). Once again the film thickness is found to correlate well with the measured diameter of the PPy structures at 16 nm. Therefore PPy nanospheres are also synthesized on HOPG in the C_{10} system.

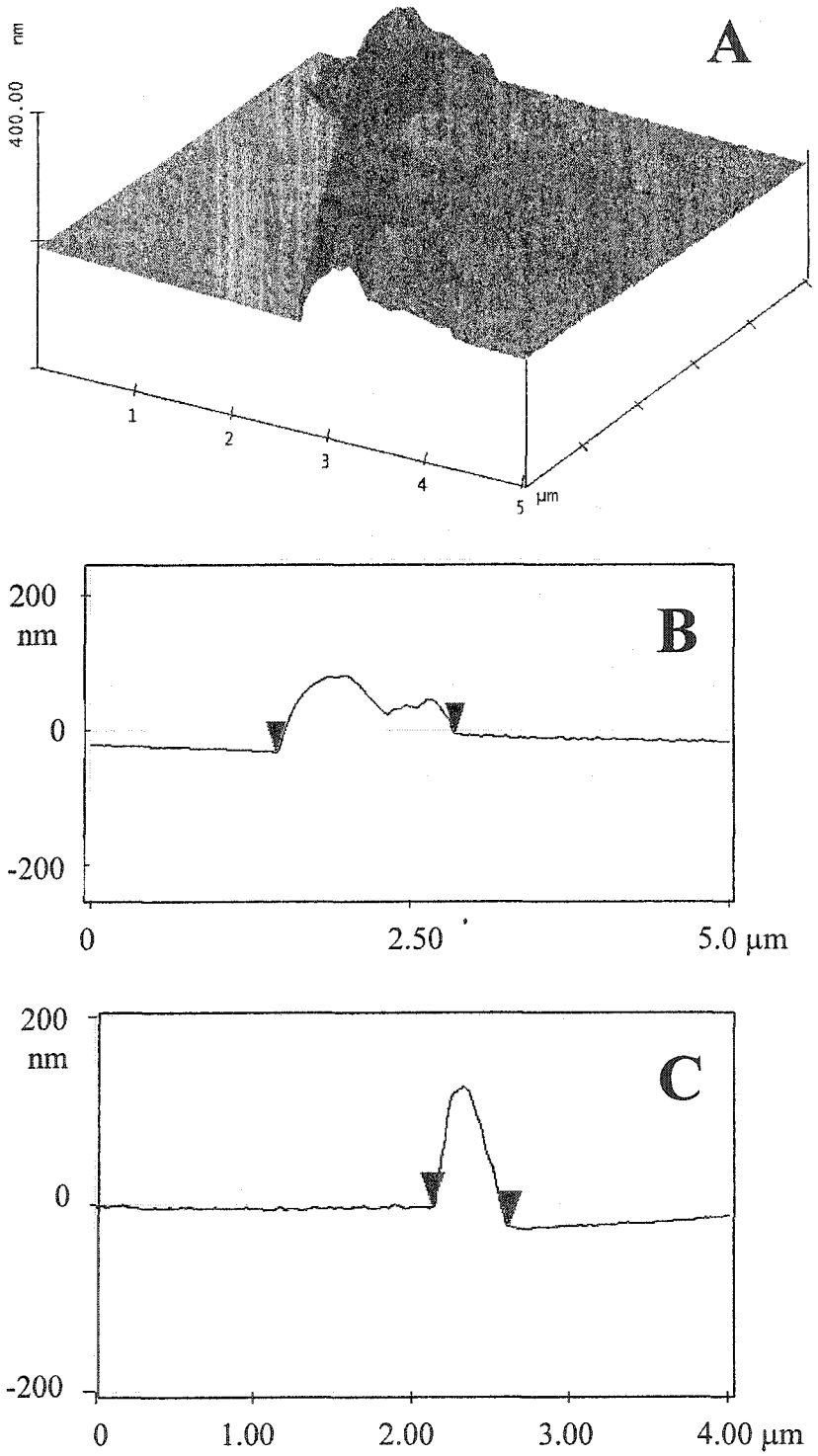


Figure 5.10. Cross-sectional analysis of PPy films for C_8 system indicating polymer film on the right side of the image and bare HOPG on the left side of the film edge (A). Height of the film measured between the markers for C_8 (B) and C_{10} (C) with heights of 26 nm and 16 nm respectively.

The question now arises as to why the PPy films are spherical and not hemi-spherical in nature. To answer this fresh HOPG was chemically modified with APS as previously described to form a more hydrophilic surface and the synthesis of PPy was carried out in an identical fashion as before. Resulting PPy films were identical in morphology and thickness to those obtained with freshly cleaved HOPG. From this result we believe that the surface of the freshly cleaved HOPG is chemically altered upon addition of APS even after the adsorption of surfactant and monomer. With SDS, the surface maintained its hydrophobicity in the presence of APS if surfactant and monomer was already adsorbed. This difference is probably due to low surface coverage of the sulfonate surfactants; since the concentration used were far below the CMC for the C_8 and C_{10} systems (0.03*cmc and 0.13*cmc respectively), while for SDS the concentrations used were roughly 0.7*cmc.

In this study we chose to keep the surfactant and monomer concentrations the same for all three surfactants, (5.4 mM and 2.7 mM respectively) irrespective of the surfactant's cmc. Surfactant concentrations of 5.4 mM correspond to approximately 0.03*cmc, 0.13*cmc and 0.45*cmc for C_8, C_{10} and C_{12} respectively,[24] where the cmc's correspond to those measured without monomer. In a different set of experiments, surfactant concentrations were fixed at 0.67*cmc, and the monomer concentration fixed at 2.7 mM. For C_8

and C_{10} systems, which had much higher surfactant concentrations than 5.4 mM, there was no noticeable coverage of polymer on the substrate indicating not enough monomer was localized at the surface. Increasing the monomer concentration so that the surfactant to monomer concentration was kept at a 2:1 ratio, as used for the other experiments, leads to large amounts of solution polymerization which in turn deposits on the graphite and obscures the surface.

III. Conclusions

Adsorbed surfactant aggregates function as templates for the formation of morphologically controlled polymer films of π-conjugated polymers with sub 100 nm features. The capability to synthesize and arrange the polymer in one step in order to retain the properties of the material by eliminating subsequent treatment or processing is key to producing organic electronic devices. The structure of the polymer film can be controlled by the addition of co-adsorbing molecules which induce phase transitions in the order of spherical → cylindrical → planar. Additionally, film morphologies are shown to be sensitive to the length of the surfactant hydrophobe, with the same sort of phase transitions occurring with changes in hydrophobe length, i.e. spherical → cylindrical → planar with increasing hydrophobe length. Unique to surface aggregation, a third variable, the

interaction between the surface and the surfactant, can be used to alter the morphology in a manner which agrees qualitatively with expectations. Other variables are also probably available to elicit structural control, including electrolyte concentration, temperature, pH, or possibly monomer type and concentration. Thorough experimentation and theoretical modeling will yield a better understanding of this phenomenon, and should lead to a technique that can be tailored to many polymers and surfaces in which one can not only synthesize, but also pattern at nanoscale dimensions.

IV. Acknowledgements

The authors would like to thank the National Science Foundation (CTS-0210485) for the financial support for this work. The authors would also like to thank Dr. Andrew Back of the Evans PHI Laboratory, Physical Electronics, Aaron Lowe and John Jacobs from the University of Wisconsin, Materials Science and Engineering, and Zhongrui Li from the University of Oklahoma, Department of Chemical Engineering and Materials Science for conducting XPS experiments.

V. References

[1] Rabe, J. P. *Curr. Opin. Colloid Interface Sci.* **1998**, 3(1), 27.

[2] Djuve, J.; Grant, L. M.; Sjöblom, J.; Goloub, T. P.; Pugh, R. J. *Langmuir* **2002**, 18, 2673.

[3] (a) Kwak, J. C. T. *Polymer-Surfactant Systems*; Marcel Dekker: New York, 1998; Vol. 77. (b) Goddard, E. D. *Colloid Surf.* **1986**, 19, 255. (c) Goddard, E. D. In *Interactions of surfactants with polymers and proteins*; Goddard, E. D., Ananthapadmanabhan, K. P., Eds.; CRC Press: Boca Raton, FL, 1993; pp 203-276. (d) Lindman, B.; Thalberg, K. In *Interactions of surfactants with polymers and proteins*; Goddard, E. D., Ananthapadmanabhan, K. P., Eds.; CRC Press: Boca Raton, FL, 1993; pp 203-276. (e) Bárány, S. *Macromol. Symp.* **2001**, 166, 71.

[4] Holdcroft S. *Adv.Mater.* **2001**, 13, 1753.

[5] Abdou, M. S. A.; Xie, Z. W.; Leung, A. M. *Synth. Met.* **1992**, 52, 159.

[6] Gorman, C. B.; Biebuyck, H. A.; Whitesides, G. M. *Chem. Mater.* **1995**, 7, 526. Rzsnyai, L. F.; Wrighton, M. S. *Langmuir* **1995**, 11, 3913.

[7] Garnier, F.; Hadjlaoui, R.; Yasser, A. Scivastava, P. *Science* **1994**, 265, 1684.

[8] Bargon, J.; Behnck, W.; Weidenbrueck, T.; Ueno, T. *Synth. Met.* **1991**, 41, 1111.

[9] Magnus Persson, S. H.; Kyreklev, P.; Inganas, O. *Adv. Mater.* **1996**, 8, 405.

[10] (a) Li, W. Z.; Xie, S. S.; Qian, L. X.; Chang, B. H.; Zou, B. S.; Zhou, W. Y.; Zhao, R. A.; Wang, G. *Science* **1996**, 274, 1701. (b) Ren, Z. F.; Huang, Z. P.; Xu, J. W.; Wang, J. H.; Bush, P.; Siegel, M. P.; Provencio, P. N. *Science* **1998**, 282, 1150. (c) Huanh, M. H.; Mao, S.; Feick, H.; Yan, H.; Wu, Y.; Kind, H.; Webber, E.; Russo, R.; Yang, P. *Science* **2001**, 292, 1897. (d) Yu, D. P.; Xing, Y. J.; Hang, Q. L.; Yang, H. F.; Xu, J.; Xi, H.; Feng, S. Q. *Physica E* **2001**, 9, 305. (e) Chen, L. C.; Chang, S. W.; Chang, C. S.; Wen, C. Y.; Wu, J. –J.; Chen, Y. F.; Huang, Y. S.; Chen, K. H. *J. Phys. Chem. Solids* **2001**, 62, 1567.

[11] Biggs, S.; Walker, L. M.; Kline S. R. *Nano Lett.* **2002**, 2(12), 1409.

[12] Liu, J. F.; and Ducker, W. A. *Langmuir* **2000**, 16, 3467.

[13] Okawa, Y.; Masakazu, A. Nanoscale Control of Chain Polymerization. Nature **2001**, *409*, 683-684.

[14] Maynor, B. W.; Filocamo, S. F.; Grinstaff, M. W.; Liu, J. *J. Am. Chem. Soc.* **2002**, 124, 522.

[15] Liang, L.; Liu, J.; Windisch, Jr., C. F.; Exarhos, G. J.; Lin, Y. *Angew. Chem. Int. Ed.* **2002**, 41(19), 3665.

[16] Ducker, W. A.; and Wanless, E. J. *Langmuir* **1996**, 12, 5915.

[17] Wanless E. J.; Ducker W. A. *J. Phys. Chem.* **1996**, 100, 3207.

[18] Kim, B. J.; Im, S. S.; Oh, S. G. *Langmuir*, **2001**, 17, 565.

[19] (a) Kim, B. J.; Oh, S. G.; Han, M. G.; Im, S. S. *Langmuir* **2000**, 16, 5841. (b) Kang, E. T.; Neoh, K. G.; Tan, T. C.; Khor, C. S. H.; Tan, K. L. *Macromolecules* **1990**, 23, 2918.

[20] Han, M. G.; Cho, S. K.; Oh, S. G.; Im, S. S. *Synth. Met.* **2002**, 126, 53.

[21] We cannot rule out that some contribution to positively charged nitrogen may come from intercalated ammonium ions beneath the polymer film.

[22] Yamada, T.; Miyake, K.; Ishida, M.; Hata, K.; Morita, R.; Yamashita, M.; Shigekawa, H. *Synth. Met.* **1999**, 103, 2653.

[23] Funkhouser, G. P.; Arévalo, M. P.; Glatzhofer, D. T.; O'Rear, E. A. *Langmuir* **1995**, 11, 1443.

[24] Rosen, M. J. *Surfactants and Interfacial Phenomena 2nd ed.*; Wiley Interscience: New York, 1989.

Chapter 6. Atomic force microscopy studies of polymer films synthesized in the presence of surfactant

A. Polyaniline synthesis on highly oriented pyrolytic graphite using sodium sulfonate surfactants

A detailed study of PAni synthesis using adsorbed SDS aggregates was performed in Chapter 5, while Chapter 5 also contained details of PPy synthesis carried out in the presence of sodium sulfonate surfactants. In more recent work, PAni film formation has been investigated in the presence of sodium sulfonate surfactants with different length hydrophobes; 1-octanesulfonate, 1-decanesulfonate, and 1-dodecanesulfonate. Experimental design was identical to previously described procedures although adsorption and reaction was carried out at 40°C to eliminate precipitation. Additionally, surfactant concentrations were chosen at two thirds of the cmc in all cases and monomer concentrations of 4mM were used.

Figure 6.1 shows an AFM image of PAni films synthesized in the presence of 1-octanesulfonate on HOPG. Spherical structures are observed with diameters on the order of 50 nm. In contrast, Figure 6.2

represents an AFM image of a PAni film fabricated in the presence of 1-decanesulfonate. Polymeric wires are present with diameters ca. 50 nm although there appears to be high degree of bundling of the wires. Also a large amount of deposited polymer on top of the film is present which is likely a result of either solution or emulsion polymerization. Interestingly the morphology of the deposited polymer appears to be spherical indicating a difference in polymer morphology in solution and on the surface of the substrate. A further increase in the surfactant hydrophobe to C_{12} (Figure 6.3) appears to induce a subsequent shape transition to a relatively flat film. Once again deposition, which is likely from solution or emulsion polymerization, is evident on the surface of the film and appears to be spherical in nature.

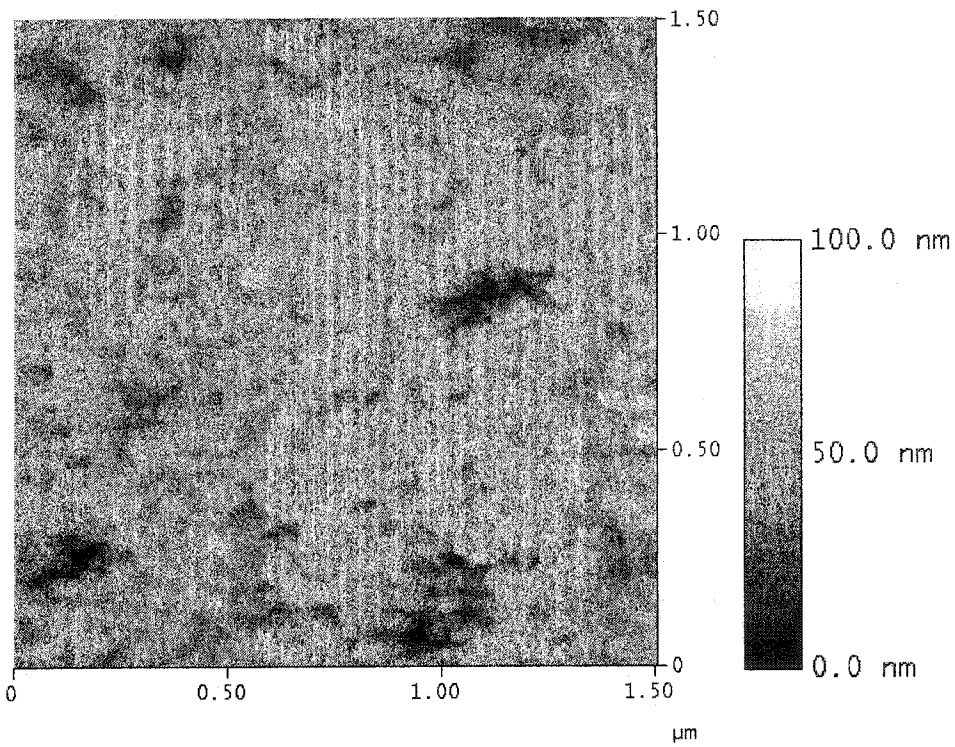


Figure 6.1. AFM image of PAni film on HOPG synthesized using C_8 sulfonate.

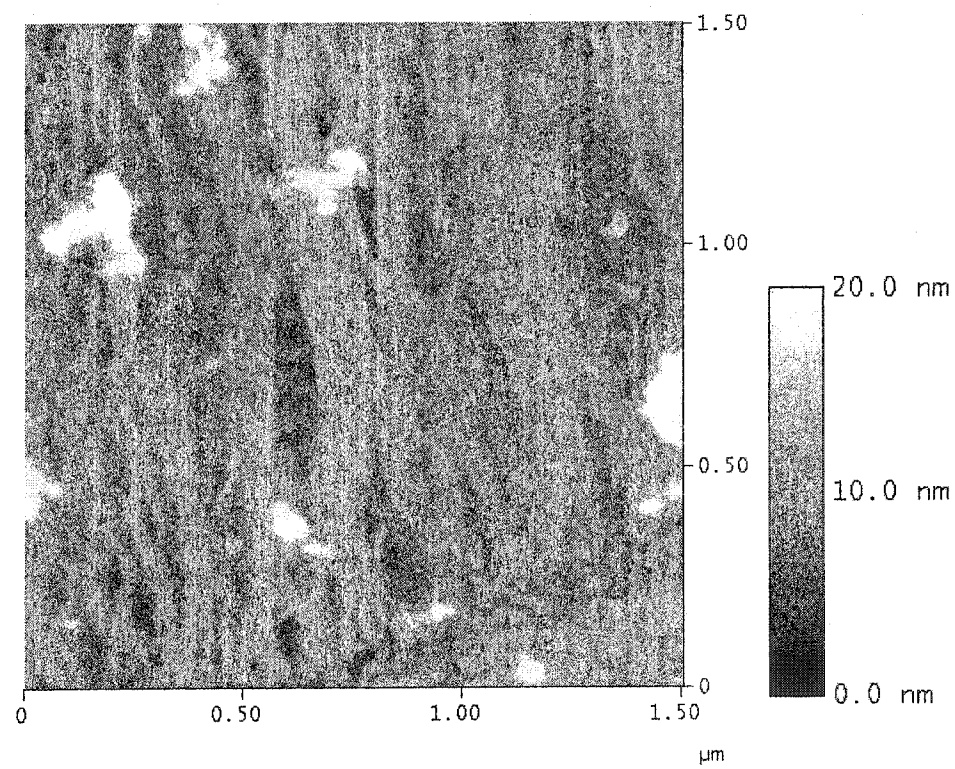


Figure 6.2. AFM image of PAni film on HOPG synthesized using C_{10} sulfonate.

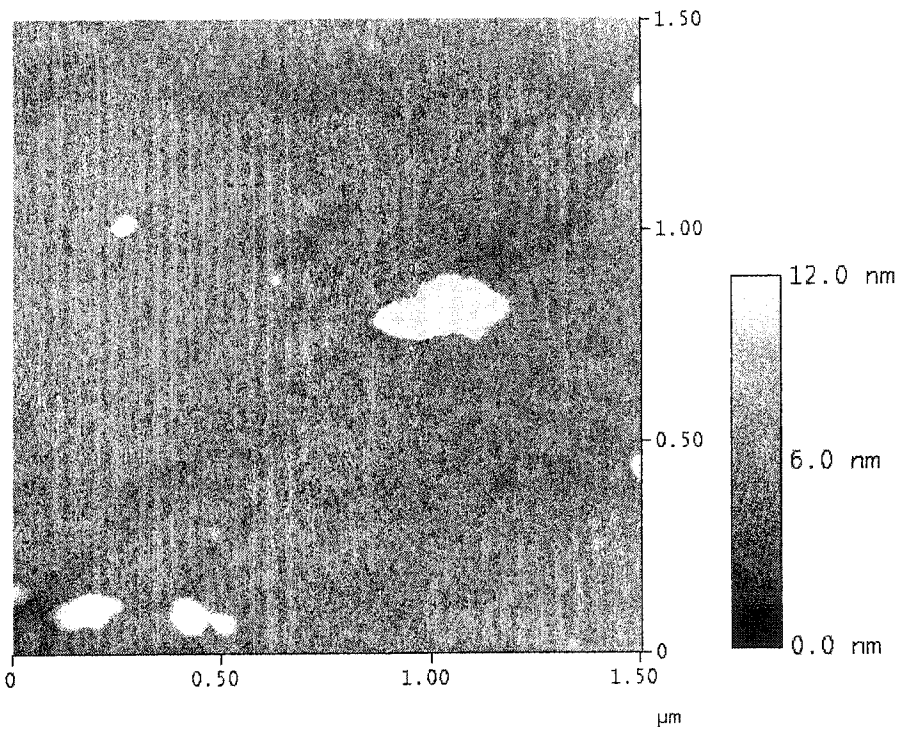


Figure 6.3. AFM image of PAni film on HOPG synthesized using C_{12} sulfonate.

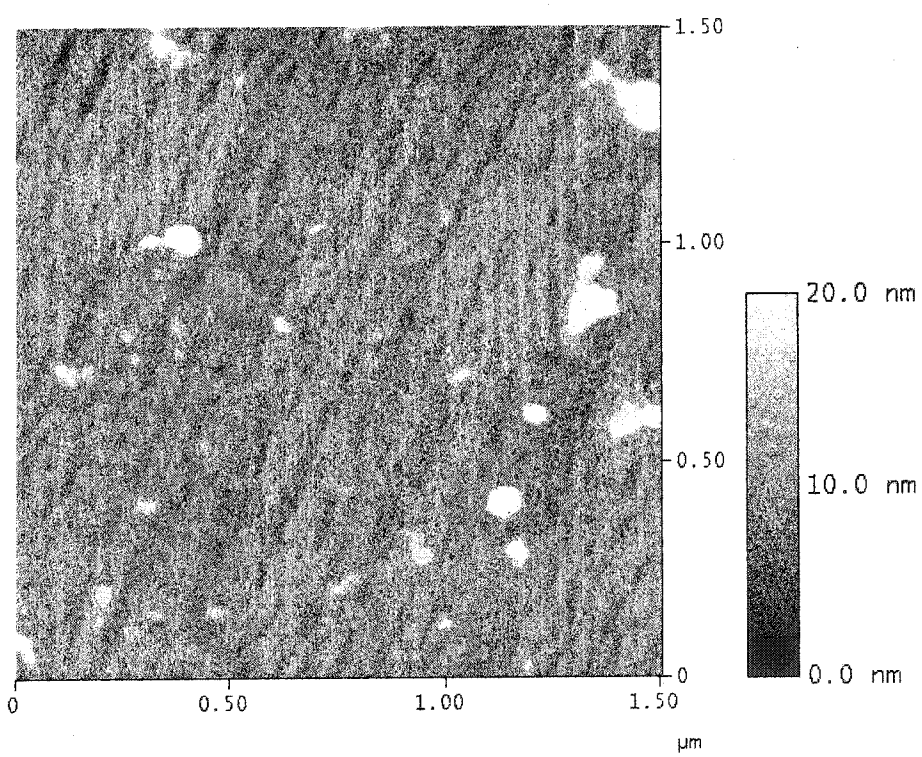


Figure 6.4. AFM image of PAni film on chemically treated HOPG synthesized using C_8 sulfonate.

In another experiment, HOPG was chemically treated (for treatment procedure see chapter 2) and then the synthesis of PAni was carried out in the presence of 1-dodecanesulfonate. Figure 6.4 indicates that there is a change in morphology from a flat film (Figure 6.3) to wires. Once again, a large amount of deposition is present on the film.

Of interest from the results explained previously is a comparison of figures 5.6 and 6.4. In Figure 5.6 PAni spheres are synthesized on chemically treated HOPG using sodium dodecyl sulfate as a template. In contrast (Figure 6.4) PAni wires are fabricated on chemically treated HOPG using sodium dodecyl sulfonate. Such a change in morphology is what would be expected as sodium dodecyl sulfate has a larger headgroup size in comparison to sodium dodecyl sulfonate. The result of a larger area occupied by the headgroup (with all other parameters being equal) is a lower value for the packing parameter. A reduction in the packing parameter favors higher curvature aggregates. Therefore the transition from sphere (for sodium dodecyl sulfate) to rod-like (for sodium dodecyl sulfonate) would be expected.

B. PAni synthesis on silicon dioxide using sodium sulfonate surfactants

Synthesis of PAni was performed on silicon dioxide in an attempt to produce nanowires on an insulating substrate. Experimental conditions were as described in the previous section of this chapter. Silicon chips having approximate dimensions of ,5 x 5 mm were used as received therefore the thickness of the oxide layer was unknown.

In Figures 6.5 through 6.8 spherical structures are observed on the surface of the substrate. The diameter of these structures decreases as hydrophobe length is increased from C_8 (Figure 6.5) to C_{10} (Figure 6.6) to C_{12} (Figure 6.7). These observations were also made in chapter 5 when investigating PPy films on HOPG with respect to hydrophobe length. In addition, the amount of polymer on the surface appears to decrease with increasing hydrophobe length. It may be interesting to note that by visual inspection during synthesis, color changes in solution (indicative of reaction) appear first for the C_{12} system, then for C_{10} and then for C_8. Such an observation may reveal that aniline monomers are more easily accessible for polymerization in the presence of surfactants with longer hydrophobic moieties.[1]

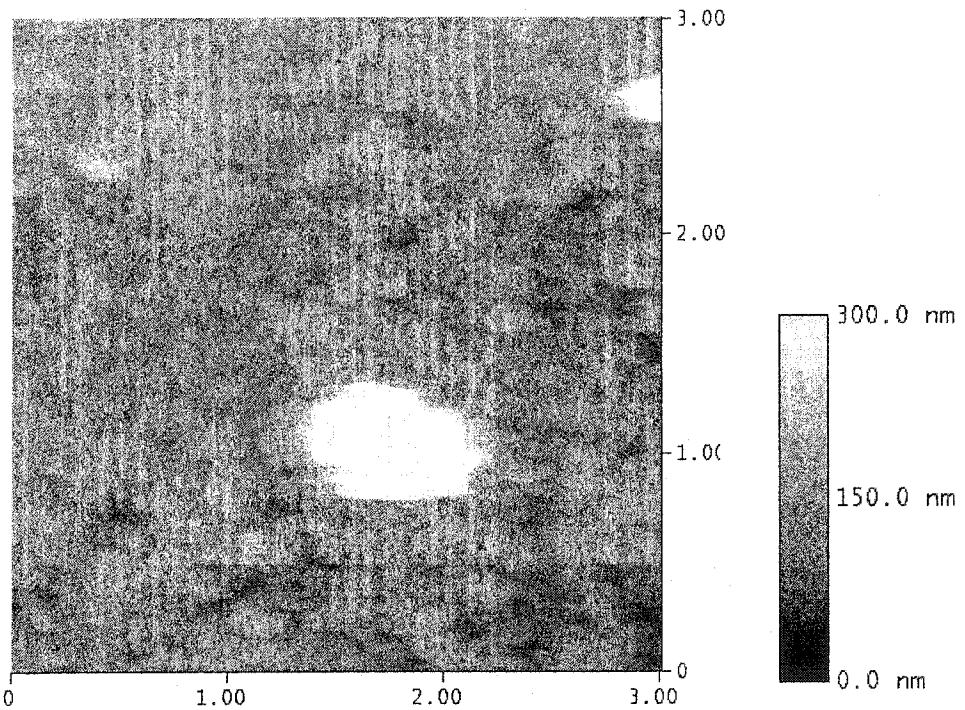


Figure 6.5. AFM image of PAni film on SiO_2 synthesized using C_8 sulfonate.

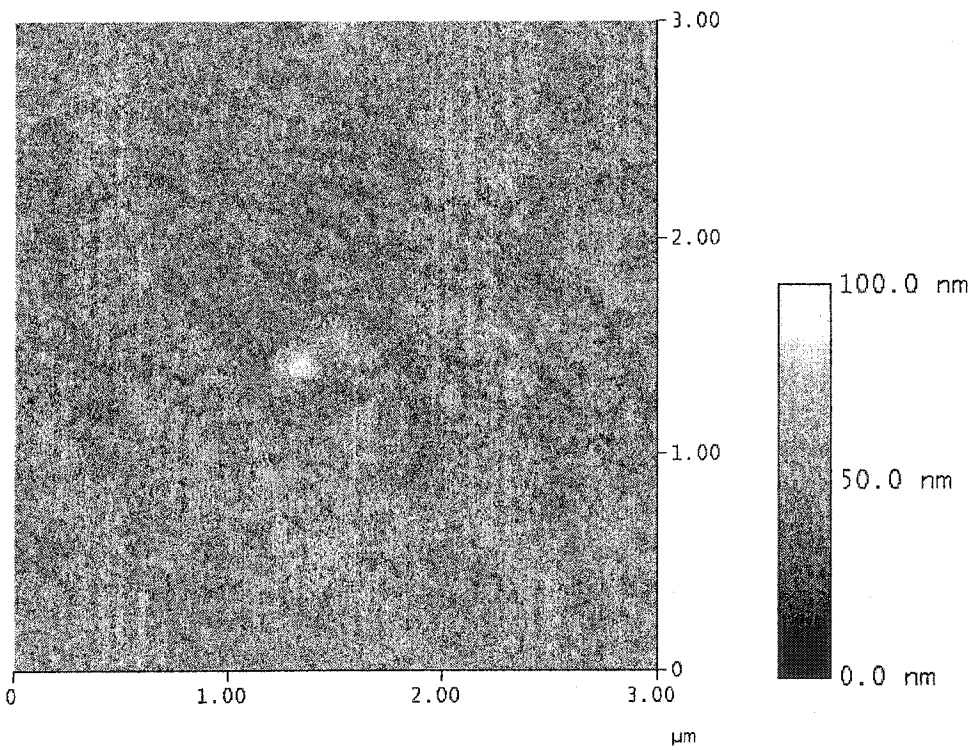


Figure 6.6. AFM image of PAni film on SiO_2 synthesized using C_{10} sulfonate.

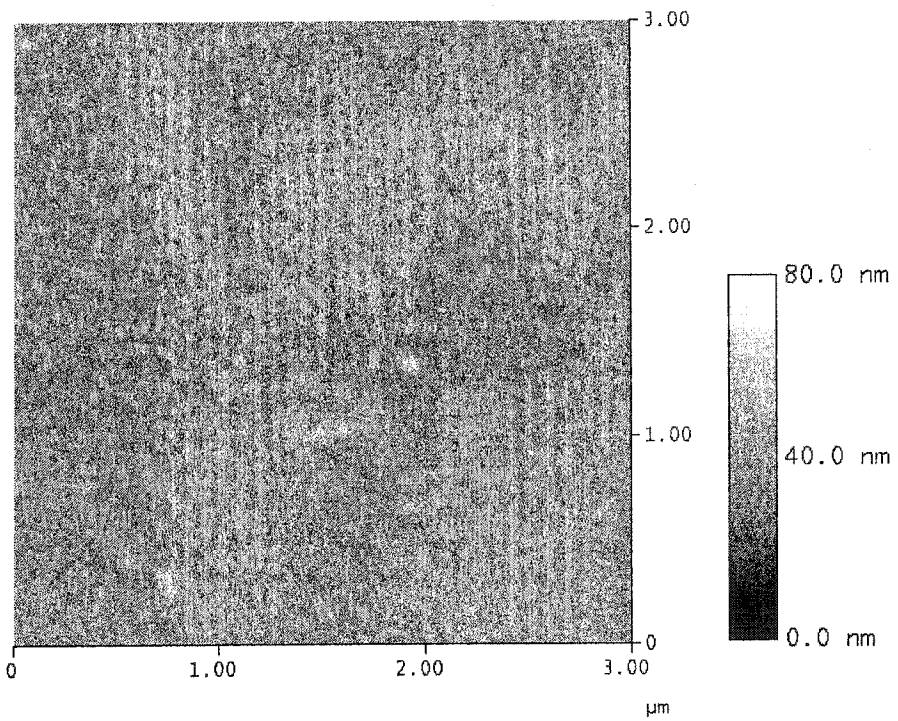


Figure 6.7. AFM image of PAni film on SiO_2 synthesized using C_{12} sulfonate.

C. PAni synthesis on mica using sodium dodecyl sulfate

PAni has been synthesized on mica in the presence of SDS (5.4mM aniline and 5.4mM SDS at 2°C). Experiments carried out at a pH of 2 adjusted with HCl did not produce polymer at the solid interface; AFM images after polymerization were consistent with freshly cleaved mica. Experiments carried out at a neutral pH produced an orange color on polymerization and did produce structures on the surface of mica. Figure 6.8 shows an aligned film covering the surface of the mica. This alignment is evident over large areas of the surface of mica with directional changes occurring at steps in the surface as shown by an optical micrograph, Figure 6.9. Figure 6.10 shows an area in which individual structures are discernable with diameters ca. 50 nm and heights ca. 12 nm.

To identify the chemical composition of these films XPS was used. Figure 6.11 shows an XPS spectra on the N1s nitrogen environment. From this spectra one can identify three different nitrogen peaks that are characteristic of PAni. Due to synthesis taking place at a neutral pH, PAni is probably of low molecular weight. In a recent study PAni that was synthesized exhibiting an orange color, as opposed to dark green, was referred to as oligomeric material.[2]

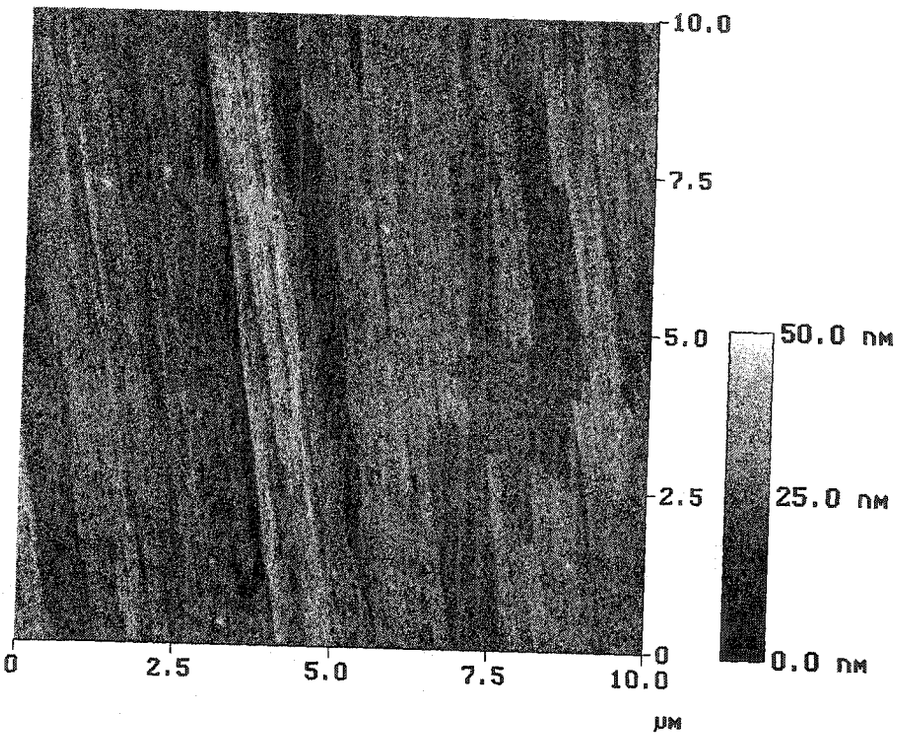


Figure 6.8. AFM image of PAni film on mica synthesized using sodium dodecyl sulfate.

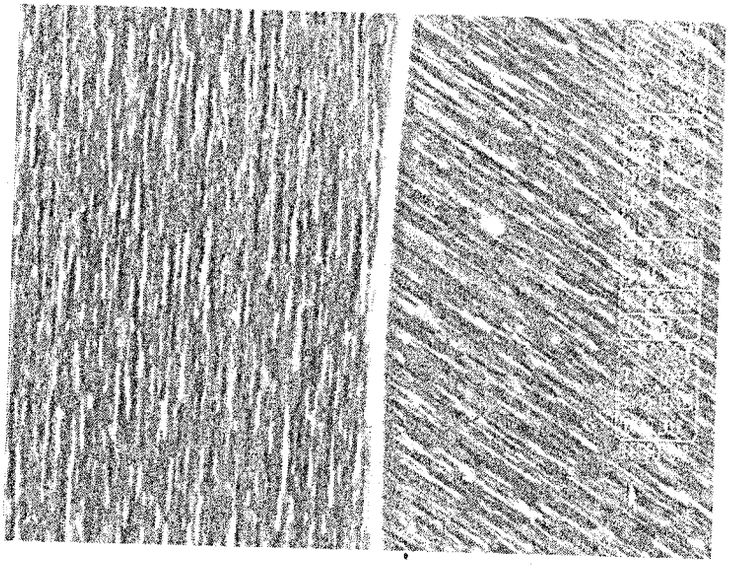


Figure 6.9. Optical micrograph of PAni film on mica indicating directional changes associated with steps in the surface. For reference the image is 100 x 75 microns.

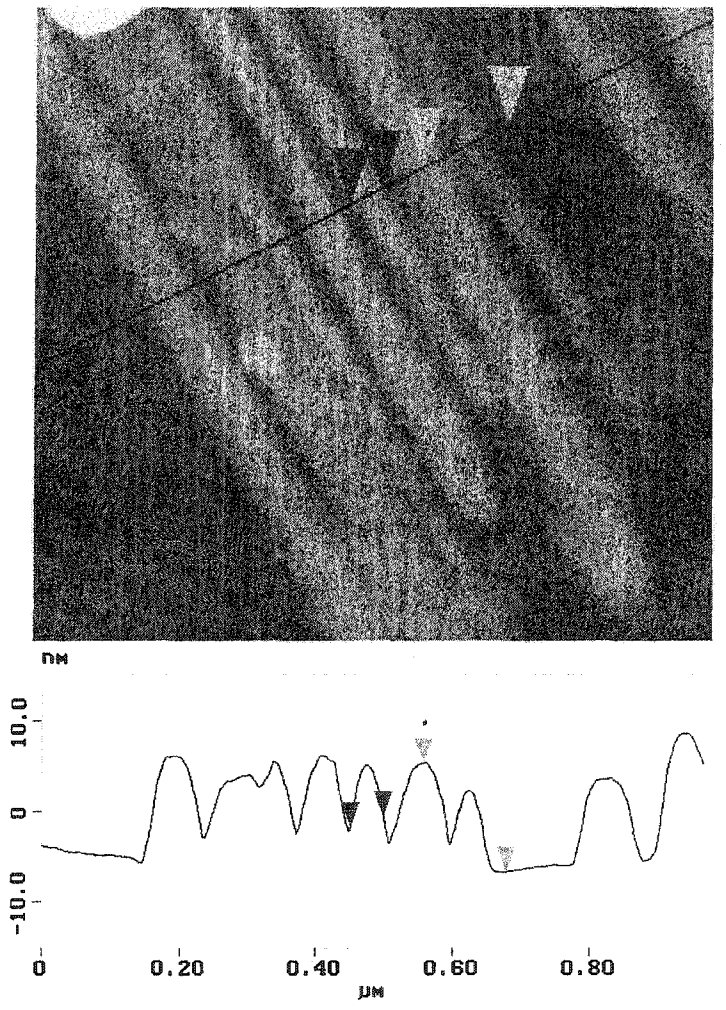


Figure 6.10. Cross section of PAni film as synthesized in Figure 6.8. Some individual wire like structures are present with diameters on the order of 50 nm. Vertical height of the film appears to be ca. 12 nm.

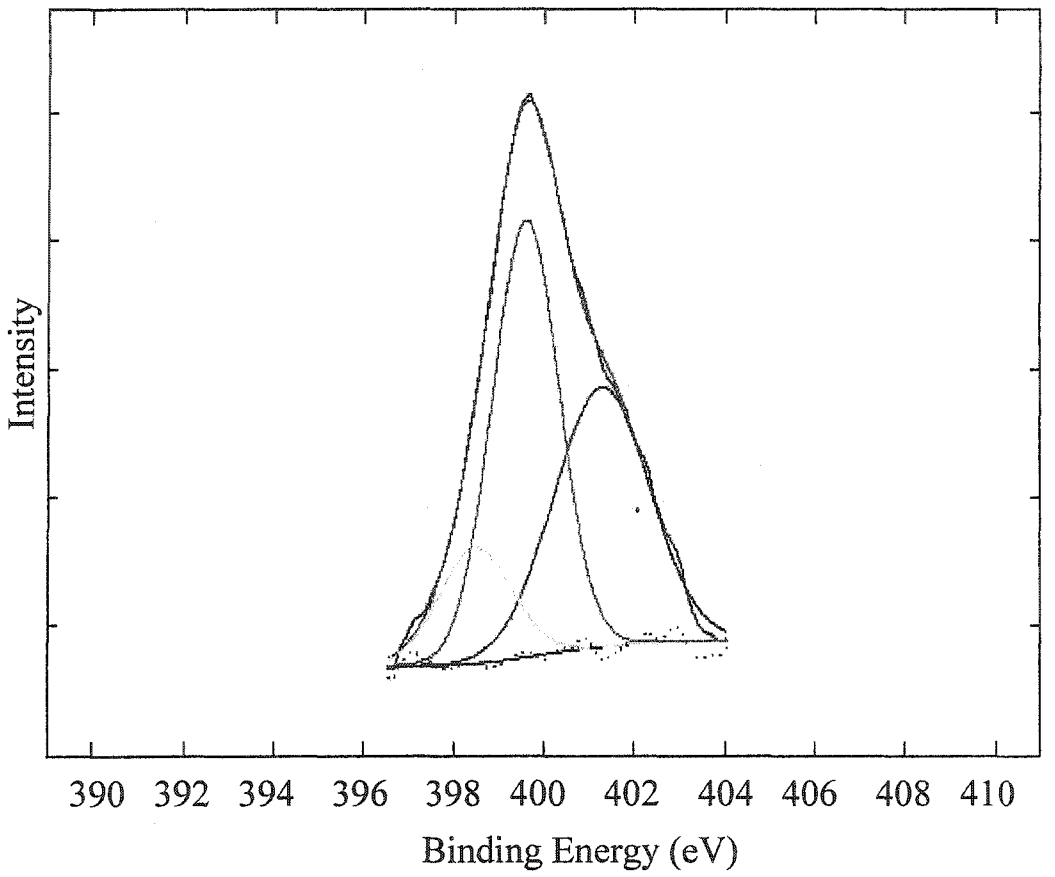


Figure 6.11. N1s nitrogen environment of PAni film synthesized on the surface of mica. Deconvolution leads to peaks centered at 398.5, 399.6, and 401.38 with areas of 13.7, 46.7, and 39.6 % respectively.

II. References

[1] A limited number of experiments have been carried out in an effort to achieve morphological control of these polymer films by the addition of long chain alcohols. These experiments have been unsuccessful at this point in time.

[2] Huang, J.; Virji, S.; Weiller, B. H.; Kaner, R. B. *J. Am. Chem. Soc.* **2003**, 125, 314.

Chapter 7. Conclusions and Recommendations

I. Conclusions

In chapter 3 the cmc of SDS was measured in the presence of adsorbing substrates. When alumina and titania was present as an adsorbent, the cmc of SDS was reduced in both instances. Measurement of the sodium ion concentration with respect to SDS in solution indicated that the concentration of sodium ions in the bulk was higher than the concentration of bulk SDS. This mismatch in sodium ion concentration was attributed to sodium counter ions being released as SDS adsorbed to the substrate. The reduction in cmc was therefore attributed to be due to free sodium ions in the bulk capable of decreasing repulsion between SDS headgroups and therefore reducing the cmc.

In other work (chapter 4) adsorbed surfactants were used in the polymerization of PAni and PPy thin films on acidic alumina. Apparent conductivity of the particles was found to increase by approximately eight orders of magnitude to ~ 10^{-1} S/cm in the presence of a conducting polymer film. For both polymers, contact conductivity reached a plateau region at approximately 15 weight percent of organics, suggestive of complete surface coverage with polymer. This result was validated by XPS and wetting experiments.

In an extension to this work, and for the first time, adsorbed surfactant templates have been used for the synthesis of morphologically controlled electrically conducting polymer films with nanoscale dimensions on flat surfaces. In chapters 5 & 6 results are presented showing that adsorbed aggregates can be used as templates to synthesize morphologically controlled structures of both PAni and PPy. In a similar fashion to adsorbed surfactant aggregates, the morphology of the polymer films can be exquisitely controlled by changes in either the surface chemistry or by the addition of co-adsorbing molecules. This technique has advantages over other techniques for the synthesis of conducting 1-D nanostructures outlined in chapter 1, as many nanowires can be fabricated on a surface in ordered arrays by a *one-step* procedure.

II. Recommendations and future work

A. Thin film modification of alumina particles with polyaniline and polypyrrole

Follow-up work can be performed with conductive fillers produced by the method outlined in chapter 4. In chapter 4 alumina particles were prepared with contact conductivities that were controllable as a function of

surface coverage. The next step would be to evaluate the use of these fillers to provide composite materials with tunable conductivities. Since there is a demand for polymeric conducting materials of which one has the ability to color, it may be possible to produce thin polymer films of either PAni or PPy on alumina which are opaque and therefore colorable. At present PPy coated alumina particles with a pale gray appearance do not afford high enough conductivities for this purpose therefore tuning of certain parameters such as reaction conditions or dopant need to be addressed.

B. Synthesis of morphologically controlled films on flat surfaces

Work reported in chapter 5 and also in chapter 6, creates many new opportunities for further investigations. At present the conductivity of individual nanowires has not been evaluated since isolation of wires on HOPG is very difficult. Conductivity may be measured if the wires are removed from HOPG and deposited on grids that are now available from companies such as Keithley. Removal of the wires may prove to be difficult requiring sonication in alcohol.

At this point it is not clear what the morphology of the surfactant/monomer aggregate is prior to polymerization. To address this issue *in-situ* AFM studies can be performed. Morphological changes during polymerization are also of interest although not easily measured due to potential damage to the cell.

Many of the films investigated in which wires are present indicate that the wires tend to form bundles. This phenomenon likely occurs during drying. Another possible explanation is that surfactant, which holds the wires in place, is removed during washing. Different drying and washing techniques may be tried in order to minimize these effects. In addition, deposition from solution is problematic in some experiments and may be a result of drawing the substrate through the liquid/air interface during removal. Other forms of removal from the reaction mixture may be investigated to minimize deposition from solution.

In chapter 5 surface modification of HOPG was attributed to intercalated species from the oxidant. A better understanding of this process may be carried out by selection of different persulfate oxidants such as sodium, potassium, or lithium. Also atomic resolution scanning probe microscopy

(SPM) images and angle resolved XPS experiments might reveal the location and organization of intercalated species.

Many potential combinations of surfaces, surfactants, and monomers are available for further investigations. I believe that surface masking techniques used in conjunction with the technique outlined in chapter 5 might lead to a method for the precise placement of electrically conducting polymeric nanostructures on surfaces. An example of this would be the use of ordered arrays of polystyrene latex spheres as a framework to deposit nanospheres of conducting polymer in interstitial sites. As the field of nanotechnology continues to emerge, the ability to not only synthesize nanostructures but also to then position them into useful architectures, will likely become invaluable. In all likelihood, as is the case with some biological systems, amphiphiles will likely hold the key to organizing and positioning molecules with nanoscale precision.